

Assessment of Various Mitigation Strategies of Alkali-Silica Reactions in Concrete and Implementing Outlier Detection Method in Industrial Applications

A Dissertation

Presented in Partial Fulfillment of the Requirements for the

Degree of Doctor of Philosophy

with a

Major in Civil Engineering

in the

College of Graduate Studies

University of Idaho

by

Abdullah S. Almakrab

Major Professor: Ahmed A. Ibrahim, Ph.D., P.E.

Committee Members: Kevin Chang, Ph.D., P.E.; S.J. Jung, Ph.D., P.E.; Suat Ay, Ph.D., P.E.

Department Administrator: Fritz R. Fiedler, Ph.D., P.E.

August 2021

Authorization to Submit Dissertation

This dissertation of Abdullah S. Almakrab, submitted for the degree of Doctor of Philosophy with a Major in Civil Engineering and titled "Assessment of Various Mitigation Strategies of Alkali-Silica Reactions in Concrete and Implementing Outlier Detection Method in Industrial Applications," has been reviewed in final form. Permission, as indicated by the signatures and dates below, is now granted to submit final copies to the College of Graduate Studies for approval.

Major Professor: _____ Date: _____
Ahmed A. Ibrahim, Ph.D.

Committee Members: _____ Date: _____
Kevin Chang, Ph.D.

_____ Date: _____
S.J. Jung, Ph.D.

_____ Date: _____
Suat Ay, Ph.D.

Department
Administrator: _____ Date: _____
Fritz R. Fiedler, Ph.D.

Abstract

The mitigation of Alkali-Silica Reaction (ASR) has become more urgent than ever before due to the high demand for concrete in an increasingly industrialized world with expanding urban infrastructure. This study investigates the efficacy of additives in cement mixtures as an effort of stopping or mitigating Alkali-Silica Reactions that damage the structural integrity of concrete members. While there is existing research on certain supplementary cementitious materials (SCMs) and their role in stopping ASR in concrete, the present study is distinguished by using various binary supplementary cementitious materials (SCMs) such as Metakaolin and waste glass powder as replacement for cement. A new cement product called NewCem Plus was also investigated as a cement replacement at various percentages. In addition, the effectiveness of other materials and admixtures such as basalt fiber and lithium were also examined. The ASTM C1260 14-day accelerated mortar bar test was used for this study, and all supplementary materials were tested separately according to ASTM standards. Moreover, concrete properties such as compressive strength and concrete flow test were also evaluated in order to complement the test results. Our preliminary findings showed that Metakaolin could effectively be implemented in concrete mixtures as an ASR mitigation waste-by-product. In the samples with 10%, 20%, and 30% where Metakaolin was added as cement replacement, the expansion was 79%, 84%, and 88% less than that of the control mixture. The glass powder decreased the expansion of control specimens by 20%, 43%, and 75% at the 10%, 20%, and 30% replacement levels, respectively. The addition of lithium to the Metakaolin mitigated the ASR. Lithium by itself was effective when added to the Metakaolin and glass powder mixtures, where it reduced the expansion below the threshold limit, which is 0.1%. The cement replacement of 10% with glass powder + lithium resulted in 0.209% expansion (51% reduction). However, the reduction for the 20% and 30% was not enough to pass the ASTM test, and the total expansion went

above the 0.1% total expansion safe limit of the test. The mixtures of NewCem Plus (NCM) and Lithium were not an effective solution for ASR reduction in concrete.

The test results of the other two materials, glass powder, and basalt fibers, showed variations between reducing and increasing the expansion level based on their percentages of cement replacements. Although the concrete expansion was slowed, it was not kept under the safe level of 0.10% as recommended by ASTM 1260. Finally, the experimental results point positively to the simultaneous addition of multiple SCMs and additives in cement mixtures to further increase its numerous properties. In addition, a comprehensive cost analysis of all the ingredients used in all mixtures was performed. The results showed that the cost would be 50% less compared to the control mixtures (100% cement) to 655% more when basalt fibers were used. The manufacturer shall perform a life cycle assessment before the final decision of the inclusion of such materials. This study showed the feasibility of using binary and ternary blends of SCMs in mitigating ASR in concrete, and it shows a comprehensive representation of how those materials should be included in concrete mixtures for future applications.

The second topic of this dissertation was focused on the application of data mining in detecting outliers in concrete testing results and how that is important to stakeholders and decision makers. The rapid development in the construction industry has induced a large amount of concrete data over the years, which are usually measured and analyzed every day. Concrete is made from numerous ingredients that have huge variability either at the design stage or at the testing stage. The main goal of this study is to quantify the anomalies and outliers during the design phase of concrete mixtures. Concrete mixtures have various percentages of ingredients such as cement, slag, fly ash, water, superplasticizer, and fine and coarse aggregates. Although machine learning and data mining are considered very thriving topics in many research fields,

their implementation in the construction industry is still limited. The concrete community needs such a tool to produce efficiently designed concrete mixtures. Outliers could occur during the evaluation of samples' measurements that might include human errors or concrete properties' inconsistency. The Local Outlier Factor (LOF) algorithm is the most common method used to determine outliers; however, the LOF has some challenges. In this study, an anomaly-based outlier detection algorithm called Isolation Forest based on a Sliding window for the Local Outlier Factor (IFS-LOF) algorithm was proposed to solve the limitations of the LOF method in evaluating 1030 concrete mixtures. The proposed algorithm worked without any previous knowledge of data distribution and executed the process within limited computer memory and with minimal computational effort. The evaluation of results proved that the IFS-LOF algorithm was more efficient in detecting the sequence of outliers and provided more efficient accuracy than other state-of-the-art LOF algorithms.

Acknowledgments

It is a happy occasion to extend my sincere thanks to everyone who supported me during my Ph.D. period, especially the Saudi cultural mission in the United States of America (SACM), for sponsoring me. I also thank the International Student Office at the University of Idaho for the help and support they gave to me as an international student. I would also like to thank my major professor, Dr. Ahmed Ibrahim, for his support and kindness during my studies. Many thanks to the Department of Civil and Environmental Engineering at the University of Idaho, represented by the department chair Dr. Fritz R. Fiedler, the administrative staff, and the academic faculty for their support and cooperation.

Dedication

I dedicate my work to my beloved wife, Dr. Ibtisam Alhasaf, who fully supports me in many ways during my work, and my beautiful children, who always give me hope for a better future. I am deeply grateful to my great parents and my brother Dr. Nasser, who has been encouraging and supporting me my whole life. I have never felt alone when I have them close to me.

Table of Contents

Authorization to Submit Dissertation	ii
Abstract.....	iii
Acknowledgments	vi
Dedication.....	vii
Table of Contents.....	viii
List of Tables	x
List of Figures.....	xii
Chapter 1: Introduction.....	1
1.1 Introduction.....	1
1.2 Research Objective	2
Chapter 2: Alkali-Silica Reaction in Concrete Structures: Mechanism, Effects, and Evaluation	
Methods Adopted in The United States	5
2.1 Introduction.....	5
2.2 Mechanism of Alkali-Silica Reaction.....	9
2.3 Effect of ASR on Concrete Structures: Pavement and Bridges	18
2.4 Evaluation of Alkali-Silica Reaction	23
2.5 Conclusions.....	33
Chapter 3: Experimental Investigation of ASR Mitigation Using Various SCMs Through Binary	
Mixtures.....	35
3.1 Introduction.....	35
3.2 Experimental Program	40
3.2 Experimental Test Results	55
3.3 Cost Analysis	83
3.4 Conclusions.....	85
Chapter 4: Improving the Outlier Detection Method in Industrial Application by Combining the	
Isolation Forest and Local Outlier Factor	91

4.1	Introduction.....	91
4.2	Related Work.....	92
4.3	Context, Dataset, And Methodology	95
4.4	Components and Workflow	97
4.5	Experimental Results and Discussion.....	102
4.6	Experimental Settings.....	103
4.7	Discussion.....	103
4.8	Benefits of Using the Outlier Detection in Concrete Mix Design	108
Chapter 5: Conclusions and Recommendations		109
References.....		113
Appendix		126
A.1.	Guidelines for Use Dosage	126
A.2.	Chemical composition of the used materials	127
A.3.	The Algorithm.....	130
A.4.	Copyright	135

List of Tables

Table 2.1 Summary of Alkali-Silica Reaction in Major Aggregate Types.....	13
Table 2.2 Mortar Bar and Concrete Prism Tests of ASR Expansion as a Function of Aggregate Size	15
Table 2.3 Mixture Proportions for the MCPT Specimen.....	32
Table 2.4 Classification of Aggregate Reactivity (Nixon & B. Fournier, 2017) ((Latifee & Rangaraju, 2015).....	33
Table 3.1 Chemical Composition of used SCMs ((Islam et al.2017) (H. Hu, Y. Liu, 2010, p.329-386)	44
Table 3.2 Details of the Mix Design.....	46
Table 3.3 Experimental Program	53
Table 3.4 Reactivity Tables (Nixon & B. Fournier, 2017) ((Latifee & Rangaraju, 2015)	54
Table 3.5 Fourteen-day expansions, standard deviations, and coefficients of variation for Group A (Specimen 1) mixtures	56
Table 3.6 Fourteen-day expansions, standard deviations, and coefficients of variation for Group A (Specimen 2,3,and4) mixtures	56
Table 3.7 Fourteen-day expansions, standard deviations, and coefficients of variation for Group B (Specimen 5,6, &7) mixtures.....	58
Table 3.8 Fourteen-day expansions, standard deviations, and coefficients of variation for Group C (Specimen 8, 9, and10) mixtures	60
Table 3.9 Fourteen-day expansions, standard deviations, and coefficients of variation for Group D (Specimen 11, 12, and13) mixtures	62
Table 3.10 Fourteen-day expansions, standard deviations, and coefficients of variation for Group G (Specimen 15, 16 and17) mixtures	65
Table 3.11 Fourteen-day expansions, standard deviations, and coefficients of variation for Group H (Specimen 18, 19 and 20) mixtures	67
Table 3.12 Fourteen-day expansions, standard deviations, and coefficients of variation for Group I (Specimen 21, 22, and23) mixtures	69
Table 3.13 Fourteen-day expansions, standard deviations, and coefficients of variation for Group J (Specimen 24, 25, and 26) mixtures	70
Table 3.14 Flow Test Results	72
Table 3.15 Compressive Strength 28 days Results.....	75
Table 3.16 Cost Analysis.....	89
Table 4.1 Range of Concrete Ingredients Used in This Study.....	96
Table 4.2 Isolation Forest [IF] Algorithm	98

Table 4.3 The Isolation Forest Based on the Sliding Window for Local Outlier Factor (IFS-LOF Algorithm)	101
Table 4.4 Accuracy Rate of the LOF, LOF-SW and IFS-LOF for Different Window Sizes	104
Table 4.5 Execution Times of the LOF, LOF-SW, and IFS-LOF for Different Window Sizes.....	107

List of Figures

Figure 2.1 Typical Example of ASR in Concrete with Stanton.....	7
Figure 2.2 Schematic of ASR Activity in Concrete Structures	9
Figure 2.3 A Schematic Diagram of ASR Chemistry	11
Figure 2.4 Schematic of the Crystalline Structures of Opal and Quartz.....	14
Figure 2.5 Composition of Pore Solution in Cement and Mortar.....	17
Figure 2.6 Images of Various Effects of Alkali-Silica Reaction	23
Figure 2.7 Different Testing Methods Used for Assessing Alkali-Silica Reaction	25
Figure 3.1 Alkali Silica Reaction Triangle (Concrete Cracking – A Destructive Kind)	41
Figure 3.2 Mold Used for Mortar Bar Preparation of 1 in. x 1 in. x 11.5 in.....	51
Figure 3.3: The 14-day AMBT expansion rate for the control specimens	55
Figure 3.4 The 14-day AMBT expansion rate for Metakaolin as SCM	56
Figure 3.5 Metakaolin as SCM.....	57
Figure 3.6: The 14-day AMBT expansion rate for Glass Powder	58
Figure 3.7: The 14-day AMBT expansion rate for Metakaolin-Glass Powder Samples	60
Figure 3.8: Metakaolin-Glass Powder Samples.....	61
Figure 3.9 The 14-day AMBT expansion rate for NewCem Plus (NCP) Samples	62
Figure 3.10 Mortar bars for Li with basalt fine aggregate Samples	64
Figure 3.11 The 14-day AMBT expansion rate for Li with MK Samples.....	65
Figure 3.12 Li with MK Samples with 30% replacement of cement.....	66
Figure 3.13 :The 14-day AMBT expansion rate for Li with GP	67
Figure 3.14:Li with GP Samples with 10% cement replacement	68
Figure 3.15 : The 14-day AMBT expansion rate for NCP with Li Samples	68
Figure 3.16 NCP with Li Samples with 10% replacement of cement	69
Figure 3.17 The 14-day AMBT expansion rate for BF Samples.....	70
Figure 3.18 The 14-day AMBT expansion rate normalized.....	71
Figure 3.19 Compression Test Results for (MK).....	76
Figure 3.20 Compression Test Results for (GP).....	77
Figure 3.21 Compression Test Results for Metakaolin-Glass Powder	77
Figure 3.22 Compression Test Results for (NCP)	78
Figure 3.23 Compression Test Results for Lithium with Metakaolin.....	79
Figure 3.24 Compression Test Results for Li with Glass Powder	80
Figure 3.25 Compression Test Results for (NCP+Li)	80
Figure 3.26 Compression Test Results for (BF)	81

Figure 3.27 Compression Test Results Normalization	82
Figure 3.28 Cost Analysis Chart.....	88
Figure 4.1 Illustration of the Outlier Categories.....	93
Figure 4.2 Illustration of Subsampling Size in the Isolation Forest for Processing Data Points	97
Figure 4.3 Illustration of the Reachable Distance in Various Data Points as $k = 4$	99
Figure 4.4 Structure of the Proposed IFS-LOF Algorithm.....	102
Figure 4.5 Comparison of Accuracy of Results Between LOF, LOF-SW, and IFS-LOF	105
Figure 4.6 Comparing accuracy result between LOF, LOF-SW, and IFS-LOF. IFS-LOF presents most consistently higher accuracy in most of the ws comparing to the other remaining algorithms	106

Chapter 1: Introduction

1.1 Introduction

Concrete is an essential material in most construction activities. It also has excellent resistance and strength, and it can be easily made from abundant, naturally occurring materials. Still, it faces problems due to the impact of such environmental conditions as weather changes that create wide swings in temperature and that may continually expose the concrete to moisture. Therefore, there is still room for researchers to develop more ideal formulas to make concrete more resistant to harsh weather conditions and to increase its durability.

Structures all around the globe experience cracking and other signs of decay due to exposure to the natural conditions of their surrounding environments. These structures start to lose structural integrity over time and need repairs, which also will be difficult to maintain in the long term, eventually requiring demolition.

The importance of improving concrete mixtures for structural applications will continue using various venues. Therefore, the enhancement of concrete durability is one of those venues. The Alkali-Silica Reaction (ASR) in concrete has become one of the main enemies due to its corrosive and deleterious impact. This is important because the chemical reaction of ASR in concrete leans to take long time to externally visible and this happens after the occurrence of irreparable damage. The diagnostic methods for ASR are complicated, although these methods have been developed as early as the 1940s when researchers became aware of the issue. Furthermore, current means of addressing or avoiding ASR generally do not create permanent solutions to ASR, necessitating further assessment and examination.

An in-depth investigation of combinations of Supplementary Cementitious Materials (SCMs) is still needed, along with evaluation of quicker methods for diagnosing the issue, such as the

ASTM 1260, which could be more reliable. In addition, the use of new waste by-products and various fiber types, should be investigated.

Furthermore, this dissertation presents a novel study of detecting outliers in concrete mixtures. Outlier detection is getting more attention in the civil engineering construction industry as a result of the extreme growth in the civil construction sector worldwide. Outlier detection is directly needed for the maintenance and repairs of existing civil infrastructures such as highways, bridges, buildings, dams, and tunnels. However, the infrastructure data may come from different sources that might include errors or odd data points. The proposed outlier algorithm will help in the precise analysis and detection of big-concrete data available. Therefore, the results of this study will help to improve the quality of concrete production.

1.2 Research Objective

ASR has been a major durability problem in concrete materials for decades, especially in concrete that has reactive ingredients such as aggregates or high alkali cement. If concrete ingredients have a certain level of silicates that react with the hydroxyl ions dissolved in the concrete pore solution, an active gel is formed. This gel is expandable when it interacts with water as a result of concrete exposure to moisture.

This study aims at increasing the knowledge related to ASR mitigation in concrete materials. Investigating ASR mitigation strategies by using waste by-products will add a great benefit to the concrete materials community. Mitigating ASR in concrete will save stakeholders and concrete structures' owners millions of dollars by enhancing concrete durability and lowering the high cost of maintenance. There is a need to develop cost-effective and feasible admixtures to inhibit ASR. In this research, various concrete mixtures with various SCMs, lithium admixtures, and fiber types were evaluated. All the tested concrete mixtures contained fine

basalt aggregate (reactive aggregate) plus high alkali content cement. In addition, various supplementary cementitious materials (SCMs) with different cement replacement percentages (0% [control], 10%, 20%, and 30%) were used in all mixtures. These particular SCMs and fibers were tested because they were identified through the review of the literature as having the potential to be good mitigating agents of ASR. Moreover, these materials are economically viable and can be integrated into concrete on a large scale. Some of the used SCMs have been chosen for this research were waste by-products (e.g., waste glass powder, NewCem Plus, and Metakaolin). The effect of including basalt and basalt fibers was also investigated. Finally, various lithium percentages were used in combination with the SCMs.

Because concrete assessment and evaluation are usually based on lab experiments, which have a high risk of human error, the use of data mining as a method of detecting data errors and outliers is justified. This further justifies the idea of using data mining as a method of detecting data errors and outliers. Finding the outliers in each concrete ingredient could improve the quality and reliability of the data to be processed. A detection method has been developed to identify outliers in big-concrete data available in the literature. The proposed algorithm generates better performance than state-of-the-art algorithms. Therefore, this research's specific objectives are as follows:

1. Evaluate Alkali-silica reaction (ASR) in concrete structures: Mechanisms, effects, and evaluation test methods adopted in the United States.
2. Deeply investigate the effect of the implementation of binary waste-by-product materials to inhibit or mitigate ASR in concrete.
3. Investigate the newly blended waste-by-product NewCem on ASR mitigation.

4. Examine the optimal concrete mixture that limits ASR expansion to less than the allowable limit recommended by the ASTM C1260.
5. Conduct a comprehensive cost analysis to investigate the feasibility of the proposed mitigation techniques proposed in Objective 2.
6. Develop a novel outlier detection algorithm for concrete mixtures.

Chapter 2: Alkali-Silica Reaction in Concrete Structures: Mechanism, Effects, and Evaluation Methods Adopted in The United States

(Published in Case Studies in Construction Materials,
<https://doi.org/10.1016/j.cscm.2021.e00563>)

2.1 Introduction

Portland Cement Concrete (PCC) consists of 60% to 75% aggregates, 10% to 15% of Portland cement and/or other supplementary cementitious materials or admixtures, and water. Concrete is recognized as the most widely used construction material in the world (Naik, 2008). The presence in PCC of reactive amorphous or poorly crystallized silica from many natural aggregates reacts with alkalis (i.e., sodium [Na] and potassium [K]) in cement or admixtures, which then produces a deleterious chemical reaction over time. This chemical reaction is widely known as the alkali-aggregate reaction (AAR), which is a prominent concrete durability problem that affects the serviceability of civil engineering infrastructure, including buildings, pavement, bridges, and other concrete structures (Forster et al., 1998; Latifee, 2016; Malvar et al., 2002; Thomas et al., 2012). AAR is sub-divided into two kinds of reactions: (a) the alkali-silica reaction (ASR) that develops due to reactive silica minerals in aggregate; and (b) the alkali-carbonate reaction (ACR), which arises in aggregates that contain carbonate and dolomite (Diamond, 1992).

Due to the high percentage of silica present in aggregate, the prominent form of AAR is ASR, which was initially observed by Stanton decades ago (Stanton, 2008; see Figure 2.1). ASR is a destructive chemical reaction that occurs between the active silica constituents (reactive minerals) of aggregate and the alkalis in the paste matrix (cement and other pozzolanic materials), causing an indefinite expansion in the presence of moisture or pore solutions in

concrete (Farney & Kosmatka, 1997). Most structures built with concrete in the United States during the 1940s developed ASR and eventually failed and required demolition after a period of time (Forster et al., 1998). ASR causes deformation that manifests as an extensive expansion -- map and other forms -- of cracking, aggregate pop-out, gel exudation, and/or white deposits on the concrete surface (Islam & Akhtar, 2013; Kandasamy & Shehata, 2014).

Much research has been conducted on ASR over the last 80 years, beginning with the pioneering work of Stanton in 1941 (Stanton, 2008). Numerous published articles on ASR were produced between 1970 to 2020, making the subject of ASR in concrete the primary area of concern in the field in terms of it being the major durability issue in the material. Hence, this review clarifies and presents the data on the current state of the ASR challenge as presented in recent years (Thomas et al., 2012). In other parts of the world, such as in Australia, Cote et al. (1981) reported harmful expansion and cracks in their dam structures. Similarly, in Japan, ASR-induced cracks have been reported in concrete structures for decades (Ono, 1988). Cracks and expansions due to ASR have also been found in pavement structures in New Zealand (Swamy, 1992). Despite ASR being well-studied over the years, it continues to be identified in critical structures. For example, the United States and Canada recently identified structural distress caused by ASR in the Seabrook Station Nuclear Power Plant (in 2013) and the Mactaquac Dams (in 2017), respectively (Beaver et al., 2013; Yu, 2017). Such recent problems call for continuous research and reviews of recent developments.



Figure 2.1 Typical Example of ASR in Concrete with Stanton

Note. Source: “Expansion of concrete through reaction between cement and aggregate,” by T. E. Stanton © 2008.

According to Diamond (1992), the deterioration of concrete caused by ASR is continual, expansive, and generally slow. The ASR reaction produces an alkali-silica gel over time, which leads to progressive deformation of concrete due to internal forces triggering loss in serviceability and longevity (Diamond, 1992; Stanton, 2008). The ASR-induced distress, in turn, leads to major damage in concrete structures and eventually causes collapse or forces the demolition of the structure. This mechanism has been highlighted in several research works (Bach et al., 1993; Berra et al., 1991; Grattan-Bellew & Mitchell, 2002; Islam, 2010; Islam & Akhtar, 2013; Islam & Ghafoori, 2011; Léger, 1996; Swamy, 1992; Wang et al., 2010).

In terms of identifying and evaluating ASR, numerous test methods have been developed to evaluate alkali-silica reactions in mortar or concrete. These test methods, as reported in the literature, are the ASTM C 295, which involves a petrographic examination of aggregates;

ASTM C 1260, which is an accelerated mortar bar test (AMBT); and the ASTM C 1293, which is a concrete prism test (CPT; American Association of State Highway and Transportation Officials [AASHTO], 2003; American Society for Testing and Materials [ASTM], 1995, 2007). However, researchers have found that these evaluation methods exhibit some shortcomings (Bueno et al., 2020; Latifee, 2013), such as yielding false results that are contrary to field performance. This issue requires that we re-evaluate these methods. In this regard, a new ASR testing method called the AASHTO TP 110-Miniature Concrete Prism Test ([MCPT], which was replaced by the AASHTO T 380 in 2019) was developed in 2014 to act as a bridge for the shortcoming of the previous testing procedures (AASHTO, 2019; Halsey & Heyen, 2019; Latifee, 2013; Rangaraju et al., 2016). Also, this method has been adopted for evaluating mitigation measures for ASR susceptibility in concrete (Afshinnia & Rangaraju, 2015; AASHTO, 2014; Latifee, 2013).

As a result of the effects of ASR on concrete's lifespan, the identified shortcomings, and the inconsistency of ASR testing methods, a review is needed that obtains first-hand information on the mechanisms of ASR, its effects, and the various evaluation procedures. Furthermore, new information on ASR, in the form of new problems as well as new research findings, continues to arise, including the development of the new AASHTO T 380 (2019). Therefore, this article provides a comprehensive and detailed examination of the ASR mechanism and its effects on concrete structures. A full description of the test procedure to determine aggregate susceptibility to ASR is also discussed along with results acquired from recent publications. Lastly, this review highlights the latest test method, AASHTO T 380, which was developed to supersede previous methods. It discusses this method extensively in terms of both ASR evaluation and mitigation approaches.

2.2 Mechanism of Alkali-Silica Reaction

2.2.1 Background on Alkali-Silica Reaction

ASR is a deleterious chemical reaction with a multi-stage process (Islam & Akhtar, 2013). The active silica constituents present in some aggregates react with alkalis in the cementitious materials, producing alkali-silica gel. The reaction product (gel) is hygroscopic, having a greater ability to absorb water. In the presence of water or pore solution, this causes an expansion, especially in the presence of certain conditions (climatic factors), and subsequently leads to cracks and other ASR-induced distress (Diamond, 1992; Farny & Kosmatka, 1997). An insufficient amount of active silica in aggregates, alkali concentration from the binder, and moisture will prevent alkali-silica gel from arising at high enough levels to cause deleterious effects. The schematic of this activity is shown in Figure 2.2.

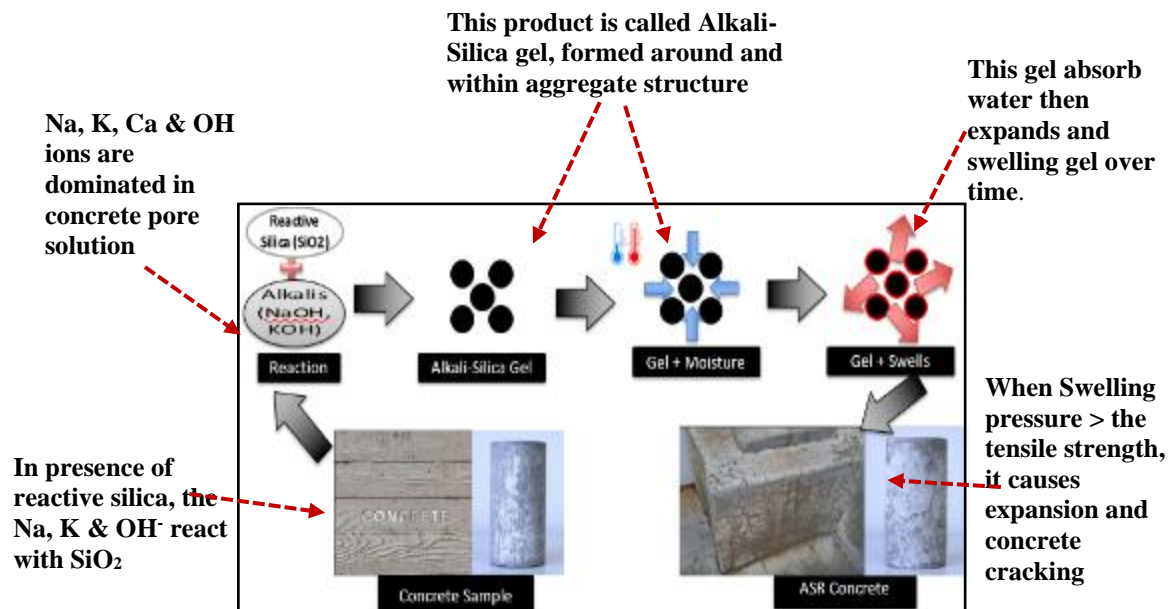
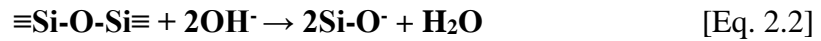
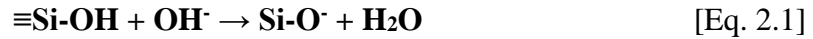


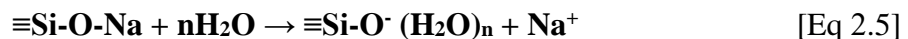
Figure 2.2 Schematic of ASR Activity in Concrete Structures

2.2.2 Chemistry of Alkali-Silica Reaction

The ASR chemical reaction occurs between reactive silica in aggregates and alkali hydroxide in the pore solution of concrete. The state of silica (SiO₂) in the aggregates is chemically passive, in the form of quartz, and mainly structured as siloxane groups ($\equiv\text{Si-O-Si}\equiv$). However, the disorderliness of crystalline silica at the surface means that it tends to attract water and produce amorphous hydrous silica (silanol group [$\equiv\text{Si-OH}$]; Thomas et al., 2011). Thereafter, the silica inclines toward dissolution in the presence of highly concentrated hydroxyl ions by first neutralizing the silanol groups ($\equiv\text{Si-OH}$) and then neutralizing the siloxane groups ($\equiv\text{Si-O-Si}\equiv$), as illustrated in Eq. 1.1 and 1.2 (Thomas et al., 2012).



As the structures ($\equiv\text{Si-OH}$, $\equiv\text{Si-O-Si}\equiv$) gradually break down, they also attract the hydroxides of the soluble alkali generated from alkali metal ions. These alkalis present abundantly in concrete pore solution as Na⁺ or K⁺ (Godart et al., 2013). The calcium hydroxide (Ca(OH)₂) and calcium silicate hydrate (C-S-H) produced from cement hydration also add to the OH⁻ in pore solution. Alkali-silicate solution/silicic acid (Si-OH) and gel (depending on the level of moisture) are the preliminary products of the reaction between these siloxane groups ($\equiv\text{Si-O-Si}\equiv$) and hydroxyl ions (see Eq. 1.3). Thereafter, the Si-OH reacts with more OH⁻ and alkali metals forming alkali silicate hydrate and water, as presented in Eq. 1.4 and Eq. 1.5 (Bažant & Steffens, 2000; Godart et al., 1993; Ichikawa & Miura, 2007; Swamy, 1992).



A diffusion process of this hydrated alkali-silicate gel occurs within the aggregates in the cement paste, which then react with the calcium ions in the paste to form alkali-calcium-silicate hydrate gel. In the presence of moisture, this final product expands, which when it occurs in excess generates cracks at the interfacial transition zone between the aggregate particles and cement paste, leading to stress and cracks in concrete structures (Diamond, 2000; Dron & Brivot, 1992, 1993; Thaulow, 1996). Figure 2.3 illustrates the schematic picture of ASR chemistry in the mortar and concrete structures (Lima et al., 2018; Saha et al., 2018; Thomas et al., 2011).

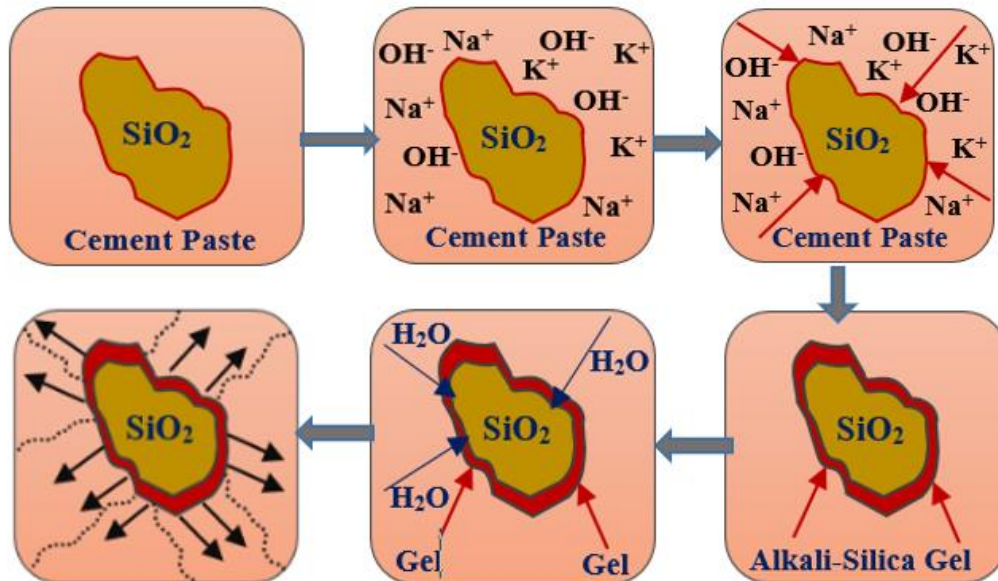


Figure 2.3 A Schematic Diagram of ASR Chemistry

Note. Adapted from Lima et al., 2018; Saha et al., 2018; Thomas et al., 2011.

2.2.3 Factors Affecting Alkali-Silica Reaction

The swelling gel of ASR does not directly cause concrete distress, but as the swelling gel absorbs moisture, it expands and induces stress. Such stresses can exceed the tensile strength

of concrete, causing progressive cracking and associated deterioration. The three main components widely regarded as essential for ASR in concrete materials are:

- Presence of reactive siliceous components in aggregates (both coarse and fine).
- Adequate alkali content from cementitious materials.
- Presence of moisture along with other factors (e.g., temperature, relative humidity, additives).

2.2.4 Reactive Aggregate

The durability and chemical stability of a concrete structure was determined by the quality of aggregates used. About 65% to 75% of the majority of concrete's volume comprises aggregates (Fanijo et al., 2020; Kolawole et al., 2020). As a result, both coarse and fine size aggregates have a substantial influence on the properties of concrete affected by ASR. According to a 2011 FHWA report, many aggregate sources are reported reactive (containing high silica content) and exhibit high ASR potential when exposed to a solution of high alkaline (Thomas et al., 2011). The chemical composition, crystallinity, and amorphous level of aggregate and the degree of solubility of the amorphous silicate in alkaline concrete pore solution all affect aggregate reactivity to ASR (Islam & Akhtar, 2013; Léger, 1996). As some researchers have confirmed (see Table 2.1), many aggregates commonly used in the United States and Canada have been found to be ASR-prone. A summary of major aggregates susceptible to ASR is presented in Table 2.1. Specifically, Berube and Frenette (1994) found that andesite, chert, opal, quartz, siliceous rocks, basalt glass, dacite, and others are reactive aggregates, while dolomite and limestone rocks were found not to be prone to ASR expansion.

Table 2.1 Summary of Alkali-Silica Reaction in Major Aggregate Types

Aggregate Type	ASR Classification	Source	Reference
Basalt	Reactive	VA, AZ U.S.	Adam (2004) Lane (1994)
Opal	Reactive	U.S.	Berube & Frenette (1994)
Dolomitic Limestone	Reactive	PA, VA U.S.	Lane (1994) Grattan-Bellew et al. (2010)
Chert	Reactive	TX/U.S.	Moser et al. (2010)
Spratt	Reactive	Ottawa CANADA	Thomas et al. (2011) Lane (1994)
Glass Aggregate	Reactive	CANADA	Shafaatian et al. (2013)
Limestone	Non-Reactive	U.S.	Stark et al. (1993) Touma et al. (2001)
Andesite	Reactive	U.S.	Adam (2004)
Dolomite	Non-Reactive	U.S.	Stark et al. (1993)
Dacite	Reactive	CANADA U.S.	Thomas et al. (2007) Touma et al. (2001) Hooton (1991)
Quartz sand	Non-Reactive	U.S.	Stark et al. (1993) Touma et al. (2001)
Rhyolite	Reactive	U.S.	Touma et al. (2001) Adam (2004)

In terms of aggregate structure, two primary groups of rocks can be differentiated based on their crystalline structure. The first of these is extremely reactive rocks, which contain amorphous silica and lack minerals with crystalline structures. These reactive aggregates contain microcrystalline silica or metastable crystals. This structure is found to be in disorder, containing micro-cracks internally, with many lattice defects that generate channels for easy penetration of alkalis from the cement paste (Glasser, 1992). As a result, the reactive silica ion can easily transfer in a larger surface area, causing more ASR to occur. The second type is “mild or non-reactive rocks,” which are made of minerals with crystalline structures (Bérubé & Frenette, 1994; Monteiro, 2001). For example, Thomas et al. (2012) compared the structure of

the reactive aggregate opal, which has an amorphous structure that makes it unstable to high pH fluids, with that of a non-reactive aggregate (quartz) (see Figure 2.4; Thomas et al., 2012). The results showed that opal particles react with alkalis present in the pore solution, causing expansion in the concrete. Meanwhile, quartz possesses orderly shaped particles, which renders it not deleterious when present in concrete in terms of reacting with alkalis.

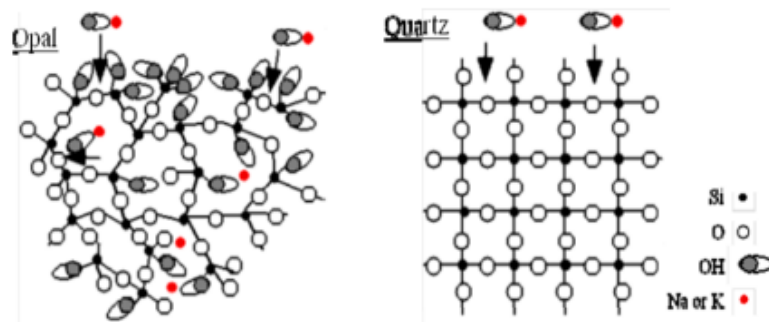


Figure 2.4 Schematic of the Crystalline Structures of Opal and Quartz

Note. Source: Thomas et al. (2012).

In addition, the aggregate degree of porosity also affects the rate of ASR expansion. A higher level of porosity increases the rate of aggregate susceptibility to ASR; causing finer aggregates to be more susceptible to ASR than are coarser aggregates (Farny & Kosmatka, 1997). This is because finer materials have a degree of order of silica minerals that are made unstable when crushed into smaller particles compared to large aggregates (Farny & Kosmatka, 1997; Xu, 1987). Also, the inverse relationship of the aggregate's internal grain size to its surface area creates a likelihood for alkali to attack (Farny & Kosmatka, 1997; Hobbs, 1988). Aggregate size has been found to have an adverse effect on the extent of ASR, making the size of reactive aggregate an important factor when determining aggregate reactivity (Stanton, 2008). In general, ASR expansion increases as particle size decreases, meaning as surface area increases. Table 2.2 illustrates the effect of aggregate size (for varied aggregate types) on ASR

susceptibility, using both mortar bar and concrete prism test, as established by different researchers.

Table 2.2 Mortar Bar and Concrete Prism Tests of ASR Expansion as a Function of Aggregate Size

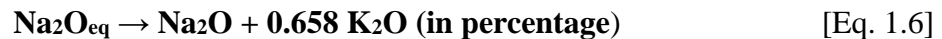
Type of Material(s)/Test	Aggregate Size Range for ASR	Reference
Siliceous Magnesium Limestone Aggregate containing Opal & Chalcedony Mortar Bar Test Concrete Prism Test	0.17 – 0.6mm	Stanton (2008)
Opaline Aggregate Particles Mortar Bar Test	0.07 - 0.85mm	Wood (1968)
Siliceous Aggregate Particles Mortar Bar Test	0.15mm	Zhang (1999)
Only Reactive Aggregate Mortar Bar Test w/0.48 mm bars	0.48mm	Kuroda et al. (2004)
Both Reactive & Non-Reactive Aggregates Mortar Bar Test	0.15 mm –0.30 mm	Kuroda et al. (2004)

Note. Source: Stanton (2008).

2.2.5 Alkalinity of Cementitious Materials

One of the major ingredients in ASR is the pore solution alkalinity, where Portland cement is the primary source of alkalis in concrete structures. Aggregates, supplementary cementitious materials (e.g., SCMs such as silica fume, natural pozzolans, slag cement, fly ash, and others), an external source (such as seawater and deicing salts), and chemical admixtures, also contribute to the additional alkali that leads to ASR in the concrete (Bérubé & Frenette, 1994; Diamond, 1992; Lindgård et al., 2012). The hydration of cement contributes to very high alkalinity being present in the pore solution in the form of $\text{Ca}(\text{OH})_2$. Efforts to minimize this could lead to low alkalinity and carbonation, resulting in corrosion, especially in reinforced concrete members. Aside from the alkalis produced by cement, reactive aggregate (especially amorphous structure aggregate) has also been found to release a certain percentage of alkalis

and increase the solution's pH (Goguel, 1995; Grattan-Bellew, 1995; Locati et al., 2010). The release and exchange of cations from aggregates with $\text{Ca}(\text{OH})_2$ present in the pore solution is the chemistry behind the dissolution of the alkalis that causes ASR gel. Though cement, aggregates, and other cementitious materials contain numerous alkali metals, it is the presence of sodium (Na^+) and potassium (K^+) ions that contribute significantly to ASR concrete damage (Lindgård et al., 2012). The quantity of alkalis in concrete in the form of Na and K is expressed in Eq. 1.6 below.



The Na_2O and K_2O are expressed as the mass percentage measured by sample chemical analysis of sodium oxide and potassium oxide. Conventional North American Portland cement contains 0.2% to 1.2% $\text{Na}_2\text{O}_{\text{eq}}$, while an alkali content as high as 1.65% or more of Na_2O is found worldwide (Lu et al., 2006). Despite the low percentage of alkalis compared to the percentage of other oxides present in Portland cement, the high solubility of these alkalis dominates the concrete pore solution. As shown in Figure 2.5, after some a period of time, the SO_4^{2-} concentration and the OH^- ions dissolve into the solution to maintain balance with the Na^+ and K^+ ions, which plays an important role in ASR-induced damage (Stark et al., 1993; Thomas et al., 2011).

Lastly, the total alkali content formed in the concrete mixture can increase as a result of external sources (e.g., seawater, water from industries that use sodium and potassium solution, and the groundwater) and admixtures (e.g., retarders, water reducers, and air-entraining agents) that may contain Na and K ions. This results in high ASR that, in turn, can potentially increase ASR expansion (Lindgård et al., 2012).

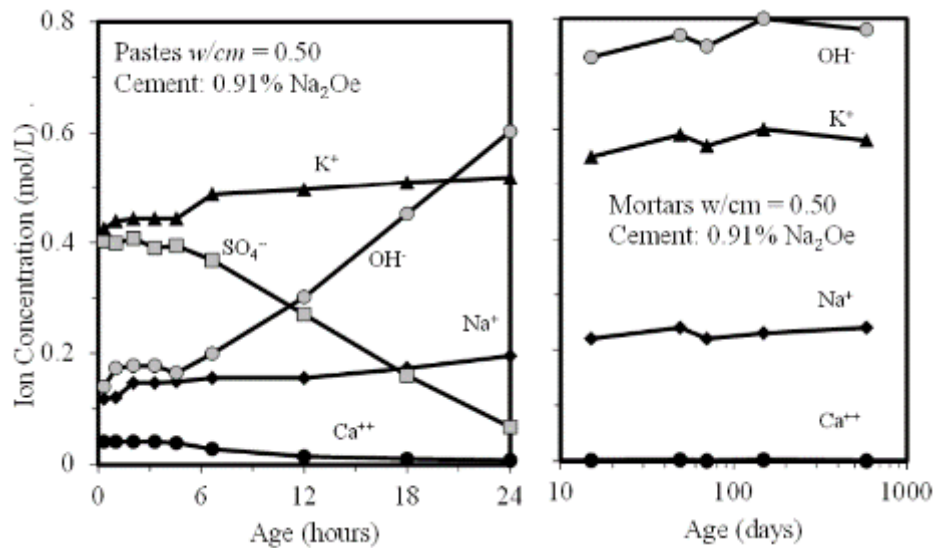


Figure 2.5 Composition of Pore Solution in Cement and Mortar

Note. Source: Diamond (2000).

2.2.6 Moisture in the Environment and Climatic Factors

There is number of environmental conditions that may increase concrete's vulnerability to ASR. The main environmental factors that affect ASR are temperature, humidity, associated concrete alkali redistribution due to seasonal climatic variations (wide seasonal variations in temperature and wetting/drying cycles), and penetration of alkalis from external sources (seawater and deicers).

The optimum combination of silica from aggregates and alkalis from cement is essential to initiating ASR, whereas these environmental factors make ASR expansive and, as a result, deleterious. Water is required to initiate alkali-silica reaction in concrete, as it acts as a transporter of alkali ions in the cement paste matrix. Moreover, water can also be absorbed into concrete externally. The pressure that causes concrete cracks starts when the gel absorbs water (as described in the following section), leading to greater expansion and cracking in the aggregates' interfacial transition zone over a long period. Therefore, high ASR expansion in a

concrete mixture is generally developed by highly reactive aggregates with high alkali cement content when exposed to a substantial amount of moisture. Highly reactive aggregates with high alkali cement content without sufficient presence of water show no or little expansion (Lu et al., 2006).

In addition, an increase in the relative humidity (RH) of concrete causes a greater effect of ASR expansion in concrete structures. Thus, there could be a sign of swelling gel in concrete at a very low relative humidity, but a relative humidity of 80% or more has been shown to be more supportive of swelling gels (Helmuth et al., 1993; Pedneault, 1996; Swamy, 1992). Additionally, the rate of ASR expansion also increases as temperature increases (Lu et al., 2006), while reducing concrete permeability, and the w/c ratio results in a decrease in ASR expansion (Shon et al., 2002).

2.3 Effect of ASR on Concrete Structures: Pavement and Bridges

As discussed above, the effects of the rise of ASR in structures are not immediate. Still, research shows that it continues over time as the reaction of silica and alkali continues, particularly in a high moisture environment. This adverse effect of ASR over a while in a concrete structure can result in sudden damage and eventually, either collapse or the requirement of demolition. ASR affects the engineering properties of concrete, such as compressive strength, tensile strength, flexural strength, and modulus elasticity over time. It also results in deflection, relative movement, permanent deformation, cracking, surface pop-outs, joints materials (sealant) extrusion, surface deposits (gel exudation and efflorescence), and discolorations. ASR effects are to a large extent characteristic of every concrete structure; however, in this review, the impact of ASR is only discussed on major highway infrastructure

(concrete pavements and bridges). The description of these effects on concrete pavement and bridge decks, as a case study, is discussed later and shown in Figure 2.6.

2.3.1 Concrete Expansion in Pavement and Bridges

Concrete expansion is one of the major consequences of ASR. The expansion of pavement generally occurs as a result of the swelling gel formed during ASR, and though the deterioration caused by this characteristic of the gel is fairly slow, it is progressive (Lu et al., 2006). Over time, this leads to a loss in durability, serviceability, and ultimately the need for the premature demolition of such concrete structures, reducing their planned lifespan. This expansion results in randomly formed map cracking, longitudinal cracks in subtle cases, and joint spalling of concrete pavement in worst cases (see Figure 2.6a; Stanton, 2008).

In bridges, alkali silica reaction expansion varies from one component to another; such distresses may manifest in such things as joint closure, deflections with the associated squeezing of sealing materials, and eventually concrete spalling joints. It can also lead to adjacent concrete structure movement, as shown in Figure 2.6b (Thomas et al., 2012).

2.3.2 Cracking in Pavement and Bridges

Concrete cracking is one of the major effects observed in concrete structures such as pavement or bridge decks. These cracks can be longitudinal and transverse and can also vary in length, depth, or width. That is, they can go around, or through the aggregates or, depending upon their location, they can affect the entire lifespan of the structure, as shown in Figure 2.6c-h (Stark et al., 1993; Thomas et al., 2011). The ASR-induced cracking that is characterized by networks of cracks is due to excessive gel expansion either in or on the structure, which occurs when reactive aggregate particles within the concrete become internally restrained and cause

internal stress, which is a pressure that exceeds the tensile strength of concrete (Farny & Kosmatka, 1997; Poole, 1991). In concrete pavement, in the initial stage of ASR development, cracking is shown on the pavement surface as randomly oriented cracks that indicate few or no substantial cracks. These cracks can be seen earlier on a smooth surface than on a grooved or textured one, with more pronouncement in the wetted surface (Stark et al., 1993). In addition to this, a well-defined longitudinal crack in the form of map cracking or pattern cracking (which develops across the width of pavement) can also occur due to ASR in concrete. This cracking increases as a result of traffic wear, especially with jointed and continuously reinforced pavement. ASR in the jointed pavement can show as severe cracking, especially left to right longitudinal cracking and interconnected cracks (fatigue cracking; Farny & Kosmatka, 1997; Godart et al., 2012; Poole, 1991). These cracks are then open to the elements and vulnerable to being filled with secondary deposits on the surface. Moreover, these cracks increase moisture content changes because they expose the concrete to rain or changes in temperature. ASR in continuous reinforced concrete pavement (CRCP) can be observed as a rectilinear crack pattern, with longitudinal cracks that are interconnected by random or transverse cracks, in smooth rather than textured pavement (Thomas et al., 2011).

Additionally, D-cracking, which is also known as durability cracking, and presents around the joints in concrete pavement, can also be caused by the mechanism of ASR when the cracks are seen to be simultaneously parallel to the adjacent joint. This type of distress cracking progresses normally away from the transverse joints and pavement slab edge (see Figure 2. 6d; Farny & Kosmatka, 1997; Godart et al., 2012; Poole, 1991; Stark et al., 1993; Thomas et al., 2011; Xu, 1987).

In bridges, ASR-associated cracking in the deck's mid-span and in bridge columns is observed as longitudinal cracks from top to bottom, interconnected by tight, short, mini-cracks that expand transversely between the longitudinal cracks; this presentation of ASR also leaves behind white deposits on columns. Most vertical cracks observed in bridge parapet walls are caused by ASR deformation, evidenced by the white deposit at the base that represents the ASR swelling gel and CaCO_3 (Naik, 2008; Stark et al., 1993). Another type of collaborative crack associated with ASR is the horizontal crack in the pier cap over water. Likewise, in the wing wall of bridge structures, lower level sub-horizontal cracks can be associated with ASR (especially in the area of free frost action). The curb section can also show distress cracking due to ASR in longitudinal and fine, random cracks. These cracks tend to increase in the presence of moisture or frost (Farny & Kosmatka, 1997; Thomas et al., 2011).

2.3.3 Pop-Outs in Pavement and Bridges

Concrete pop-outs occur as a result of weak or poor bonding between the cement paste and the aggregate particles. Pop-outs can also occur when a fragment of concrete breaks out of its surface. Pop-out distress related to ASR occurs when surface reactive aggregates undergo damaging expansion, inducing a detachment and separation from the bottom aggregates. This effect is more pronounced during frost action, to which the concrete aggregate surface is susceptible (Diamond, 1992). In this scenario of ASR, the gel forms beneath the pop-out aggregate and is indicated on the concrete's surface by holes (Farny & Kosmatka, 1997; Godart et al., 2012; Stark et al., 1993). These holes in the concrete usually range from one to two inches in width, depending on the site location (see Figure 2.6i). Likewise, concrete pop-outs associated with ASR are also dependent on the floor finishes and coverings and the composition of the slab sub-grade, such as the wet cohesive soils that are common with the pavement. The

durability and serviceability of concrete not generally affected by this kind of distress; however, it can lead to a rough concrete surface due to constant traffic (Poole, 1992; Thomas et al., 2011).

2.3.4 Surface Deposits and Color Changes

Surface deposits created by gel exudation and efflorescence often occur along concrete cracks and range from white to dark grey. ASR gel exuding from the concrete's surface can also exhibit as a colorless fluid or be viscous and yellowish or rubber-like in terms of color and shape (Poole, 1992). Though these color traces may not show ASR-related distress effects (suggesting that the traces are caused by frost action); however, the presence of gel formation on the crack surface ascertains ASR. These traces may increase in the presence of frost action, frost susceptible aggregate, and the presence of moisture. According to Poole (1991), surface discoloration has been revealed to be common in bridge decks and appears in combination with cracking. This surface discoloration area is generally bleached brown or pinkish in color and extends several inches from the crack regions (see Figure 2.6j; Thomas et al., 2011).

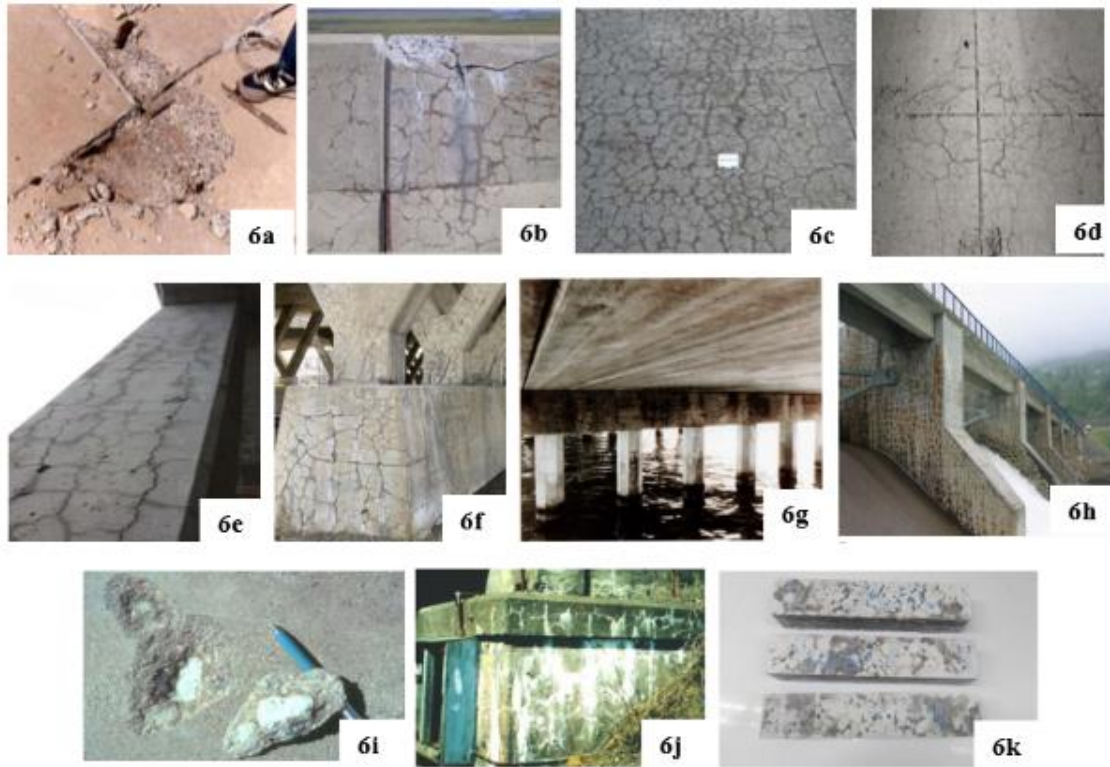


Figure 2.6 Images of Various Effects of Alkali-Silica Reaction

Note. (6a) Concrete spalling joint induced by ASR; (6b) Parapet wall of a bridge; (6c) Well-developed cracks associated with ASR; (6d) D-cracking associated with ASR; (6e) Longitudinal cracking related to ASR in bridge columns; (6f) Vertical cracks shown in parapet walls; (6g) Horizontal cracking on pier cap of a bridge; (6h) Map cracking in bridge wing walls caused by ASR; (6i) Pop-outs; (6j) Surface discoloration and exudation; and (6k) Expansion and cracks seen in a testing specimen (Thomas et al., 2011).

2.4 Evaluation of Alkali-Silica Reaction

Various methods have been developed and proposed to test and evaluate aggregate or concrete sample susceptibility to ASR. Furthermore, efforts are continually made to develop better versions of earlier testing methods to address the issue of potential aggregate reactivity in concrete. Figure 2.6 shows an illustration of the major published test methods from 1940 to 2015. From the literature review, it is clear that there are few testing methods in place in the United States to evaluate aggregate or concrete susceptibility to ASR. These are ASTM C295

- aggregate petrographic examination; ASTM C1260 - accelerated mortar bar test, concrete prism test; ASTM C1293 - concrete prism test (CPT), and the new testing method, AASHTO T 380 - Miniature Concrete Prism Test (MCPT). These well-vetted ASR evaluation methods are discussed below.

2.4.1 Aggregate Petrographic Examination - ASTM C295

The petrographic examination method was first developed in 1954 by K. Mather and Mather (1950), which was modified in 2008 (and renamed ASTM C295-08; ASTM, 2003). According to K. Mather and Mather (1950), this method was developed as a way to determine the chemical and physical properties of aggregates; to classify and evaluate the quantity of particle element present in the aggregate; and to differentiate aggregate samples from a specific source from those of another source with known performance data (K. Mather & Mather, 1950).

This test method is a reliable and fast way to identify reactive aggregate susceptible to alkali-silica reaction. A visual and microscopic examination is performed on the prepared potential aggregate samples using sieve analysis or an optical microscope. A thin section of aggregate is carefully examined. A petrographic examination may also be achieved using X-ray diffraction (XRD), scanning electron microscopy (SEM), or infrared spectroscopy (IR). However, some limitations of ASTM C295 make it unsuitable for examining certain specific aggregates for ASR; these shortcomings include: (a) the inability to characterize slow reactive aggregates, (b) the inability to determine the level of reactivity of aggregate in concrete, (c) the need for an expert and skillful petrographic examiner, and (d) that the processes involved consume much time and energy to identify aggregate reactivity. Also, the obtained results are dependent on the findings of other testing methods to evaluate aggregate susceptibility to ASR (Nixon & Sims, 1996; Touma et al., 2001).

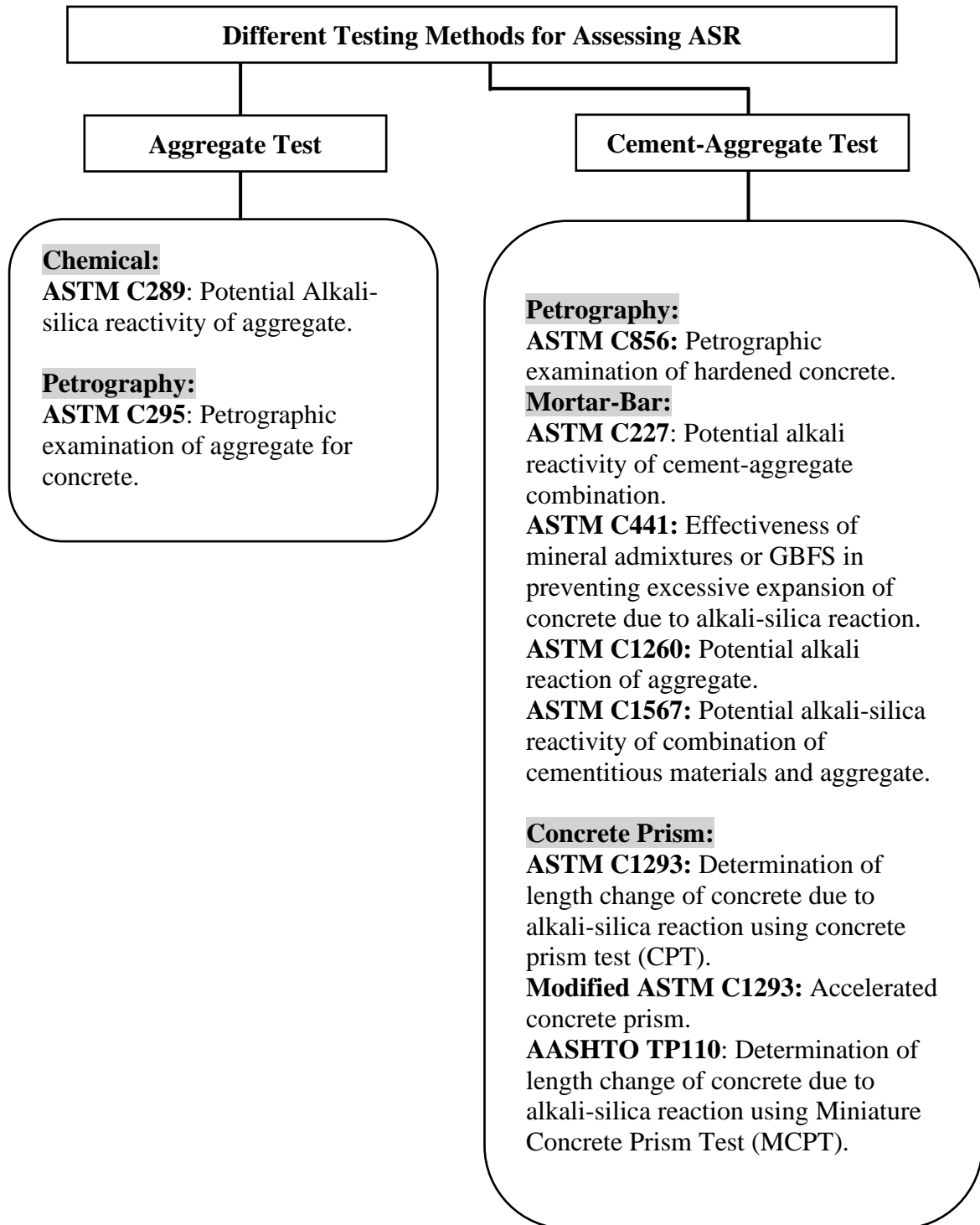


Figure 2.7 Different Testing Methods Used for Assessing Alkali-Silica Reaction

2.4.2 Accelerated Mortar Bar Test - ASTM C1260

The accelerated mortar bar test (AMBT), ASTM C1260, was invented in South Africa by Oberholseter and Davies in 1986 at the National Building Research Institute (NBRI), which was later approved in 1989, and revised/reapproved in 2007 as ASTM C1260 – 07. The test method involves the preparation of 1 in. x 1 in. x 11.25 in.) mortar samples following the standard aggregate gradation of ASTM C33 or ASTM C150 specifications. However, the autoclave expansion of the cement is limited to 0.20%. The test procedure is carried out by complete immersion of the samples in a sodium hydroxide (NaOH) at 80 oC (176 oF) for 14 days. The results are produced within 16 days from the casting date.

An expansion of less than 0.10% of the mortar bar is considered to be harmless, and that the aggregate is non-reactive and therefore more suitable for structures. Suppose the average expansion is between 0.10% and 0.20%. In that case, the aggregate is considered to be slow reactive, which indicates further testing should be done using other methods (CPT) or field performance should be incorporated into the determination of reactivity. An expansion greater than 0.20% is considered to be reactive and therefore deleterious. Some researchers – including Folliard et al. (2006), Malvar and Lenke (2006), and Jin (1999) -- concluded that the expansion threshold of 0.10% is inadequate to characterize some aggregates' susceptibility to ASR expansion; hence, Hooton (1991) proposed the extension of testing days to 28 days and 56 days with an expansion limit of 0.28% and 0.48% respectively, for proper classification of slow reactive aggregates.

The shortcomings of this test have been reported to include its aggressive approach, which may produce a false-negative, where test results show an aggregate as deleterious when its field performance is good, and false-positive result, where the test identifies an aggregate as not

deleterious but the aggregate is found to be reactive when examined using other tests or observed in the field (Folliard et al., 2006; Hooten, 1991). For example, Folliard et al. (2006) reported that four aggregates that passed the ASTM C1260 mortar bar test failed the 1-year ASTM C1293 test. Likewise, there are the false-negative cases of aggregates Gm-46c, Ad-130c, and Ad-174c, which were recently reported on by the Idaho Transportation Department (ITD) in its report on ASR (Gillerman & Weppner, 2014). These aggregates were reported non-reactive using the AMBT method but found to be reactive when the 1-year CPT method was used. Although many agencies widely accept this test method, a number of studies have indicated notable limitations (Bérubé et al., 2002; Bérubé & Fournier, 1993; Folliard et al., 2006).

One of the controversies associated with ASTM C 1260 is the test duration. For instance, Shi et al. (2015) concluded that 16 days of testing is sufficient to characterize aggregates with slow reactivity and Fernandez-Jimenez et al. (2007) also supported this recommendation, confirming that some aggregates (zeolite) exhibit greater expansion even before the end of 14 days (Fernández-Jiménez et al., 2007; C. Shi et al., 2015). This is contrary to the recommendation of Hooton (1991), noted earlier, for an extension of testing to 28 and 56 days. Likewise, Palacios and Purta (2006) also proposed an extension of testing time to 28 days and more. Another drawback to ASTM C1260 is the extensive crushing and aggregate treatment involved that alters the degree of expansion (Latifee & Rangaraju, 2015; Lu et al., 2008). Under this method, the test samples are subjected to an aggressive environment that includes high temperature and harsh curing medium (Bérubé, 1992). For example, Ideker et al. (2010) found that the expansion result of many tested aggregates is inconsistent with their field performance; this is because AMBT samples are subjected to a very harsh medium compared to what will

occur naturally in the field. Clearly, based on the highlighted shortcomings, the test procedure is problematic for job mix design or mitigation purposes. The overall finding is that this method should be utilized mainly to accept aggregates rather than eliminate them (Ideker et al., 2010; Thomas et al., 2006). These factors led to the development and adoption of the ASTM C1293.

2.4.3 Concrete Prism Test - ASTM C1293

One-Year Concrete Prism Test

The one-year CPT is a standard test method for determining the expansion of concrete over time using a concrete prism sample. This method was created to overcome the limitations of other testing types to assess aggregate susceptibility to ASR that incorporates a concrete test method rather than an aggregate test or mortar bar test. This test was developed by Gillott and Swenson (1969) during the 1950s in Canada, which involves the use of high-alkali cement with alkali content of $0.90\% \pm 0.10\%$ and the addition of sodium hydroxide to the mix water in order to raise the cement alkalis to 1.25%. A concrete prism formed from such a mix measuring 3 in. x 3 in. x 11.25 in. is cured in water for one full year at 100 oF. Expansion of less than 0.04% after 1 year is considered acceptable, whereas values above this are considered reactive; for mitigation purposes, concrete prism expansion of less than 0.04% for 2 years is considered acceptable. Unlike the AMBT method, this test method may be used to assess both fine and coarse aggregates using the concrete prism and without the excessive crushing that might distort the determination of reactivity. ASTM C1293 has been proven to be the most consistent and dependable of methods for quantifying reactivity (Ideker et al., 2010; Lu et al., 2008; Thomas et al., 2006).

The two major limitations of this test method are the long test duration, where the exposure of the concrete prism to the harsh condition of alkali for 1 year is impractical for specific short-

term projects' aggregate screening and ASR evaluation. The other limitation is alkali leaching. Researchers have shown that about 35% of the alkalis originally in the concrete prism leach out into the water storage over the term of the test (1 year), with about 20% leaching out after just 90 days (Rivard et al., 2003, 2007; Thomas et al., 2012). Such leaching potentially may skew the findings on ASR. To account for these issues, the method has been modified by boosting the alkali to 1.25% Na₂O_{eq} in the concrete specimen, as suggested by Thomas et al. (2006), and limiting the testing term to 13 or 26 weeks (Thomas et al., 2006). This evolved test method is called the Accelerated Concrete Prism Test (Thomas et al., 2006), which will be examined next.

Accelerated (6-Month) Concrete Prism Test

This method is a modification of the ASTM C1293 test introduced by Ranc and Debray (1992) to overcome the earlier highlighted shortcomings of the 1-year CPT method. The idea was to reduce the test duration from 1 year to just 6 months by subjecting samples to a more aggressive environment than the one required by the 1-year CPT. The test procedure maintains the high-alkali cement (alkali content of 0.90% ± 0.10%) and adds sodium hydroxide to the mix water to raise the cement alkalis to 1.25%. Similar to the 1-year CPT test, a sample size of 3 in. x 3 in. x 11.25 in. is prepared and cured in water for 6 months at 140 oF (60 oC). Other test periods have been suggested; for instance, a test period of 26 weeks within the expansion limit of 0.04%, was adopted by Latifee and Rangaraju (2015). Also, Thomas et al. (2006) found that the 3-month expansion results of the accelerated concrete prism tests showed good correlation ($R^2 = 0.9808$) with results from the extended 1-year concrete prism test.

For decades, the 14-day AMBT and the 1-year CPT have been generally adopted for ASR testing in mortar bar and concrete prism, respectively. However, the two methods were found to be inconsistent with one another. Therefore, there is a need for a well-validated method that

can be used to evaluate the susceptibility of aggregates to ASR within a reasonable timeframe. This gave way to the development of a new test procedure: AASHTO TP 110 – Miniature Concrete Prism Test (MCPT).

2.4.4 Miniature Concrete Prism Test – AASHTO T 380

The miniature concrete prism test (MCPT) method was developed by Latifee and Rangarajuin (2015) to overcome the challenges encountered when using the ASTM 1260 and ASTM 1293 test methods. The MCPT method has been found to provide good correlation with ASTM C1293 results as well as field performance (Latifee & Rangaraju, 2015). Also, the method is confirmed as providing reliable results on aggregate susceptibility to ASR (Latifee & Rangaraju, 2015). In achieving this reliable outcome through the new method, characteristics of AMBT and CPT were adequately modified; and the shortcomings of extended time duration, excessive crushing and treatment of fine aggregates (< 4.75 mm), high storage temperature of 80 0C (176 0F), and small test specimen size employed by ASTM C1260 (AMBT), were addressed. Likewise, ASTM C1293 (CPT) drawbacks, including the lower test temperature that requires a longer test duration and the storage of test specimens in a 100% RH environment that allows for alkali leaching from specimens, were accommodated through needed modifications.

The new test adopted the use of a concrete prism with the dimensions of 50 mm x 50 mm x 285 mm (2 in. x 2 in. x 11.25 in.), rather than the dimensions of 25 mm x 25 mm x 285 mm and 75 mm x 75 mm x 285 mm adopted in the ASTM C1260 and ASTM C1293, respectively, making the prism more suitable for assessing aggregate susceptibility to ASR within a more reasonable period (Latifee, 2013, 2016). Here, concrete prism expansion of less than 0.04% after 56 days is considered acceptable; values above this are considered reactive (see Table 2.3; Latifee et al., 2015; Latifee & Rangaraju, 2015). Furthermore, allowances are made for an

additional 28 days (for a total of 84 days) to determine any slow reactive aggregates. The MCPT adopted the storage of test specimens in sodium hydroxide solution to accelerate ASR used in the AMBT method. Likewise, it also implemented the beneficial features of the CPT method, such as boosting equivalent alkali to 1.25% in concrete and using the concrete prism instead of mortar bar specimen (Latifee & Rangaraju, 2015). In addition, to accelerate the ASR reaction, the test employed 25 mm (½ in.) maximum coarse aggregate size rather than 19 mm (¾ in.) maximum size (as used in CPT), without crushing the aggregates, as done in the AMBT. Table 2.3 summarizes the main features of the MCPT, and Table 2.4 describes the classification of aggregate reactivity for each test method (Latifee & Rangaraju, 2015).

Table 2.3 Mixture Proportions for the MCPT Specimen

Item Mix	Proportion
Specimen Size	2 in. x 2 in. x 11.25 in.
Test Duration	56 days – 84 days
Storage Temperature	60 °C (140 °F)
Storage Environment	NaOH Solution (Soak)
Initial Length (zero)	24 hrs. in H ₂ O @ 60 °C (140 °F)
Cement Type	420 kg/m ³
Cement Alkali Content	0.9% +/- 0.1 Na ₂ O _{eq}
Alkali Boost (Total Alkali Content)	1.25% Na ₂ O _{eq}
Coarse Aggregate (Dry Volume Fraction)	0.65
Coarse Aggregate	Maximum size of 12.5 mm (1/2 in.)
Coarse Aggregate Proportion (% by weight)	(1) 12.5 mm – 9.5 mm
	(2) 9.5 mm – 4.75 mm
12.5 mm – 9.5 mm	57.5%
9.5 mm – 4.75 mm	42.5%
Fine Aggregate	Determined based on ACI 211; Absolute Volume Method: $(1 - V_{H_2O} + V_{cg} + V_{cem})$
Water-to-Cement Ratio:	0.45

Note. Source: Bérubé & Fournier (1993).

Table 2.4 Classification of Aggregate Reactivity (Nixon & B. Fournier, 2017) ((Latifee & Rangaraju, 2015)

Reactivity	1-Year Expansion in CPT, %	14-Day Expansion in AMBT, %	56-day Expansion in MCPT, %
R0 Non-Reactive	≤ 0.04	≤ 0.10	≤ 0.03
R00 Slow/Low Reactive			$> 0.031, \leq 0.040$
R1 Moderately Reactive	$> 0.04, \leq 0.12$	$> 0.10, \leq 0.30$	$> 0.041, \leq 0.012$
R2 Highly Reactive	$> 0.12, \leq 0.24$	$> 0.30, \leq 0.45$	$> 0.121, \leq 0.240$
R3 Very Highly Reactive	> 0.24	> 0.45	> 0.241

2.5 Conclusions

This chapter reviewed the alkali-silica reaction (ASR) associated with concrete, focusing on its mechanism, effects, and evaluation methods for identifying and assessing it. ASR affects concrete's physical, chemical, and mechanical properties, causing excessive expansion, cracking, discoloration, exudation, and the eventual requirement of demolition of concrete structures. The multiple stages, dependence on many factors, complexity, and sluggish nature of the chemical reactions involved in ASR make it challenging to understand. Thus, the best way to address the ASR problem is by avoiding it at inception. This can be achieved namely by assisting material engineers, companies, departments of transportation (DOTs), and other relevant agencies to save millions of dollars required by the cost of repair and rehabilitation of structures associated with the impacts of ASR. Out of the many methods developed from 1940 to 2015 to assess alkali-silica reactivity, the ASTM C1260 and ASTM C1293 are the two most well-known and widely accepted standard test methods to characterize the potentials of aggregates to alkali-silica reaction. However, these methods have been proven from a research point of view to be dependable. The aggressiveness and extended time required of the ASTM

C1260 and ASTM C 1293 tests, respectively, made them unsuitable for some types of aggregates or projects. Therefore, evaluations of aggregates that employ these tests should be utilized solely to confirm those results obtained from a petrographic test or involve a blending of those results obtained from a petrographic test or involve blending two more methods to ascertain ASR susceptibility fully.

The development of a rapid and reliable method – the AASHTO TP 110 method – was discussed. This method arose from research that exposed the shortcomings of the various existing test methods, and it recognizes that there are many factors associated with alkali-silica reactivity that must be considered in testing methodology. The AASHTO TP 110 method (MCPT) has been proven to correlate with the 1-year CPT, fair correlation with the 14-day AMBT, and most importantly, strong correlation with the field performance of aggregates in concrete. These factors greatly bolster the MCPT method as a reliable and rapid predictor of aggregate alkali-silica reactivity.

Chapter 3: Experimental Investigation of ASR Mitigation Using Various SCMs Through Binary Mixtures

3.1 Introduction

The literature on mitigation of ASR is plentiful, with new experiments and research being performed every year. Over the years, cement has been one of the main forces in driving the economy and the industrial sector to its success. Recently, we have seen that research in supplementary cementitious materials has increased. With the advancement of technology and the available high-tech equipment, it is time to look for modern methods that not only mitigate deleterious reactions in concrete but also make it stronger. ASR is one of the major problems that occur in concrete in various places. The reasons for ASR might be due to using reactive aggregates or cement made with high alkali. The following sections summarize the previous effort that has been made in the area of ASR mitigation.

Farny & Kerkhoff (2007) have studied the mechanisms of alkali-silica reactions in cement and how it causes concrete to crack and expand. The cement mixture and aggregate have a high concentration of crystallized and amorphous (non-crystallized) silica, as it is a combination of different ores, rocks, and clay types. Some silica in the mixture is more susceptible to reactions or has a higher degree of reactivity than the others. When concrete is formed, moisture or water may run through its microscopic pores. This water, in the presence of cement metals like sodium, potassium, and calcium, forms an alkaline solution similar to the standard bar tests. This solution reacts with the amorphous silica molecules to form a gel that is very susceptible to water absorption. According to (Farny & Kerkhoff, 2007), the gel itself does nothing to harm the concrete; it is the water absorption that causes the gel to expand in

such a way that it puts the whole structure under stress and vulnerable to cracking. Therefore, if we need to protect a concrete structure from further damage in the case of deleterious ASR, then waterproofing the structure might save further damage to the structure.

Aquino et al. (2001) performed experiments on concrete aggregate mixtures using the ASTM C1260 standard for a period of twenty-one days. They used pozzolanic Silica fume (SF) and High Reactivity Metakaolin (HRM) in alkaline cement and aggregate mixtures to study the inhibiting effects of these SCMs in Concrete. They used American standards dipping the concrete bar in one molar sodium hydroxide solution and taking readings after periodic intervals. Their tests confirmed that the use of SCMs had played an essential role in the mitigation of ASR reaction since the expansion in concrete made with SF and HRM was significantly less than the control baselines of unadulterated Concrete. It showed that metakaolin could be used to inhibit ASR in concrete and if the 7-day test would produce similar results. Moreover, by doing X-ray analysis, they found out that the calcium in the concrete increases with time as the ASR progresses. The increase in calcium content in the concrete mixture is a byproduct of the alkali-silica reaction that slowly consumes the silica in concrete with the aggregates in the presence of an alkaline solution.

Justyna (2017) also tested the properties of high reactivity metakaolin in limiting the corrosive action caused by the alkali-silica reactions in Concrete. Justyna found out that some of the pozzolanic materials had properties that helped in stopping the ASR from happening. When Metakaolin was mixed in percentages of 5-20%, it produced results that showed a significant reduction in ASR activity in concrete mortar bars and through thermogravimetric analysis (TGA). Mixtures of cement mortar that had at least 5% Metakaolin showed a decrease in ASR as it depleted the calcium hydroxide concentration in Concrete, making the solution

less alkaline and reducing aggregate reactivity. However, to establish a safe level in concrete expansion, the concentration of Metakaolin was increased to about 20% in the mortars. This level of Metakaolin showed test results that were under safe levels in the Accelerated Mortar Bar Test. Thus, metakaolin is effective in stopping ASR in percentages of 20% or more.

Ke, et al. (2018) used waste glass powder as a supplementary cement material to study the effects of mitigation in ASR in Concrete. Waste glass comprises of ground glass particles that are used to strengthen cement mixtures producing weather-resistant Concrete. The waste glass is ground to microparticles of sizes in the range of 300 μm or less. The study observed that glass particles greater than 300um were not effective in mitigating ASR but played a role in worsening the reaction by increasing the calcium present in Concrete. The study concluded that microparticles of glass powder less than 300 μm (ideally from 38-58 micrometers), when mixed in 20% of the mass of cement mixture, were effective in mitigating the adverse ASR reaction in Concrete.

Kara De Meijer (2014) studied the use of waste glass powder as an environment friendly material in Portland cement mixtures to mitigate the effects of ASR in concrete. According to the author, waste glass in itself will not mitigate ASR in Concrete, but when finally ground to less than 150 μm , it has the potential to stop ASR in concrete structures just like other pozzolanic supplementary cement materials used in Concrete. Waste glass powder, when ground to a slurry with very tiny particles, showed cementitious properties. The best results were shown when the glass powder was finely ground to particles of size 10 micrometers or less; it showed results similar to other mainstream pozzolanic materials, and the reactivity of ASR was mitigated.

Lipatov et al. (2015) studied the properties of basalt glass melted down into basalt fibers of sizes of around 20 μm and studied its alkali resistance and fiber strength properties. The study found that when basalt fibers were subjected to an alkaline solution, a protective layer of material was formed on the fibers that significantly increased its alkali resistance and made the material more resistant to tensile stresses. The fibers were mixed with a zirconium silicate powder, and the study found that basalt fibers significantly increased the alkali resistance of the mixture and its strength. The study also proved the benefits when including basalt fibers in concrete for mitigating ASR.

Haddad et al. (2004) Performed research on the properties of concrete made with propylene fibers, which describes as fibers of steel coated with a layer of resistance material like brass and subjecting it to chemical solution tests for 25 days and then 85 days. The study found out that although the fibers did not mitigate the ASR and cracking in concrete in the long run, the process was delayed by introducing propylene in concrete. Moreover, the tensile strength of concrete samples showed noticeable improvement. The cost of mixing these elements in concrete is small compared to its advantages.

Guo et al. (2018) studied the alkali resistance of basalt fibers in concrete and its effects on the structural integrity of the system. The study was performed in China, where concrete was reinforced by the Basalt fibers while also studying the mitigating effects of fibers on ASR. The study found out that basalt fiber reinforced concrete did not affect the compressive strength of Concrete, but the flexural and tensile moduli showed noticeable improvements. The fibers also reacted to changes in temperature and alkalinity of the experimental environment, but overall, the results needed more investigation and research.

Moisture accompanied by other aggregates that are reactive is the factor needed for ASR occurrence. That means its elimination reduces ASR occurrence. Studies on the elimination of water content from concrete are discussed to get a deeper understanding of the mechanic of ASR.

Hobbs (1988) studied the content of water availability in concrete and how to control it. The study found out that the water from the drainage system was harmful to the underlying concrete structure. It must be ensured that the water drains away from a concrete element rather than through parts of it or into the structure itself. De Beauchamp (1995) indicated that there is a membrane that is waterproof like Polyvinyl chloride, which has been applied on the concrete dams hence being protected from ingress of water inside concrete structures.

Durand (1995) reported that when construction Joints or macro cracks are being filled with cement epoxy or grout resins, structural continuity can be restored. The water penetration, as well, to the ASR affected areas could be limited, as indicated in (Charlwood and Solymar's, 1995) research. The filling is also commonly done right before you apply a sealing that is waterproof or a water repellent agent. However, once a structure starts showing signs of ASR reaction, the deleterious reaction cannot be permanently stopped. It usually reappears as the concrete has already absorbed enough moisture to restart the ASR.

Bérubé et al. (1987 and Ishuzuka et al., (1989) indicated that when flexible modern grouts are injected for leakage prevention through cracks or joints in a concrete structure in which the expansion of ASR is still ongoing, it can be more effective compared to epoxy resins.

A lot of conducted research has indicated that ASR remains constant or continues to grow when its internal humidity is 80- 85 percent or higher (Stark, 1990). Stark's research also showed that thin elements of concrete are rarely likely to be impacted by ASR, especially when

they are kept in dry outdoor or indoor conditions. There has to be no moisture supply from outside. And when they are immersed in seawater or freshwater due to alkalis in the pore fluid of concrete leaching. But when it comes to substantial concrete members, they are occasionally at risk of contracting ASR, including the concrete in arid areas due to the high humidity maintained (Stark and Depuy, 1987).

When preventing water penetration for an extended period, surface film coatings like water repellent agents and polyurethane, i.e., water-based silicates, are ineffective (Putterill et al. 1985). Hobbs (1988) researched the cracked piers which offer support to the expressway in Japan, and in his study, the docks were repaired when they were seven years old. It was done through cracks filling using epoxy resin, which was injected with pressure, and they coated with saline impregnation or epoxy resin and, finally, the topcoat where polymer cement paste was utilized. His conclusion was that this method was not as active. It just had a delayed effect because after some years of wide exposure, cracks were observed in (1989) also indicated that crack injection to eliminate humidity and surface coating on structures was ineffective, and it had limited results.

3.2 Experimental Program

The primary goal of this study was to investigate the effectiveness of different supplementary cementitious materials in inhibiting ASR in concrete. The SCMs included in the experimental work were Metakaolin and waste glass powder, in addition to basalt fiber, and lithium as an additional admixture. The Accelerated Mortar Bar Test ASTM 1260 was used to determine the effects of the implementation of those SCMs on ASR expansion. The control mixtures were made of 100% highly alkaline cement and fine reactive basalt aggregate without the inclusion of SCMs. The main objective of the experimental work was to perform intensive ASR testing

of binary and ternary concrete mixtures. Those mixtures have been prepared by incorporating a high percentage of waste-by-product, lithium admixtures, and basalt fibers in binary and ternary mixes. The study results should answer the “why” question, which is determining the optimum percentage(s) of the SCMs that inhibit or prevent ASR in concrete using the ASTM C1260-7 procedures. The following section presents details of materials, mixture design, and testing procedures.

3.1.1 Materials

Raw materials were selected carefully according to their chemical composition to achieve the desired reduction of ASR, as shown in Figure 3.1. Thus, the best way to stop or reduce ASR is through prevention. Defining nonreactive concrete blends should break the chemical interaction between the alkali, silica, and water during the concrete mixtures' design stage.



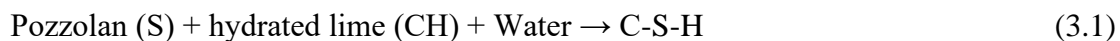
Figure 3.1 Alkali Silica Reaction Triangle (Concrete Cracking – A Destructive Kind)

Various supplementary cementitious materials (SCMs) have been identified in this study for further investigation as ASR mitigation materials. The materials used were Metakaolin, waste glass powder, basalt fibers, NewCem-Plus, and Lithium admixture. They were selected because they are in the market and they are not fully implemented in concrete mixtures, the author

thought that it worth to study those materials (MK, GP, NewCem Plus) in combinations to see their effect in helping ASR mitigation. Moreover, these materials are economically viable and can be integrated into concrete on a large scale without adding much cost, mainly because some of the SCMs chosen for this research are waste by-products. The Metakaolin and waste glass powder are identified as pozzolanic materials with a pozzolanic reaction due to the size of their particles that is, on average less than $100 \mu m$. There are three conditions to be met for a material to be pozzolanic: High silicate content ($SiO_2_{eq} = SiO_2 + Al_2O_3 + Fe_2O_3$), amorphous structure, and large surface area, Glasser F.P (1992). All three of those conditions are identical for the Metakaolin and glass powder, as shown in Table 3.1. In addition, due to its high alkalinity ($ph > 12.5$), concrete pore solution provides a strong medium of dissolution of the amorphous silicates, which helps accelerate the pozzolanic reaction.

The pozzolanic reaction is a reaction between silicates and $Ca(OH)_2$, which is a cement hydration byproduct. Pozzolanic materials chemically react in similar behavior to the cementitious materials adding more strength to the concrete over a long-time. When a chemical reaction occurs between water and a pozzolan or cement or hydrated lime, calcium-silicate-hydrates (C-S-H) form, as shown in (Equation 3.1). C-S-H is the main binder phase and the source of strength in concrete.

The formation of C-S-H causes depletion of Alkali ions in hydrates and reduces ASR. This process is defined as alkali binding, which reduces calcium and silica ratio and facilitates a higher percentage of alkali ions for entrapment.



The calcination of pure kaolinite produces metakaolin. The structure of Metakaolin is based on the purity of kaolin and the temperature of calcination. SCMs such as metakaolin are richly

composed of SiO₂ or silica and Al₂O₃ or alumina (Table 3.1). Also, it has been observed that metakaolin has a higher Alumina (Al₂O₃) composition compared to other SCMs such as slag and fly ash. The author has chosen Metakaolin as an ASR potential inhibitor because there is limited research that has been done in this area. In addition, Metakaolin is composed of reactive silica that can react with OH ions present in the concrete pore solution to produce the C-S-H phase and promotes alkali ions trap.

Furthermore, Metakaolin reduces the rate of reaction between alkali and reactive aggregate. The reactive silica presents in Metakaolin can react with aluminum and produces aluminosilicate. These aluminosilicates are stable under alkali and act as a passivation layer. This passivation layer is responsible for stopping the further dissolution of reactive silica and mitigating ASR. Finally, SCMs such as Metakaolin and glass powder increase the surface area of SiO₂, which results in decreasing OH ions concentration at the aggregate surface. This mechanism slows down the dissolution rate of aggregate. It lowers the availability of OH ions at the surface of aggregate per unit silicate area, resulting in a lower ASR rate.

NewCem Plus is a relatively newly developed cement introduced to the concrete industry by Lafarge Inc. NewCem-Plus, a blend of fly and ground granulated blast furnace slag (GGBFS). It has specifications that exceed the requirements of ASTM C1697 for blended SCMs. This type of new blended cement has superior performance in terms of strength, compatibility with admixtures, and suitability for various concrete applications. The chemical compositions of NewCem-Plus are shown in Table 3.1. Its performance in mitigating ASR is not investigated yet. It combines the benefits of pure Portland cement, fly ash, and slag as SCMs.

In general, using SCMs tends to control ASR based on the work cited from the literature, but they may decrease compressive strength (Toutanji et al.2004). Therefore, lithium (Li) has been

used as an additional chemical admixture in some mixes to enhance the compressive strength. Table 3.1 shows the chemical composition of used SCMs.

On the other hand, Portland cement contains a high percentage of lime CaO, which promotes the Alkali reaction (Toutanji et al., 2004) with a lower percentage of amorphous silicates. Therefore, it would be effective to replace cement with another material that has low CaO in its chemical composition. As shown in Table 3.1, the chemical composition of Metakaolin, glass powder, and basalt fibers show low weights of CaO, and a high percentage of SiO₂. Various research has been done to investigate the effect of implementing low alkali materials as cement replacements to find the relationship between alkali/silica compounds and the mechanical properties of concrete.

Table 3.1 Chemical Composition of used SCMs ((Islam et al.2017) (H. Hu, Y. Liu, 2010, p.329-386)
(See Appendix A.2))

Material	Chemical Composition	Percentage (%)	Particle Size
Portland Cement	CaO	60 – 67	7 -200 μm
	SiO ₂	17 – 25	
	Al ₂ O ₃	3 - 8	
	Fe ₂ O ₃	0.5 – 6	
Metakaolin	SiO ₂	50 - 55	2 μm
	Al ₂ O ₃	40 - 45	
Glass Powder	SiO ₂	68	200 μm
	CaO	14.5	
	K ₂ O	0.8	
Basalt Fibers	SiO ₂	51 - 59	N/A
	Al ₂ O ₃	14.6 – 18.3	
	CaO	5.9 – 9.4	
	MgO	3 – 5.3	
NewCem-Plus	CaO	15	12.34 μm
	Other Alkali	2.5	
	SO ₃	3	

3.1.2 *Mix Design*

The control concrete mixture was designed following ASTM C1260 to achieve 7500 psi compressive strength at 28 days. All mixtures were made using Type I Portland cement according to ASTM C150. The cement and water contents were 440 kg/m³ and 207 kg/m³, respectively. The water-to-cement ratio (w/c) was 0.47. Basalt aggregate with five different particle gradings of 2.36 mm, 1.18 mm, 600 μm, 300 μm, and 15 μm were used.

Twenty-six different concrete mixtures were prepared by replacing cement with Metakaolin (MK), Glass Powder (GP), Lithium (Li), NCP, and Fibers using different replacement ratios (10%, 20%, and 30%). Table 3.2 illustrates the details of the mix design. Specific gravities (G) were used to determine the required quantities. Metakaolin has a specific gravity of 2.30; Glass Powder has G of 2.73; NCP has G of 2.75 and 2.65 for Basalt fibers

Table 3.2 Details of the Mix Design

MIX	Description		Fine Aggregate (Basalt) (kg/m ³)					Water (lit)	Cement (kg/m ³)	Admixtures (NaOH) (kg/m ³)	MK (kg/m ³)	GP (kg/m ³)	NCP (kg/m ³)	Li (lit)	Basalt Fibers (kg/m ³)
	Description	Cement Replacement %	2.36 mm	1.18 mm	0.600 mm	0.300 mm	0.150 mm								
1	Control	0%	124	235	235	235	161	207	440	4.37	0	0	0	0	0
2	MK	10%	124	235	235	235	161	207	396	4.37	32.12	0	0	0	0
3	MK	20%	124	235	235	235	161	207	352	4.37	64.25	0	0	0	0
4	MK	30%	124	235	235	235	161	207	308	4.37	96.36	0	0	0	0
5	GP	10%	124	235	235	235	161	207	396	4.37	0	38.13	0	0	0
6	GP	20%	124	235	235	235	161	207	352	4.37	0	76.26	0	0	0
7	GP	30%	124	235	235	235	161	207	308	4.37	0	114.40	0	0	0
8	GP+ MK	10%	124	235	235	235	161	207	396	4.37	16.06	19.06	0	0	0
9	GP+ MK	20%	124	235	235	235	161	207	352	4.37	32.125	38.13	0	0	0
10	GP+ MK	30%	124	235	235	235	161	207	308	4.37	48.18	57.20	0	0	0
11	NCP	10%	124	235	235	235	161	207	396	4.37	0	0	38.41	0	0
12	NCP	20%	124	235	235	235	161	207	352	4.37	0	0	76.82	0	0
13	NCP	30%	124	235	235	235	161	207	308	4.37	0	0	115.24	0	0
14	Li	0%	124	235	235	235	161	207	440	4.37	0	0	0	0.13	0
15	MK + Li	10%	124	235	235	235	161	207	396	4.37	32.12	0	0	0.13	0
16	MK + Li	20%	124	235	235	235	161	207	352	4.37	64.25	0	0	0.13	0
17	MK + Li	30%	124	235	235	235	161	207	308	4.37	96.36	0	0	0.13	0
18	GP + Li	10%	124	235	235	235	161	207	396	4.37	0	38.13	0	0.13	0
19	GP + Li	20%	124	235	235	235	161	207	352	4.37	0	76.26	0	0.13	0
20	GP + Li	30%	124	235	235	235	161	207	308	4.37	0	114.40	0	0.13	0

MIX	Description		Fine Aggregate (Basalt) (kg/m ³)					Water (lit)	Cement (kg/m ³)	Admixtures (NaOH) (kg/m ³)	MK (kg/m ³)	GP (kg/m ³)	NCP (kg/m ³)	Li (lit)	Basalt Fibers (kg/m ³)
	Description	Cement Replacement %	2.36 mm	1.18 mm	0.600 mm	0.300 mm	0.150 mm								
21	NCP + Li	10%	124	235	235	235	161	207	396	4.37	0	0	38.41	0.13	0
22	NCP + Li	20%	124	235	235	235	161	207	352	4.37	0	0	76.82	0.13	0
23	NCP + Li	30%	124	235	235	235	161	207	308	4.37	0	0	115.24	0.13	0
24	Fibers	1.5%	124	235	235	235	161	207	440	4.37	0	0	0	0	5.55
25	Fibers	2.5%	124	235	235	235	161	207	440	4.37	0	0	0	0	11.10
26	Fibers	3.5%	124	235	235	235	161	207	440	4.37	0	0	0	0	16.65

- 180 g of NaOH has been used for soak solution
- 4050 ml of water has been used for soak solution
- 270 ml of distilled water has been used for soak solution

3.1.3 Testing Procedures

In order to measure the effectiveness of ASR mitigation methods, it is possible to use any test available in the civil engineering literature. Since the mitigation methods vary across regions, determining their effectiveness plays a vital role in confirming the overall competency of these methods. The main test method used in this study was the ASTM C1260-7 (14-day AMBT), which is known as the accelerated mortar bar test. It is used to measure expansion due to ASR under severe accelerated environmental exposure.

3.1.3.a Accelerator Mortar Bar Test

The ASTM C1260-7 belongs to the family of accelerated mortar bar tests or AMBTs researched by South African civil engineers in 1986. The test takes a total of 14 days to execute and involves the immersion of cement bars in one molar sodium hydroxide solution. This test helps in identifying and assessing the reacting agents in concrete aggregates that are causing ASR. All national and international standards of the AMBTs are based on the National Building Research Institute (NBRI), which is the original source of the mortar bar test method. The different tests in this family are the American ASTM C1260, the AMBT RILEM AAR-2, the British DD249 method of AMBT, and the Canadian CSA method. These tests are based on the AMBT technique, but they have slight differences in terms of execution time and severity of the exposure.

To conduct this test, three mortar bars of 1.0 x 1.0 x 11.5 in. were immersed in a hydroxide solution. The bars were made only from cement mortar, where aggregate and cement were mixed in the presence of water and allowed to harden in a steel mold. They were then exposed to water for one day to establish the standard initial dimension that was used for expansion calculations afterward. The three bars were then immersed in a NaOH solution under a

temperature of 80 °F throughout the procedure. The test continued for 14 days, during which the cement bars were taken out at pre-specified intervals for the purposes of taking measurements. The results of the tests were then evaluated using the guidelines given in the ASTM (Lenke et al., 2009).

Currently, the AMBT C1260 is one of the best tests available because it accurately measures the effect of ASR inhibitors in concrete mixtures and because it has a short execution time. The AMBT C1260 takes 14 days to show results that are similar to those of the 56-day Miniature Concrete Prism Test (MCPT). The MCPT might take an additional 28 days to show results if the aggregates are slower in reactivity. The test results based on AMBT and MCPT are closely correlated, and AMBT is the more efficient one. More importantly, we were using fine aggregates in this experimentation phase; given this, AMBT was determined to be the most suitable test for evaluating fine aggregate samples. The 56-day MCPT is vital for future research of coarse aggregate samples as well. The 14-day AMBT cannot be used for coarse aggregates (Lu et al., 2006).

3.1.3.b Flow Test

The ASTM C1437 flow test was used to measure the workability of the mortar samples. Workability or flow is the measure of the ease with which the mortar could be set. A sample with more flow percentage is easier to work with during construction. The flow test used is specified in the ASTM standard C1437 (ASTM, 2007). For this test, the mortar of the sample mixture was placed inside a mold and pressed to ensure uniformity of edges. A clean tabletop was prepared with measurement scales to record any changes in mortar mass. The mortar was placed in the center, and the mold was lifted. Disturbances were introduced in the system for 15 seconds to ensure the spread of mortar mass. Afterward, changes in diameter were measured

with a caliper and recorded in two perpendicular directions. The flow was calculated as a percent increase in diameter.

3.1.3.c Compression Test

The ASTM C109/C109M test was used to measure the compressive strength of the concrete to determine its load bearing capabilities. The mortar was made and set into molds of size of 2 in. x 2 in. x 2 in., with the control mixture having no additives. Afterward, mortars were prepared with SCMs and also tested according to the test specifications

The prepared concrete specimens were placed inside the holding plates of a hydraulic press with a reading scale to record force in pounds per square inch. To ensure the uniform spread of compressive force, the upper platen of the machine was placed on a spherical bolt so that it could be adjusted to any tilt in the specimen surface. The hydraulic press increases force gradually until the concrete sample breaks. The maximum applied force was recorded and was tabulated for analysis.

3.1.4 Methodology

The cement in all mixtures was replaced with all four percentages of additives or SCMs (i.e., 0%, 10%, 20%, and 30%). The first batch of 20 bars was made without adding the additives to establish control parameters. After the mortar bars were removed from molds, they were subjected to a water solution for 24 hours. The water was kept at a steady 80 °F. Afterward, the bars were immersed in one molar sodium hydroxide solution for the period of the time of the test, which was 7-14 days in this case. After periodic intervals, the bars were taken out, and readings of length change were conducted to measure expansion changes according to Eq. 5.1. The results were then tabulated for analysis.

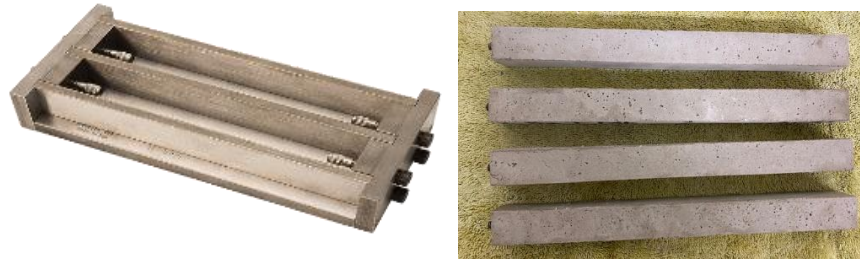


Figure 3.2 Mold Used for Mortar Bar Preparation of 1 in. x 1 in. x 11.5 in

An expansion in the dimension of the mortar bars greater than 0.13% would constitute a failure to stop the ASR reaction of the detrimentally reactive aggregate with the alkaline solution. The expansion parameter of the mortar bars was reduced to 0.06% to determine a safe level. The results of the 14-day tests were comparable to the 1-year and 2-year Concrete Prism Tests (CPT), performed using similar procedures (Lenke et al., 2009). The formula used to measure concrete expansion is shown below, where the percentage of length change in the test specimens at any age (X days) is:

$$L\% = \frac{Lx - Li}{G} \times 100 \quad [\text{Eq. 3-2}]$$

Where, L = Change in Length at X Days, %

Lx = Comparator Reading of Test Prism at X days minus the Comparator reading of the Reference Bar at X Days.

Li = Comparator Reading of Test Prism at Zero Day minus the Comparator reading of the Reference Bar at Zero Day.

G = Nominal Gauge Length, 10 in.

For measurement of the reactivity of the concrete mixtures, Table 3.4 was used as a guideline. The 14-day expansion using AMBT criteria was used in this study, where results show non-reactive ingredients if the expansion stays below 0.1%; where with a range of 0.1% to 0.3%,

the reactivity is classified as moderate; and anything above that is termed highly and very highly reactive (see Table 3.4).

The first batch of cement mixture was made up of the control mixture only; alkali cement and fine basalt aggregate were used. This mixture was used to establish a control case for the baseline test. The mixture was allowed to settle in the rectangular molds according to the AMBT using ASTM C1260 standards. The bars were immersed in one molar sodium hydroxide solution for 14 days, and data was collected at periodical intervals by measuring the bars' length change. For this to be a successful baseline test, the concrete bars must expand beyond the safety level of 0.1% in 14 days to ensure that the aggregate and the cement were producing sufficient ASR.

The next step was to include the SCMs in the cement mixtures one at a time to test their individual effect on the reactive elements inside the concrete mixture. The first group of mortar bars was produced by mixing the prescribed quantity of waste glass powder with the cement and aggregates (Table 3.2). The mixtures were prepared by repeating the process with different waste glass powder replacements as in the control test.

The second group was made with Metakaolin with the same percentage of cement replacement. The third one was made by adding basalt fibers at various percentages. The fourth group was prepared using a combination of waste glass powder and Metakaolin (binary mix) to study the combined effect of these two SCMs on the reactivity of aggregates used. The rest of the procedure was repeated similarly for the other SCMs with different percentages of cement replacements. The test results were tabulated and compared for the calculation of the results.

Table 3.3 Experimental Program

Group	Specimen	Variables	Cement Replacement	Alkali Silica Reaction (Mortar Bars)	Compressive Test (Cubes)			Workability (Base-Flow Test)
					7 Days	14 Days	28 Days	
A	1	Control	0%	4	3	3	3	Once/Batch
	2	MK	10%	4	3	3	3	
	3	MK	20%	4	3	3	3	
	4	MK	30%	4	3	3	3	
B	5	GP	10%	4	3	3	3	Once/Batch
	6	GP	20%	4	3	3	3	
	7	GP	30%	4	3	3	3	
C	8	GP+ MK	10%	4	3	3	3	Once/Batch
	9	GP+ MK	20%	4	3	3	3	
	10	GP+ MK	30%	4	3	3	3	
D	11	NCP	10%	4	3	3	3	Once/Batch
	12	NCP	20%	4	3	3	3	
	13	NCP	30%	4	3	3	3	
F	14	Li	N/A	4	3	3	3	Once/Batch
G	15	MK + Li	10%	4	3	3	3	Once/Batch
	16	MK + Li	20%	4	3	3	3	
	17	MK + Li	30%	4	3	3	3	
H	18	GP + Li	10%	4	3	3	3	Once/Batch
	19	GP + Li	20%	4	3	3	3	
	20	GP + Li	30%	4	3	3	3	
I	21	NCP + Li	10%	4	3	3	3	Once/Batch
	22	NCP + Li	20%	4	3	3	3	
	23	NCP + Li	30%	4	3	3	3	
J	24	Fibers	1.5%-Fibers (0.2 g)	4	3	3	3	Once/Batch
	25	Fibers	2.5%-Fibers (0.3 g)	4	3	3	3	
	26	Fibers	3.5%-Fibers (0.4 g)	4	3	3	3	
Total No. of Specimens				112	84	84	84	
				112 Mortar Bars	252 Cubes			

Table 3.4 Reactivity Tables (Nixon & B. Fournier, 2017) ((Latifee & Rangaraju, 2015)

Reactivity	One-Year Expansion in CPT %	14-Day Expansion in AMBT %	56-Day Expansion in MCPT %
R0 Non-Reactive	≤ 0.04	≤ 0.10	≤ 0.03
R00 Slow/Less Reactive			$> 0.031, \leq 0.040$
R1 Moderately Reactive	$> 0.04, \leq 0.12$	$> 0.10, \leq 0.30$	$> 0.041, \leq 0.012$
R2 Highly Reactive	$> 0.12, \leq 0.24$	$> 0.30, \leq 0.45$	$> 0.121, \leq 0.240$
R3 Very Highly Reactive	> 0.24	> 0.45	> 0.241

3.2 Experimental Test Results

3.2.1 Accelerator Mortar Bar Test Results

Group A (Control Specimen)

The control test was performed without adding any additives to observe concrete expansion when subjected to the NaOH solution for 14 days. The concrete bars showed an expansion of 0.425% on the 14th day, which exceeded the ASTM threshold value of 0.10%. This was expected due to the active aggregate, and the alkali cement included. This degree of expansion is considered unsafe for the structural integrity of the concrete. The 14-day trend of rising expansion over time is shown in Figure 3.3. Table 3.5 shows the average expansion of the four bars tested and the standard error in 14 days of measurements with a coefficient of variation of 4.51% despite the smaller number of specimens.

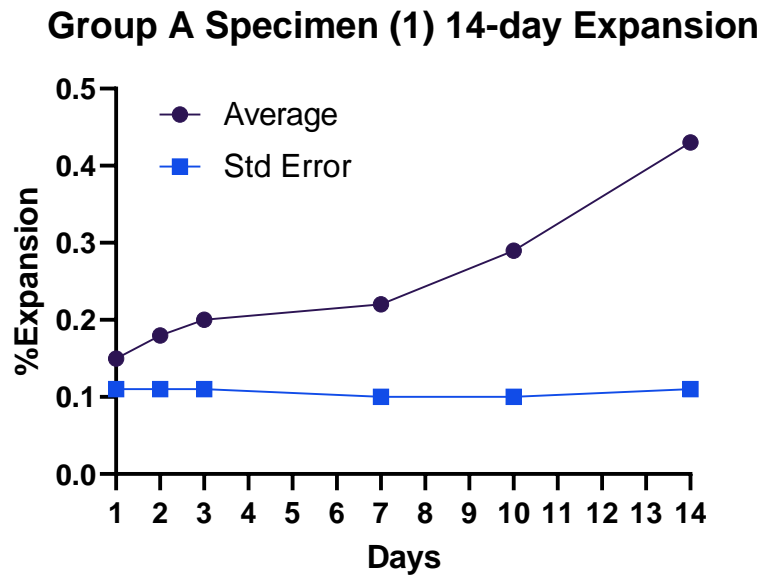


Figure 3.3: The 14-day AMBT expansion rate for the control specimens

Table 3.5 Fourteen-day expansions, standard deviations, and coefficients of variation for Group A (Specimen 1) mixtures

Mixture	Avg 14-day expansion (%)	Standard errors in 14-day measurement	Coefficient of variation (%)
1	0.425	0.011	4.51

Group A (Specimen 2, 3, &4)

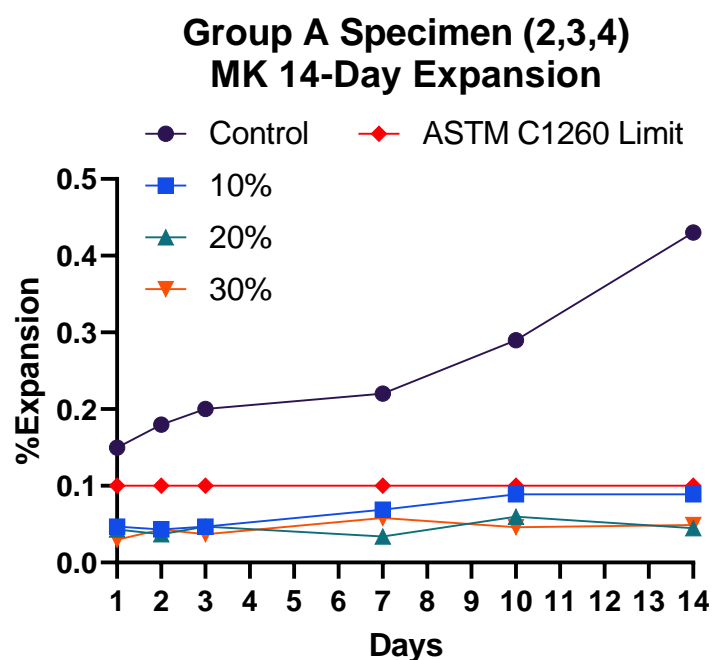


Figure 3.4 The 14-day AMBT expansion rate for Metakaolin as SCM

Table 3.6 Fourteen-day expansions, standard deviations, and coefficients of variation for Group A (Specimen 2,3,and4) mixtures

Mixture	Avg 14-day expansion (%)	Standard errors in 14-day measurement	Coefficient of variation (%)
2	0.0890	0.0024	2.64
3	0.0450	0.0042	9.43
4	0.0490	0.0019	3.82

Metakaolin has a very fine particle size that ranges between 1-2 μm (Figure 3.5). All the samples with 10% MK, 20% MK, and 30% MK cement replacement showed signs of significant ASR reduction and kept the concrete's expansion under the ASTM safe level of 0.100% (Table 3.6). As noted, without the addition of any SCM, the control sample of concrete showed an expansion of 0.425% (see Figure 3.4). In the samples with 10%, 20%, and 30% where Metakaolin was added, the expansion was 79%, 89%, and 88% less than that of the control specimen. Metakaolin significantly reduced the ASR in concrete samples, as shown in Figure 3.6. The highest coefficient of variation was for mix 3 (20% replacement), and the lowest was for mix 2 (10% replacement) (Table 3.6).



Figure 3.5 Metakaolin as SCM

Group B (Specimens 5,6, &7)

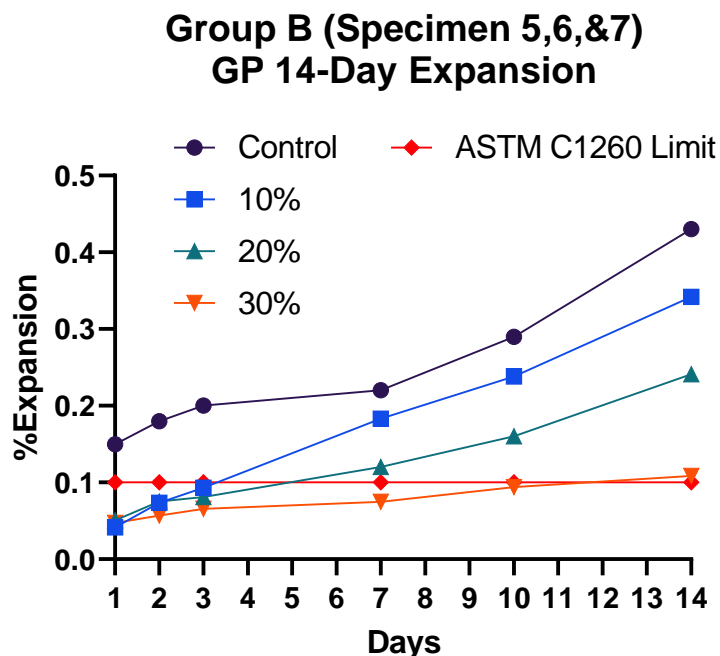


Figure 3.6: The 14-day AMBT expansion rate for Glass Powder

Table 3.7 Fourteen-day expansions, standard deviations, and coefficients of variation for Group B (Specimen 5,6, &7) mixtures

Mixture	Avg 14-day expansion (%)	Standard errors in 14-day measurement	Coefficient of variation (%)
5	0.342	0.0074	2.17
6	0.241	0.0035	1.47
7	0.108	0.0012	1.15

The microparticles of waste glass powder were used in three different percentages for mixtures five, six, and seven under group B, as SCM replacement of cement. Figure 3.6 shows that glass powder alone is not a good SCM for controlling ASR from spreading in concrete. All samples with 10% to 30% GP replacements exceeded the threshold limit starting at the age of three days (Figure 3.6) by the 14-day mark. However, the specimens containing 30% GP as replacement of cement slowed the ASR gel formation around the aggregate particles. Still, the implementation of glass powder is classified as moderate reactive materials and not

recommended to mitigate ASR by itself. The very high percentage of silicates that exist in the glass powder might be the reason for activating the ASR. The GP and the calcium hydroxide react and produce additional C-S-H that reduces CH, and a higher content of GP lowers the alkalinity of the concrete pore solution. The particle size of GP has a great effect on the production of C-S-H and on the ASR potential. The GP decreased the expansion compared to control specimens by 20%, 43%, and 75% at the 10%, 20%, and 30% replacement levels, respectively (Table 3.7). The 30% replacement level expansion was barely close to the ASTM 1260 limit, while the other replacement percentages exceeded that limit. It can be concluded that GP of 30% replacement level is strongly recommended to control ASR.

Group C (Specimens 8, 9, &10)

The last stage of experimentation was performed by incorporating two SCMs into a single mixture (binary mixtures) of concrete to study their combined effect. The AMBT tests showed a reduction in alkali reactivity of aggregate particles due to the presence of Metakaolin that was comparable to the test results achieved with the addition of only a single MK. Samples with 20% and 30% MK/GP combined ratios were successful in mitigating the harmful ASR in concrete. However, it must be noted that the sample with very fine microparticles of glass powder mixed with Metakaolin at a 10% ratio was not effective in reducing ASR expansion. In that sample, the safety limit was crossed at day 7, as shown in Figure 3.7. The standard error at 14 days was found to be .0048, 0.028, and 0.042 for mixtures 8, 9, and 10, respectively, as shown in Table 3.8. Mixtures 9 and 10 showed a significant reduction of ASR by 86% and 90% for the 20% and 30% replacement levels, respectively (Table 3.8). The binary mixtures of

GP+MK at the 20% and 30% levels were more effective than the individual mixtures of MK or GP in reducing the ASR below the threshold limit.

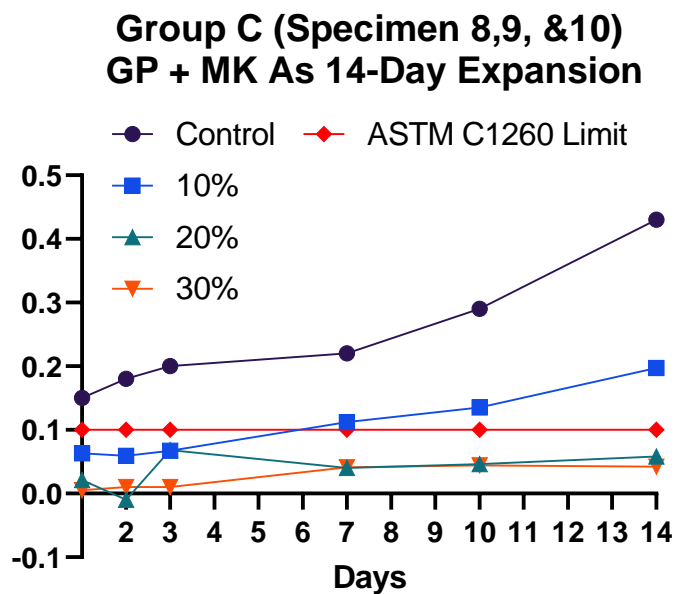


Figure 3.7: The 14-day AMBT expansion rate for Metakaolin-Glass Powder Samples

Table 3.8 Fourteen-day expansions, standard deviations, and coefficients of variation for Group C (Specimen 8, 9, and 10) mixtures

Mixture	Avg 14-day expansion (%)	Standard errors in 14-day measurement	Coefficient of variation (%)
8	0.197	0.0048	2.42
9	0.058	0.028	48.6
10	0.042	0.042	0.010

Group D (Specimens 11,12, &13)

NewCem Plus (NCP) is an additive material for cement mixtures produced commercially by Lafarge Industries. It is a blend of ground blast furnace slag and Class F fly ash mixed in an equal proportion (Figure 3.8). Literature on the use of NewCem Plus as a mitigator of ASR is still limited and vague. The product NewCem is believed to improve the properties of concrete

by making it stronger and more durable. NCP was tested in this study as a potential solution to mitigate ASR in concrete as one of the SCMs. The concrete bars with added NCP showed no reduction in the deleterious ASR reaction, and concrete showed expansion surpassing the ASTM 1260 expansion safety limit of 0.1%. Moreover, NCP mixture in quantities greater than 10% cement replacement makes the concrete very unstable and brittle. There was a reduction in the compressive strength of concrete. The mixtures were effective in decreasing the ASR expansion (60 % reduction) compared to the control mixture at 10% replacement. However, the effective threshold limit was not achieved. The NCP offers cheap cementitious waste-by-product material but is not that effective in resisting ASR. The literature suggested having a minimum of 15% to 35% Fly ash replacement levels for effective ASR mitigation.



Figure 3.8: Metakaolin-Glass Powder Samples

Group D (Specimen 11,12, &13) NCP 14-Days Expansion

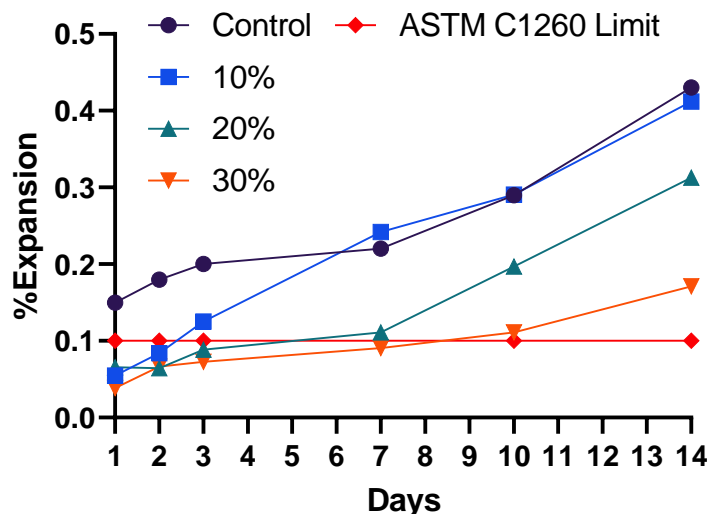


Figure 3.9 The 14-day AMBT expansion rate for NewCem Plus (NCP) Samples

Table 3.9 Fourteen-day expansions, standard deviations, and coefficients of variation for Group D (Specimen 11, 12, and 13) mixtures

Mixture	Avg 14-day expansion (%)	Standard errors in 14-day measurement	Coefficient of variation (%)
11	0.412	0.012	3.09
12	0.313	0.018	5.93
13	0.171	0.018	10.59

Three samples were made with 10%, 20%, and 30% of the total cement mixture quantity replaced with the NCP blend. The 14-day ASTM 1260 test results of the three samples, along with the control and limit, are shown in Figure 3.9. The 10% cement replacement did not show any effect on the ASR mitigation on the 14th day, and the 20% sample reduced expansion in the concrete bars to 26% compared to the control case. The largest reduction in expansion of concrete was observed in the 30% sample, bringing the total expansion in concrete to around

60 % less than the control mixture. However, none of the samples kept the expansion in length under the ASTM safe limit of 0.1%.

Group F (Specimen 14)

Lithium is the second element in the first group of the periodic table. It has an atomic mass of 6.941g and an atomic number of 3. Lithium is an alkali-metal and is found to be very reactive in its natural state. The outermost shell of lithium has a single valence electron, which makes it react with water and moisture. Stable lithium compounds for commercial use are found in the form of lithium carbonates (Li_2CO_3), sulphates, nitrates, and chlorides. The first group of metals all forms similar compounds because of their similar chemical nature. The alkali metals in Group 1 of the periodic tables are extremely reactive and make salts like NaCl with an exothermic reaction. Due to its high reactivity, lithium is not found in nature in its elemental forms. It is found as a component in compounds like brine as chloride of lithium, which is easily dissolved. The mineral spodumene ($\text{LiAlSi}_2\text{O}_6$) is a naturally occurring abundant source of lithium metal.

The main commercial use of lithium is in the construction industry as an admixture added to the concrete. Being a very reactive metal, lithium reacts with the silicates and carbonates inside the concrete and reduces the alkalinity of the pore solution, which leads to forming unreactive compounds that inhibit the alkali-silica reaction due to the presence of moisture. Moreover, lithium is used commercially in the making of lithium-ion batteries, which are used almost everywhere these days. All modern gadgets, such as laptops, smartwatches, cellphones, and tablets, run on lithium batteries. Therefore, there has been an increase in lithium demand and production.

The use of lithium in concrete mixtures has resulted in reducing the adverse effect of ASR (Thomas, Fournier, Folliard, Ideker, & Resendez, 2007). Lithium nitrate (LiNO_3) solution with a concentration of 30% is used in concrete admixture to mitigate ASR. The nature of the concrete mixture is important in determining the concentration of the lithium nitrate solution used. Reactive aggregate types require a high concentration of lithium ions to achieve a significant reduction in ASR. A lithium-to-sodium-and-potassium ratio of 0.74 eliminates ASR in the most reactive aggregates used in making concrete mixtures (McCoy & Caldwell, 1951). The ratio of 0.74 is now the standard for reactive aggregates in the industry, and to achieve it, 4.6 L of 30 % lithium nitrate needs to be added to every 1 KG of sodium oxide present in the mixture (Thomas et al., 2007).

The lithium used in Group F was mixed with basalt aggregate without adding SCMs to ensure that the lithium admixture would control the expansion rate over time. As expected, the results in Figure 3.10 show a negative expansion rate (no signs of visual ASR cracks) due to the chemical interaction between fine basalt aggregate and lithium for the 14-day measurement under harsh conditions according to the accelerated mortar bar test method.



Figure 3.10 Mortar bars for Li with basalt fine aggregate Samples

Group G (Specimens 15, 16 and 17)

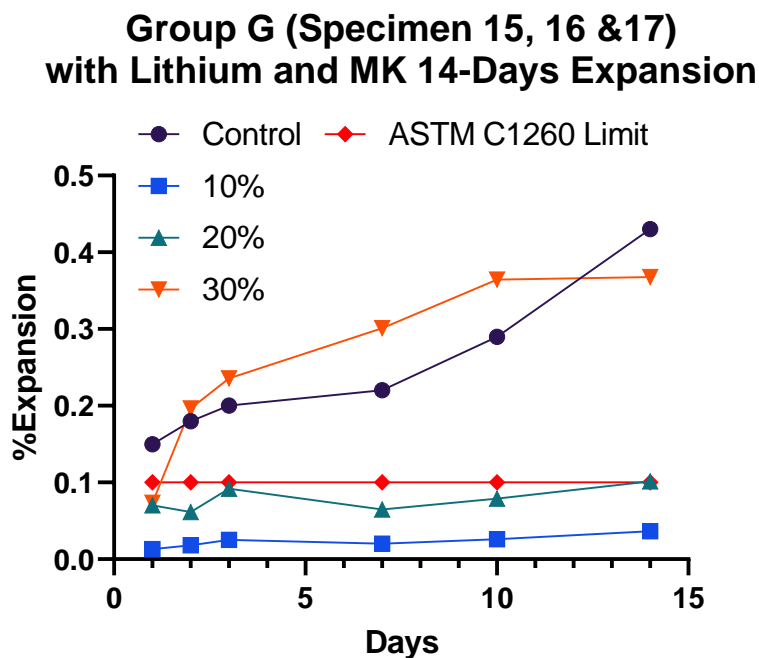


Figure 3.11 The 14-day AMBT expansion rate for Li with MK Samples

Table 3.10 Fourteen-day expansions, standard deviations, and coefficients of variation for Group G (Specimen 15, 16 and 17) mixtures

Mixture	Avg 14-day expansion (%)	Standard errors in 14-day measurement	Coefficient of variation (%)
15	0.036	0.0021	1.96
16	0.101	0.0031	3.10
17	0.368	0.0243	6.61

Samples were made with lithium and Metakaolin with cement replacement ratios of 10%, 20%, and 30%. The sample with 10% Lithium and MK showed an excellent reduction in the expansion caused by ASR (92% reduction), where the total expansion observed on the 14th day of the test was 0.036%. Therefore, MK and Lithium are good at reducing expansion in concrete. The sample with 20% +lithium admixture showed an increase in the concrete expansion compared to the 10% sample. The 14th day results showed a total expansion of almost 0.1%,

which is at the safe condition of the ASTM 1260 test. On the other hand, the sample with 30% cement replacement showed abnormal and random spurts of expansions in the concrete. The 30% mixture was deemed unsafe for construction and should not be used.



Figure 3.12 Li with MK Samples with 30% replacement of cement

Group H (Specimens 18, 19, and 20)

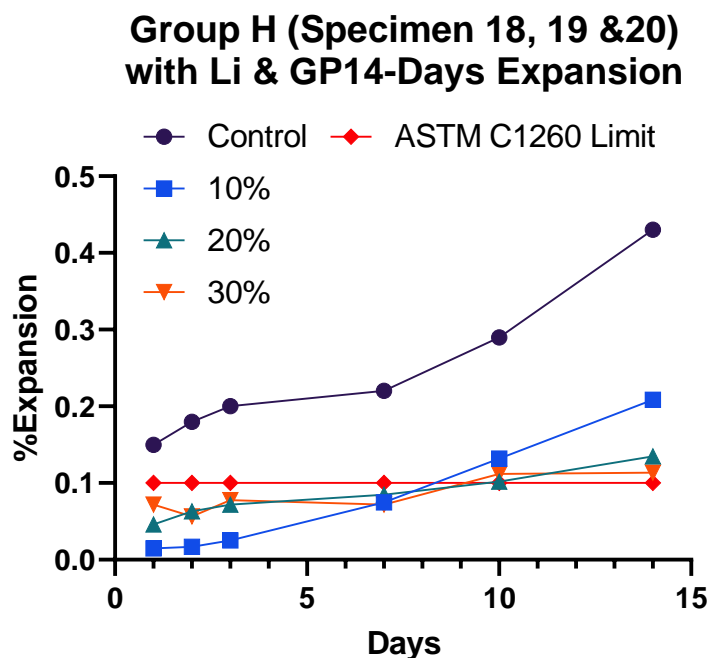


Figure 3.13 .The 14-day AMBT expansion rate for Li with GP

Table 3.11 Fourteen-day expansions, standard deviations, and coefficients of variation for Group H (Specimen 18, 19, and 20) mixtures

Mixture	Avg 14-day expansion (%)	Standard errors in 14-day measurement	Coefficient of variation (%)
18	0.209	0.0012	0.57
19	0.135	0.0035	2.58
20	0.114	0.0027	2.36

Three samples with GP+lithium were made, having a cement replacement ratio of 10%, 20%, and 30%. The samples with lithium and waste glass powder were kept in the NaOH solution for 14 days, and expansion in the concrete was measured and then compared to an earlier control sample. The addition of these GP+lithium reduced the expansion effects of ASR. A cement replacement of 10% with the SCM resulted in 0.209% expansion (51% reduction). The sample with 20% cement further improved the reduction to 68%, and the sample with 30% took it

further to 73%. The reduction rate for the expansion of samples was notable as compared to the control samples. However, the 20% and 30% reduction was not enough to pass the ASTM test, and the total expansion went above the 0.1% total expansion safe limit of the test. The final values of total expansion from the three samples were 0.209%, 0.135%, and 0.114%.



Figure 3.14: Li with GP Samples with 10% cement replacement

Group I (Specimen 21, 22, and 23)

**Group I (Specimen 21, 22, &23)
with NCP + Li 14-Days Expansion**

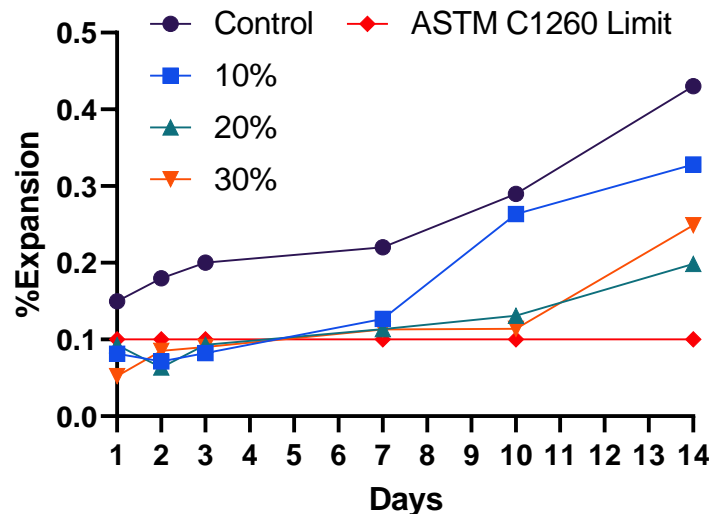


Figure 3.15 : The 14-day AMBT expansion rate for NCP with Li Samples

Table 3.12 Fourteen-day expansions, standard deviations, and coefficients of variation for Group I (Specimen 21, 22, and 23) mixtures

Mixture	Avg 14-day expansion (%)	Standard errors in 14-day measurement	Coefficient of variation (%)
21	0.328	0.0035	1.06
22	0.199	0.0017	0.83
23	0.249	0.0012	0.50

The last three samples were made with a mixture of NCP and lithium. The 14-day test results exhibited a decrease in expansion as compared to untreated concrete. The three samples produced a total expansion of 0.328%, 0.199%, and 0.249%, respectively. Sample 2 (20% replacement) produced the minimum expansion at 0.2% compared to 0.43% expansion in the control sample. The 10% and 30% replacement levels were not successful in significantly mitigating the adverse effects of ASR. However, none of the samples passed the ASTM 1260 test by keeping the concrete under the ASTM safe limit of 0.1% total expansion. Therefore, the mixture of NCM and Lithium was not an effective solution for ASR reduction in concrete.



Figure 3.16 NCP with Li Samples with 10% replacement of cement

Group J (Specimen 24, 25, and 26)

Basalt microfibers were mixed in concrete in very small proportions. Specifically, three samples with 1.5%, 2.5%, and 3.5% BF were created by the weight of the mixture. Their weights were 0.2 g, 0.3 g, and 0.4 g, respectively. The other values were the same, and the results are presented in Figure 3.17. The results showed that basalt fibers were not helping in stopping ASR in concrete. After the third day, all samples had crossed the safety threshold of 0.10% expansion, and the results were very comparable to the control mixtures.

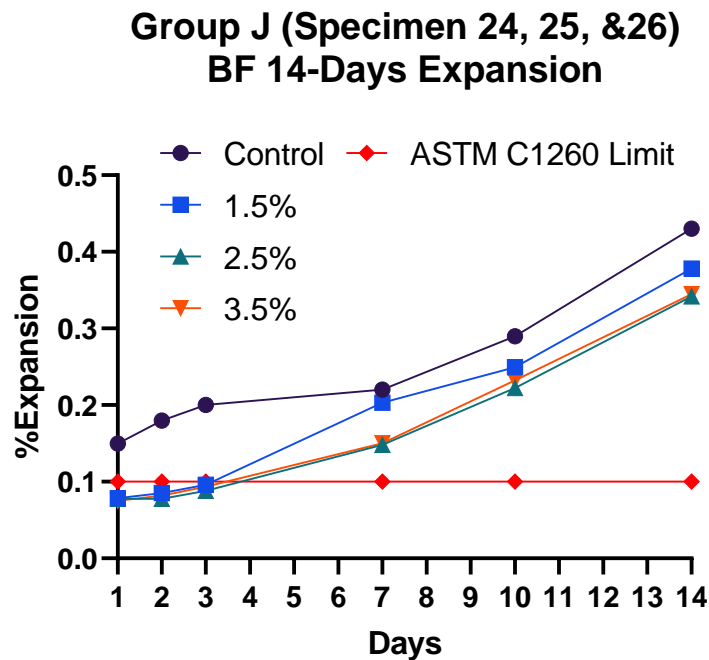


Figure 3.17 The 14-day AMBT expansion rate for BF Samples

Table 3.13 Fourteen-day expansions, standard deviations, and coefficients of variation for Group J (Specimen 24, 25, and 26) mixtures

Mixture	Avg 14-day expansion (%)	Standard errors in 14-day measurement	Coefficient of variation (%)
24	0.378	0.0104	2.74
25	0.342	0.0076	2.22
26	0.345	0.0037	1.06

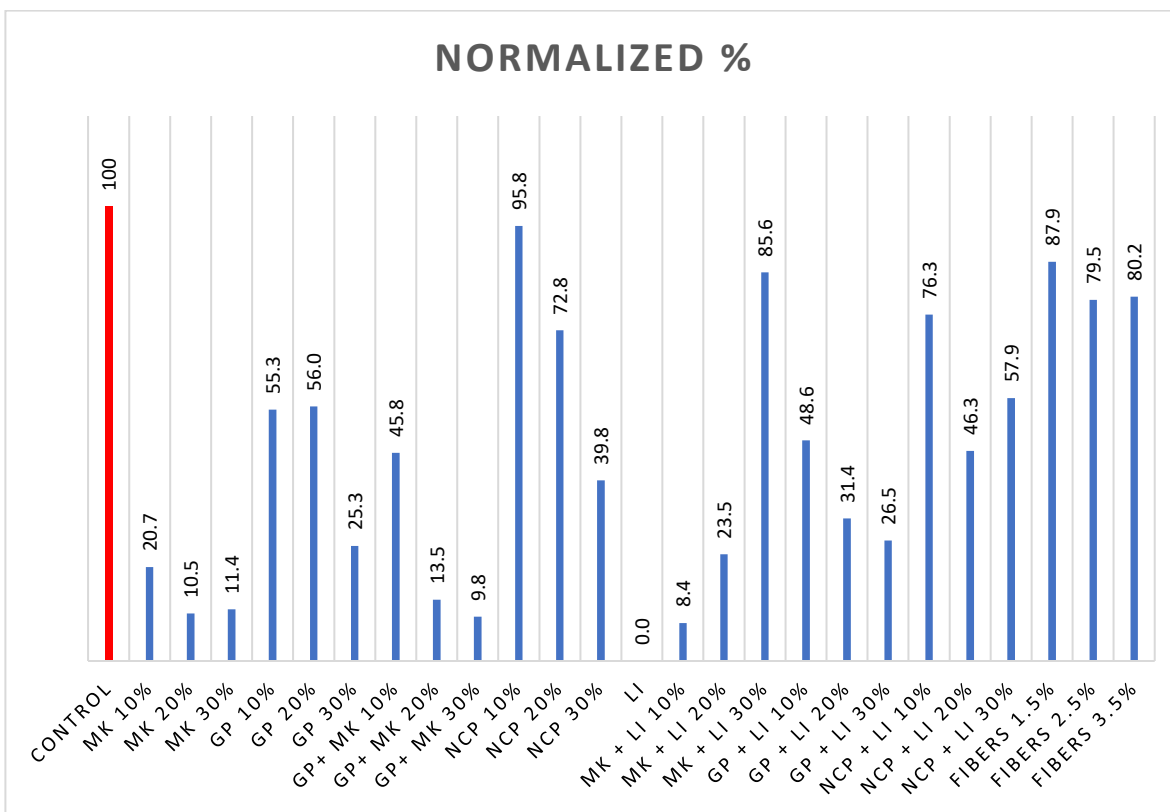


Figure 3.18 The 14-day AMBT expansion rate normalized

Figure 3.18 shows the normalized response percentages from all test samples versus the control and ASTM C1260 limits. In order to get all normalized values, the average expansion of each material was calculated by combining the 10%, 20%, and 30% results. Thereafter, all the material averages were normalized for each time point in the expansion cycles from day 1 to day 14 relative to the control mixture. The results showed that the average response of MK mixtures had a significant reduction in the ASR expansion. In addition, the Li results showed very low expansion as expected. The addition of the GP+MK at 20% and 30% levels were also promising. The NCP and Basalt fibers showed higher expansion relative to the control mixture.

3.2.1 Flow Test Results

Table 3.14 present the results of the flow test for all specimen groups.

Table 3.14 Flow Test Results

Group	Specimen	Variables	Cement Replacement	Flow Test Average Diameter (cm)	Flow%
A	1	Control	0%	20.5	103
	2	MK	10%	6.4	60
	3	MK	20%	5.825	46
	4	MK	30%	4.75	19
B	5	GP	10%	18	78
	6	GP	20%	19	88
	7	GP	30%	19.3	91
C	8	GP+ MK	10%	17.7	74
	9	GP+ MK	20%	19	63
	10	GP+ MK	30%	19.3	47
D	11	NCP	10%	16.5	63
	12	NCP	20%	11.4	13
	13	NCP	30%	10.7	6
G	15	MK + Li	10%	17.2	70
	16	MK + Li	20%	14	39
	17	MK + Li	30%	10.7	6
H	18	GP + Li	10%	20.8	103
	19	GP + Li	20%	17.2	70
	20	GP + Li	30%	14.3	41
I	21	NCP + Li	10%	20.3	100
	22	NCP + Li	20%	13.9	38
	23	NCP + Li	30%	11.4	13
J	24	Fibers	1.5%-Fibers (0.2 g)	18.7	85
	25	Fibers	2.5%-Fibers (0.3 g)	18.3	81
	26	Fibers	3.5%Fibers (0.4 g)	19	88

For group A, the workability was tested following the guidelines in ASTM C1437 flow test.

The percentage of the flow was calculated based on the average diameter (diameters measured

in two perpendicular directions) of the inner mold. The workability of the basalt mixture without adding any SCMs materials was 103%, which had a very good flow rate. However, the workability was reduced as the percentage of MK replacement increased due to the angular shape of the MK particles. The sample with 10% MK showed good workability, but the 20% and 30% MK samples showed a reduction in workability, as shown in Table 3.14. For Group B, with GP replacing cement, the workability was significantly increased with all samples with the glass powder. That was due to the spherical nature of the GP particles (rolling effect). Also, as the percentage of glass powder increased, the workability increased slightly.

For Group C, mixtures made with GP and MK, the base flow test showed decreasing workability at the higher replacement percentages. Mixture with 10% replacement showed decreased workability by 74%, for 20%, 63% and for 30%, 47%. Group D, made with NCP, has revealed a reduction in the flow from 16.5cm to 10.7cm at a 10% replacement level. The other two samples made with greater percentages of NCP further reduced workability to almost the same as the original diameter for the mold. Therefore, these concentrations of cement replacement are not good for practical purposes.

The results for Group H made with Li and MK showed a reduction with the addition of SCM. SCMs quickly absorbed extra moisture from concrete, making workability difficult. The 30% blend had abnormally low workability due to a large amount of GP+lithium, which caused the mix to dry very quickly. Finally, the workability of 10% was similar to that of concrete without SCM (control mix). However, workability decreased in the 20% and 30% samples as the concrete retains less water and thickens very quickly.

Finally, in Group I, the base flow test for a mix of NCP and Li showed that the workability of the 20% and 30% cement replacement samples were significantly decreased. However, these concrete and mortar mixes cannot be used commercially or industrially due to impracticality. The 10% sample showed no change in workability, and the flow of the mix was equal to that of the original control sample. In Group J, the flow test showed greater workability (81% to 88%) for all samples with the basalt fiber mixtures.

3.2.2 Compressive Strength Results

Group A (Specimen 1)

Compression tests for the control mixture were performed on standard 2 in. x 2 in. x 2 in. cubes. Figure 3.29 shows the compressive strength test results at 7 days, 14 days, and 28 days, respectively. These results were based on the averages of two samples per mix. As expected, the compressive strength of concrete cubes increased steadily over time and achieved the designed compressive strength of 7500 psi. Table 3.15 shows compressive strength results for all specimens.

Table 3.15 Compressive Strength 28 days Results.

Group	Specimen	Variables	Cement Replacement	Compressive Strength after 28 days (psi)	Percent (Increase / Decrease)
A	1	Control	0%	7886.25	100
	2	MK	10%	8793.75	112
	3	MK	20%	9265.25	117
	4	MK	30%	7596.25	96
B	5	GP	10%	7886.25	100
	6	GP	20%	5382.5	68
	7	GP	30%	5392.0	68
C	8	GP+ MK	10%	7233.75	92
	9	GP+ MK	20%	6423.75	81
	10	GP+ MK	30%	6637.5	84
D	11	NCP	10%	8557.5	109
	12	NCP	20%	6320.0	80
	13	NCP	30%	4988.75	63
G	15	MK + Li	10%	8390.0	106
	16	MK + Li	20%	7826.25	99
	17	MK + Li	30%	6542.5	83
H	18	GP + Li	10%	8318.75	105
	19	GP + Li	20%	7112.5	90
	20	GP + Li	30%	6311.25	80
I	21	NCP + Li	10%	8390.0	106
	22	NCP + Li	20%	7826.25	99
	23	NCP + Li	30%	6542.5	83
J	24	Fibers	1.5%-Fibers (0.2 g)	8470.0	107
	25	Fibers	2.5%-Fibers (0.3 g)	4891.25	62
	26	Fibers	3.5%Fibers (0.4 g)	5663.75	72

Group A (Specimens 2,3 &4)

The 10% and 20% mixtures made with Metakaolin showed an increase in compressive strength compared to the cubes made with 0.0% cement replacement at day 28 (Figure 3.30). The addition of micro Metakaolin particles increased the rate of hydration and produced more C-S-H that contributed significantly to the strength. Across these MK samples, the results showed that concrete strength increased according to age.

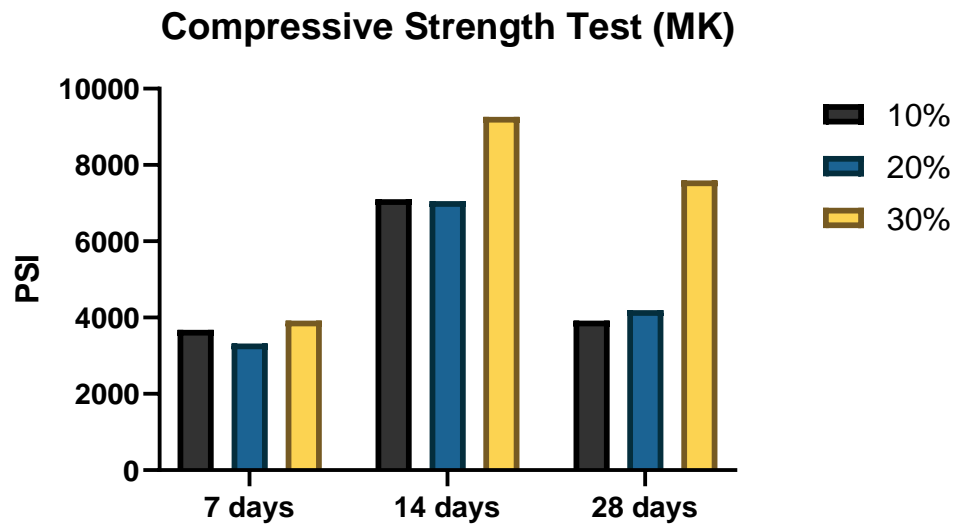


Figure 3.19 Compression Test Results for (MK)

Group B (Specimen 5,6 &7)

The compression test results showed that the 10% GP sample's strength was comparable to that of the control sample (see Figure 3.31). However, increasing the GP replacement levels to 20% and 30% decreased the compressive strength to 68% compared to the control mixture.

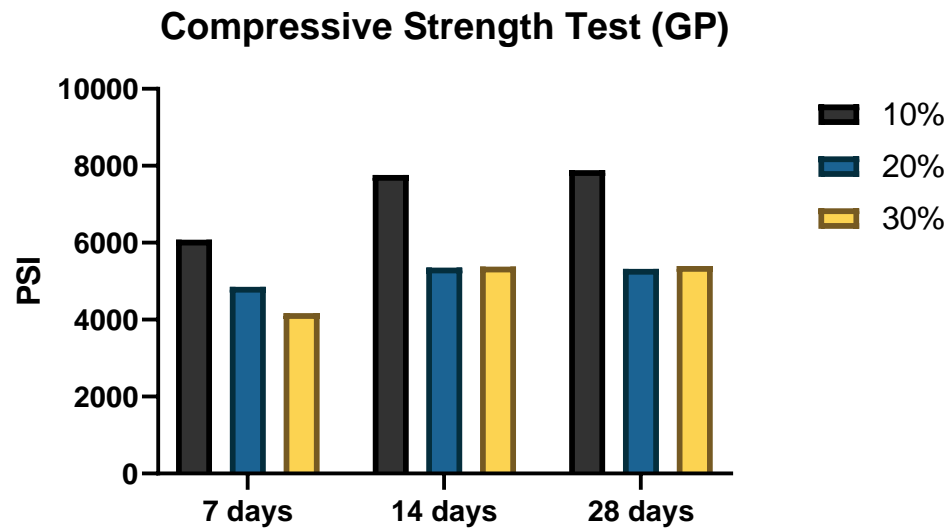


Figure 3.20 Compression Test Results for (GP)

Group C (Specimen 8,9 &10)

The compressive test results for the binary mixtures of MK and GP samples are presented in Figure 3.32. It was observed that the compressive strength of concrete was reduced in the case of the 20% and 30% MK/GP samples by 81% and 84%, respectively. This indicates that the SCM mixtures with higher concentrations of combined MK/GP weakened the concrete prisms.

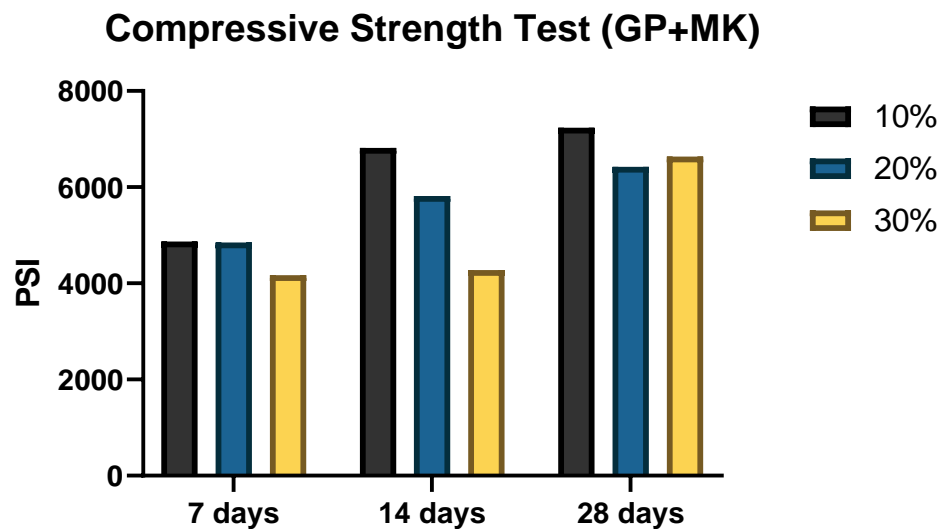


Figure 3.21 Compression Test Results for Metakaolin-Glass Powder

Group D (Specimen 11,12, &13)

The sample made with 10% cement replacement with NCM did not negatively affect the concrete strength; it increased the compressive strength compared to the control mixture. However, the 20% and 30% samples significantly reduced the compressive strength by 80% and 63%, respectively, as shown in Figure 3.33. The addition of more than 10% NCM is not recommended as it adversely affects the compressive strength of concrete.

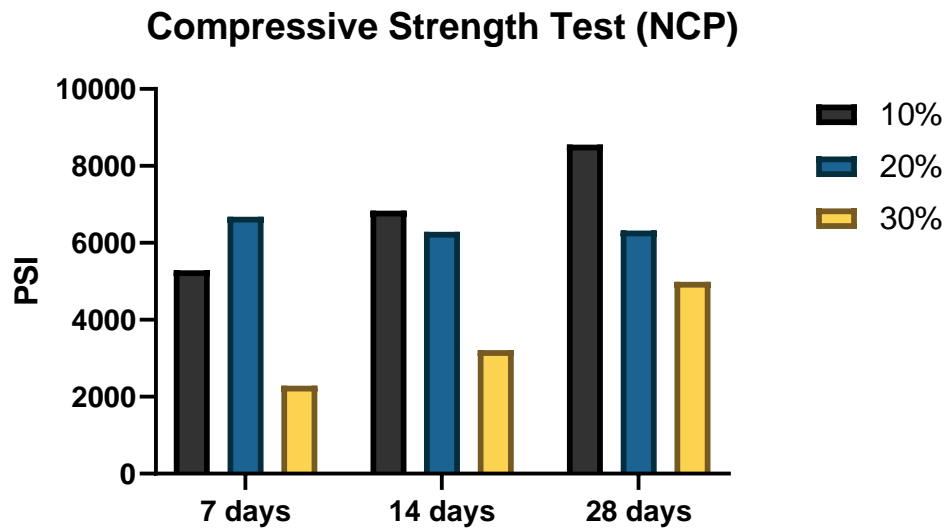


Figure 3.22 Compression Test Results for (NCP)

Group G (Specimens 15,16, &17)

The samples prepared with 10% and 20% MK + Li showed comparable strength to the control concrete blocks. This is attributed to that lithium inhibits the reaction between the alkali in cement and the reactive aggregate. However, the third sample with 30% replacement resulted in an 18% reduction in concrete strength, as shown in Figure 3.23.

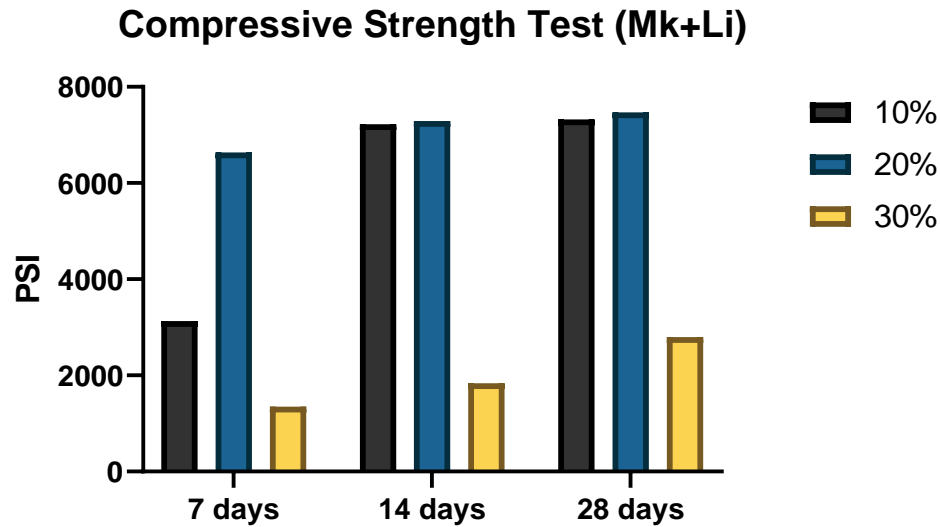


Figure 3.23 Compression Test Results for Lithium with Metakaolin

Group H (Specimens 18,19 &20)

The day-28 results of the three replacement percentages of the GP+Li are shown in Figure 3.24. The sample with 10% cement replacement had a breaking strength of 8318.75 psi, which was greater than the control sample (7886.25 psi). The addition of 10% lithium and GP mixture improved concrete strength by about 5.5%, as tested on the 28th day. On the other hand, cement replacement of 20% and 30% resulted in decreased concrete strength by 10% and 20%, respectively.

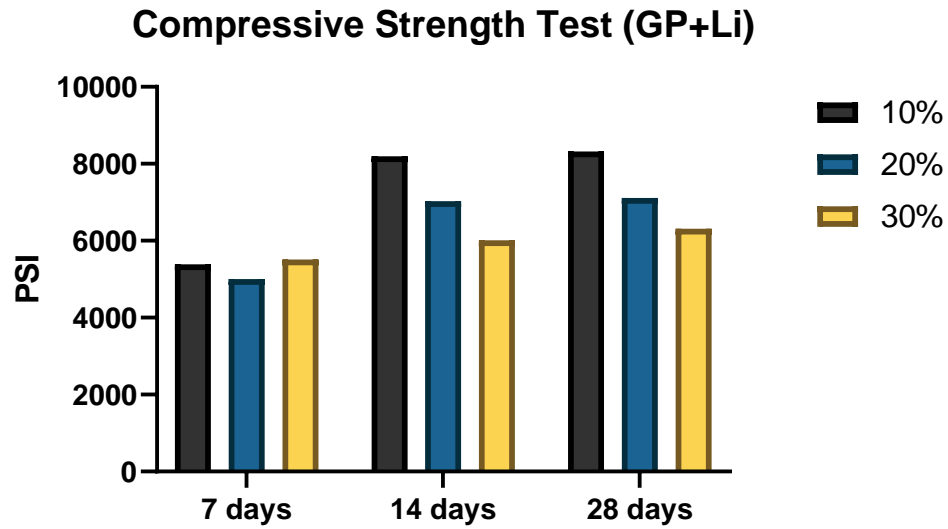


Figure 3.24 Compression Test Results for Li with Glass Powder

Group I (Specimens 21,22,23)

The results show that the 10% and 20% samples had similar compressive strengths comparable to the control case (Figure 3.25). However, the sample with 30% of NCP + Li reduced the compressive strength by 18%, resulting in compressive strength of 6542.5 psi.

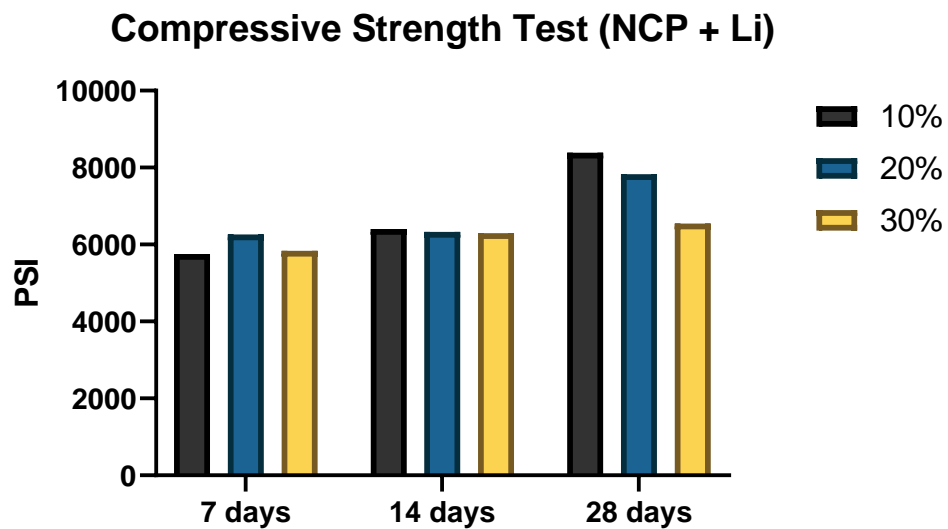


Figure 3.25 Compression Test Results for (NCP+Li)

Group J (Specimens 24,25,26)

The compressive strength testing of basalt fiber samples showed that higher fiber concentrations decreased the material's compressive strength compared to that of the control sample. This is attributed to that fibers create more air bubbles around themselves during mixing, which increases the air voids in the concrete microstructure and therefore decreases the compressive strength. The first sample (Figure 3.26) showed increased compressive strength at the 14- and 28-day marks. (The control sample had a strength of 7886.25 psi at day 28.).

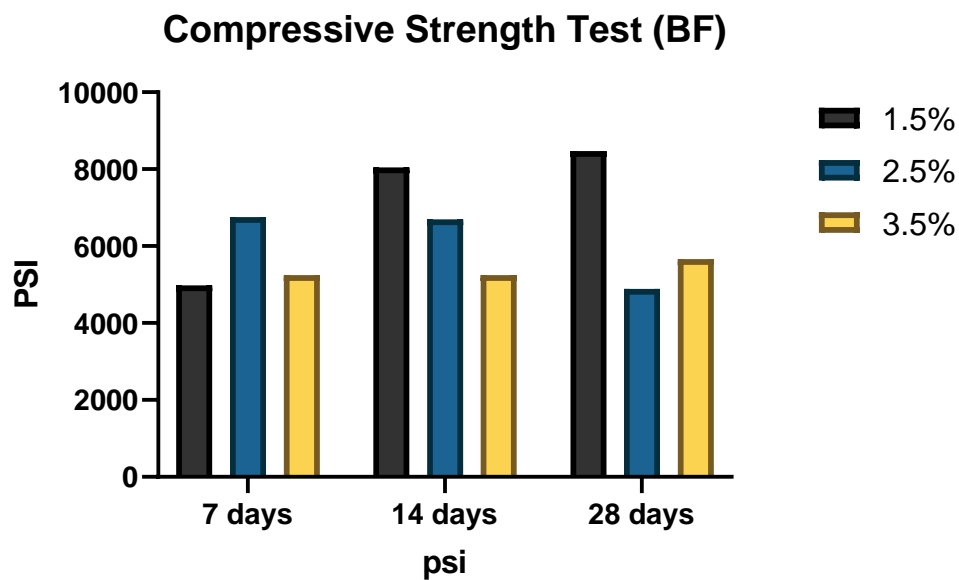


Figure 3.26 Compression Test Results for (BF)

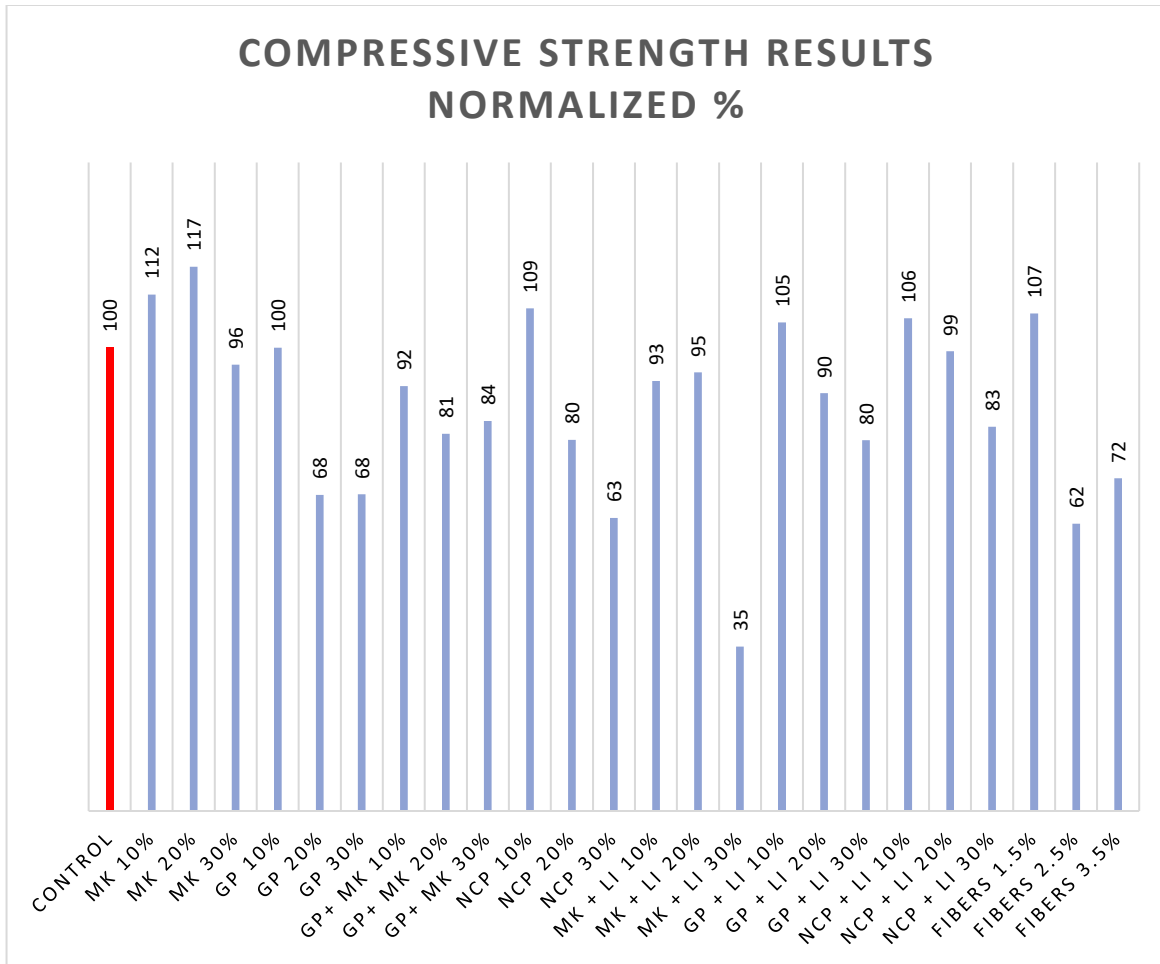


Figure 3.27 Compression Test Results Normalization

The normalized results from the compressive strength test for all mixtures are shown in Figure 3.27. The normalized response from all samples shows that the compressive strength from specimens with added SCM materials remains between a minimum of 63% in NCP (30% replacement of cement) to 109% at maximum strength compared with the control samples. The trend in all samples shows that the strength increases from day 7 to day 14 and keeps increasing till day 28. However, we see some reduction in the compressive strength in some samples, and this concrete still could be used in various applications with that reduced strength. The normal weight concrete that is currently used in various elements usually has 4000-5000 psi

compressive strength. The lowest strength obtained from all mixtures was 4891.25 psi (2.5% fiber), still considered a very good concrete and could be implemented.

3.3 Cost Analysis

The concrete mix cost plays a substantial role in the concrete quality; thus, concrete suppliers are trying to keep their prices reasonable for more production. On the other hand, concrete price directly impacts the construction market, so cubic yard or cubic meter price is considered an important factor. However, in this study, the cost of the used materials in the experimental work was calculated and compared with the control mixture to comprehend individual prices for each component and investigate whether the proposed combination of materials would make this research more economically valuable. The concrete market is experiencing high demand and competition between producers, leading to low-quality concrete and limited solutions to the ASR problem. The control mixture for the preformed experiment contains conventional concrete materials such as Portland cement and basalt aggregate that are widely used in the industry.

Supplementary cementitious materials and concrete admixtures usually increase the mixture's cost, as shown in Table 3.15. Using the SCMs is promising economically and environmentally (Najafi and Jayasekaran, 2017).

The cost of the materials used in this study has been analyzed to show a clear image of the impact on the overall cost per cubic meter for each mixture. All prices have been analyzed by adding the cost of SCMs and admixtures to the overall concrete mix. At the same time, it will show the economic feasibility of each added material. The cost of these materials was taken

directly from the concrete suppliers and reported as shown in Table 3.23 per unit price. The following equation has been used to calculate the numbers shown in Table 3.16.

Unit Price ($\$/\text{m}^3$) = Cost of the materials for each kg/m^3 x The quantity of used materials for each mixture in kg/m^3

The price for the control specimen was $\$52.8/\text{m}^3$. The highest cost was attributed to the Basalt fibers, which was classified as the most expensive ingredient according to the cost analysis. The microparticle waste glass powder (GP) is the second highest-priced material after basalt fiber. According to (Islam et al.), the increased price of the GP is due to the cost of milling.

The hybrid materials (MK&GP) price has shown an increase of 39% to 118%, with increasing cement replacement. On the other hand, the Metakaolin has a better price and was the material that effectively inhibited ASR. Although the NewCem plus (NCP) materials cost was close to the control mixture cost, it showed poor performance to mitigate the ASR, especially at 10 % replacement level with a cost of $\$52.5/\text{m}^3$. The (Li) admixture is expensive and usually has higher price compared to other chemical admixtures, however the cost of mixtures that has Li was $\$53.83$, which was very close to the cost of the control mixture.

The following conclusions have been drawn from the cost analysis:

- The cost of the control mixture (no SCMs) was \$ 52.8
- The highest cost was for the mixture made with 3.5% fiber volume fraction (655% higher than the control mixture).
- The cheapest mixture was for the one made with 30% NCP (2% lower than the control mixture)

- Mixtures included 10%, 20%, and 30% MK revealed a cost of 29.5%, 59.1%, and 88.6% higher than the control mixture, respectively.

3.4 Conclusions

After comparing the results of the different tests, we can see that all the SCMs used in our experiments have varied between either decreasing or increasing the mortar bars ASR expansion based on the SCM replacement level. Metakaolin has been shown to be a great ASR mitigating agent by reducing the amount of ASR gel formed in concrete. Metakaolin, which has pozzolanic properties, was mixed in different ratios as cement replacement. When Metakaolin was used at a 10% replacement, it completely mitigated the harmful effects of ASR in concrete by showing a significant reduction of the concrete expansion below the 0.1% threshold level. However, Metakaolin reduced the flow of concrete and slightly reduced compressive strength at 7 and 14-days.

Microparticles of waste glass powder did not show positive results in the mitigation of ASR reaction in concrete. The mortar bars made with these particles showed no resistance to changes in length and crossed the safety thresholds. Basalt fiber did not show promising results in mitigating the harmful effects of ASR in concrete. All samples went straight into expansion without delay. Moreover, the tiny fibers did not affect the concrete compressive strength.

The combination of waste glass powder and Metakaolin showed good positive results. The concrete showed increased resistance to alkalinity and increases in compressive strength. The ASR mitigation was effective at concentrations of 20% or more. The 10% cement replacement was not that effective at stopping the expansion of concrete. Overall, the method used for testing, the AMBT C1260, was an effective, quick measure of the effectivity of the reactivity of aggregate particles and the highly alkaline concrete mixtures. Specific conclusions were:

- In the samples with 10%, 20%, and 30% where Metakaolin was added, the expansion was 79%, 89%, and 88% less than that of the control specimen.
- The GP decreased the expansion compared to control specimens by 20%, 43%, and 75% at the 10%, 20%, and 30% replacement levels, respectively. It can be concluded that GP of 30% replacement level is recommended.
- Mixtures 9 and 10 of MK+GP showed a significant reduction of ASR by 86% and 90% for the 20% and 30% replacement levels, respectively.
- The binary mixtures of GP+MK at the 20% and 30% levels were more effective than the individual mixtures of MK or GP in reducing the ASR below the threshold limit. The mixtures were effective in decreasing the ASR expansion (60 % reduction) compared to the control mixture at 10% replacement.
- The sample with 10% Lithium and MK showed an excellent reduction in the expansion caused by ASR (92% reduction). The 14th day results showed a total expansion was almost 0.1%, which is at the safe condition of the ASTM 1260 test.
- The cement replacement of 10% with GP+lithium, resulted in 0.209% expansion (51% reduction). However, the 20% and 30% reduction was not enough to pass the ASTM test, and the total expansion went above the 0.1% total expansion safe limit of the test.
- Therefore, the mixture of NCM and Lithium was not an effective solution for ASR reduction in concrete.
- The results showed that basalt fibers were not helping in stopping ASR in concrete. After the third day, all samples had crossed the safety threshold of 0.10% expansion, and the results were very comparable to the control mixtures.

The study suggests using more than one SCM in concrete to make it more resistant to varying parameters. More research is needed to reach reliable and specific results for the concrete mixtures, especially with the continuous demand for concrete mixes. Using manufacturing materials in future research can support the concrete durability and help have better solutions for ASR.

In addition, a cost analysis of the mixtures has been conducted based on the unit price of each material and the quantities used in all mixtures. All mixture's cost was compared to the cost of the control mixture (100% cement). The labor cost was not taken into account. It was found that the MK mixtures were higher in price compared to the control mixtures by 29%, 59%, and 88% for the 10%, 20%, and 30% replacement levels. It can be seen that as the percentage of replacement increases, the cost increases; however, MK has proved to be very effective in reducing the ASR expansion levels. The most expensive mixture was for the 30% replacement level of GP as a SCM, where the cost has reached 148% more compared to the control mixture. The cheapest mixture was for the NCP at a 10% replacement level, where the cost was almost 50% less than the control mixture (100% cement). In addition, the 3.5% basalt fiber has shown 655% more costly than the control mixture. In conclusion, the manufacturer should compare the high initial cost of using SCMs such as MK and GP compared to the maintenance and rehabilitation of the concrete members. A life cycle assessment should be conducted before making any final decisions.

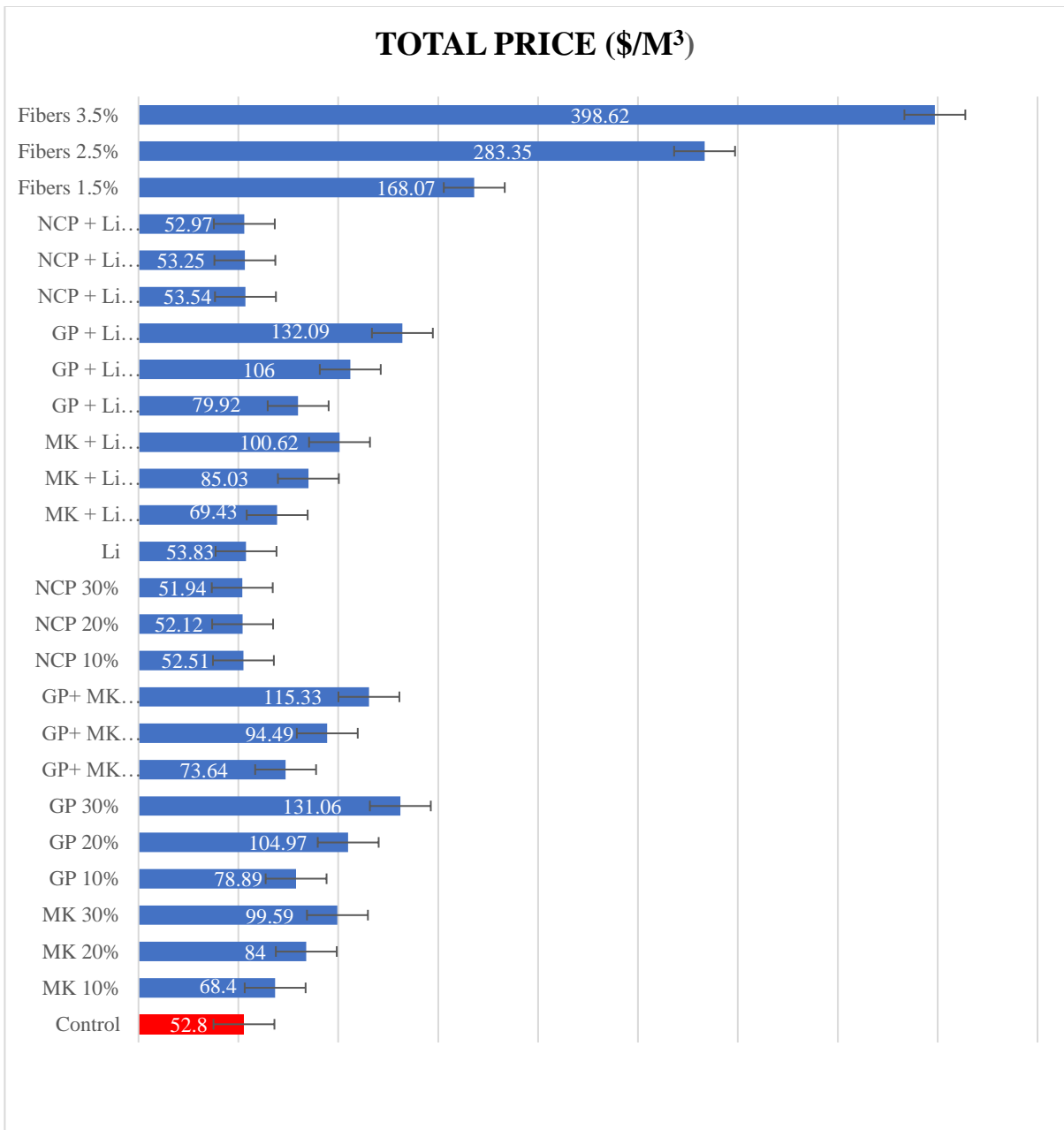


Figure 3.28 Cost Analysis Chart

Table 3.16 Cost Analysis

MIX	Description	Cement (120\$/ton)		MK (650\$/ton)		GP (18.92\$/23kg Bag)		NCP (130\$/ton)		Li (30\$/gallon)		Basalt Fibers (27\$/1.3kg Bag)		Total Price
		Weight (kg/m ³)	Unit Price (\$/m ³)	Weight (kg/m ³)	Unit Price (\$/m ³)	Weight (kg/m ³)	Unit Price (\$/m ³)	Weight (kg/m ³)	Unit Price (\$/m ³)	Weight (lit/m ³)	Unit Price (\$/m ³)	Weight (kg/m ³)	Unit Price (\$/m ³)	(\$/m ³)
1	Control	440	52.80	0	0	0	0	0	0	0	0	0	0	52.8
2	MK 10%	396	47.52	32.12	20.88	0	0	0	0	0	0	0	0	68.4
3	MK 20%	352	42.24	64.25	41.76	0	0	0	0	0	0	0	0	84
4	MK 30%	308	36.96	96.36	62.63	0	0	0	0	0	0	0	0	99.59
5	GP 10%	396	47.52	0	0	38.13	31.37	0	0	0	0	0	0	78.89
6	GP 20%	352	42.24	0	0	76.26	62.73	0	0	0	0	0	0	104.97
7	GP 30%	308	36.96	0	0	114.40	94.10	0	0	0	0	0	0	131.06
8	GP+ MK 10%	396	47.52	16.06	10.44	19.06	15.68	0	0	0	0	0	0	73.64
9	GP+ MK 20%	352	42.24	32.125	20.88	38.13	31.37	0	0	0	0	0	0	94.49
10	GP+ MK 30%	308	36.96	48.18	31.32	57.20	47.05	0	0	0	0	0	0	115.33
11	NCP 10%	396	47.52	0	0	0	0	38.41	4.99	0	0	0	0	52.51
12	NCP 20%	352	42.24	0	0	0	0	76.82	9.98	0	0	0	0	52.12
13	NCP 30%	308	36.96	0	0	0	0	115.24	14.98	0	0	0	0	51.94
14	Li	440	52.80	0	0	0	0	0	0	0.130	1.03	0	0	53.83
15	MK + Li 10%	396	47.52	32.12	20.88	0	0	0	0	0.130	1.03	0	0	69.43
16	MK + Li 20%	352	42.24	64.25	41.76	0	0	0	0	0.130	1.03	0	0	85.03

MIX	Description	Cement (120\$/ton)		MK (650\$/ton)		GP (18.92\$/23kg Bag)		NCP (130\$/ton)		Li (30\$/gallon)		Basalt Fibers (27\$/1.3kg Bag)		Total Price
		Weight (kg/m ³)	Unit Price (\$/m ³)	Weight (kg/m ³)	Unit Price (\$/m ³)	Weight (kg/m ³)	Unit Price (\$/m ³)	Weight (kg/m ³)	Unit Price (\$/m ³)	Weight (kg/m ³)	Unit Price (\$/m ³)	Weight (kg/m ³)	Unit Price (\$/m ³)	(\$/m ³)
17	MK + Li 30%	308	36.96	96.36	62.63	0	0	0	0	0.130	1.03	0	0	100.62
18	GP + Li 10%	396	47.52	0	0	38.13	31.37	0		0.130	1.03	0	0	79.92
19	GP + Li 20%	352	42.24	0	0	76.26	62.73	0		0.130	1.03	0	0	106
20	GP + Li 30%	308	36.96	0	0	114.40	94.10	0		0.130	1.03	0	0	132.09
21	NCP + Li 10%	396	47.52	0	0	0	0	38.41	4.99	0.130	1.03	0	0	53.54
22	NCP + Li 20%	352	42.24	0	0	0	0	76.82	9.98	0.130	1.03	0	0	53.25
23	NCP + Li 30%	308	36.96	0	0	0	0	115.24	14.98	0.130	1.03	0	0	52.97
24	Fibers 1.5%	440	52.80	0	0	0	0	0	0	0	0	5.55	115.27	168.07
25	Fibers 2.5%	440	52.80	0	0	0	0	0	0	0	0	11.10	230.55	283.35
26	Fibers 3.5%	440	52.80	0	0	0	0	0	0	0	0	16.65	345.82	398.62

Chapter 4: Improving the Outlier Detection Method in Industrial Application by Combining the Isolation Forest and Local Outlier Factor

(Published In construction and Building Material, DOI:10.1016/j.conbuildmat.2020.121396)

4.1 Introduction

Throughout the Big Data era, massive data is generated from numerous sources. One of the challenges in big data processing is how to quantify outliers. This is clearly significant in the concrete industry, especially since concrete is considered the second largest usable material globally after water. Concrete is a heterogeneous material, and its fresh and mechanical properties depend on various parameters (percentages of ingredients). Generally, the properties of concrete directly influence the stability and reliability of any construction project; these properties include compressive, flexural, and tensile strengths and elastic modulus (Zhang et al., 2019). The quality of data in the construction industry may be limited and challenged. For example, field data collection might include some missing values, wrong measurements, or outliers (Yan et al., 2020). Due to the efficiency of outlier detection in various areas, many outlier detection techniques have been developed to detect the anomaly known as an outlier.

The distance-based method is the most often used technique for outlier detection. Despite its accessibility, it results in poor accuracy when applied to multi-density data such as concrete mixtures input that have multiple variables. The density-based outlier method deals with multi-density data by the comparison of the density points with nearby local neighbors. The Local Outlier Factor (LOF) is the most practical procedure in the density-based approach (Breunig et al., 2000). The LOF handles dense data without assuming any underlying or predefined distribution. It also finds the dataset in heterogeneous densities (Malvar et al., 2002; Thomas et

al., 2012). However, the LOF faces some limitations, such as calculating the distance between points requires a large amount of memory, which affects execution time. In addition, the LOF is incapable of dealing with the sequence of outliers. Another technique for outlier detection, called Isolation Forest (IF), solves the issues found in the LOF by isolating the outlier instead of processing the whole dataset. IF is an unverified learning process for abnormality detection that depends on the principle of separating anomalies. Despite its accuracy, the IF method has a weakness when it comes to a local outlier. Cheng et al. 2019 proposed pruning techniques by finding the outlier candidate set to calculate the outlier score. Thus far, this is the approach most successful in solving the limitations of both the IF and LOF methods.

To further improve the accuracy of both the IF and LOF in detecting the outlier, this paper introduces a new method called the Isolation Forest based on a Sliding window for Local Outlier Factor (IFS-LOF) detection. The IFS-LOF merges both methods (IF and LOF) with a sliding window to increase the rate of accuracy and to detect input with different window sizes (ws). The IFS-LOF was evaluated through a series of experiments that were performed through concrete mixtures with various ingredients. The proposed algorithm demonstrated considerable accuracy based on the experimental results compared to the state-of-the-art standalone LOF method. The remainder of this paper is organized as follows. The next section provides a review of related methods; the third section describes the structure of the IFS-LOF method; following that, the experimental results are presented. Finally, the last section states the conclusions.

4.2 Related Work

Outlier detection is a significant research issue in machine learning and data mining for detecting a rare object in real applications, such as finance, industry, health, and materials science. When it comes to the construction industry, outlier detection has been rarely used in

evaluating the quality of the measured or collected data. According to Yan et al. (2020), only very few articles have discussed outlier detection methods used for measuring the source of the data.

The core concept of outlier detection is to identify abnormal data points that are different relative to the majority of the data trend. Outliers are divided into two categories: global outliers and local outliers. Global outliers occur when various data points are far from all other data points. For example, in Figure 4.1, the data points p_3 and p_4 are considered a global outlier. In Niennattrakul et al. (2010), the authors explained how to locate a global outlier by using the sliding window technique. For local outliers, the distance between points is usually computed according to a local neighborhood, known as the K-Nearest Neighbors (KNN) algorithm. As seen in Figure 4.1, points p_1 and p_2 are considered local outliers.

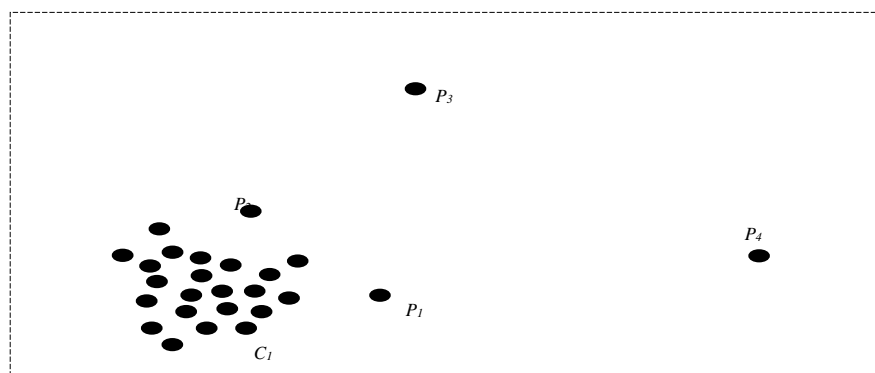


Figure 4.1 Illustration of the Outlier Categories

Note. Global outliers (p_3, p_4) and a local outlier (p_1, p_2) in a two-dimensional space.

A variety of academic articles outlined various methods for outlier detection in data mining; they included Distance-based outlier detection, Density-based outlier detection, Clustering-based outlier detection, and Ensemble-based outlier detection (Farny & Kosmatka, 1997;

Kandasamy & Shehata). Distance-based outlier detection is measured according to the distance between points. Knorr and Ng (1998) introduced the concept of the distance-based model, where data points that are located far from their closest neighbor are understood as outliers (Wang et al., 2019). The KNN is the most common method used to evaluate outliers when based on their local neighbors. For example, Dang et al. (2015) applied the KNN concept to detect the outliers based on traffic data collection from various cities. The K-mean algorithm is another method used to calculate the distance between the objects of data points of neighbors (Ramaswamy et al., 2000).

Density-based outlier detection evaluates the points in the whole dataset by comparing the density of data points with nearby local neighbors. Those densities that are distant from their nearest neighbors are called outliers. The LOF is the most popular strategy to find an outlier based on a degree, such as an outlier score. The LOF is an example of the density-based model that uses the KNN to detect data points using local reachability density. Despite the accuracy in detecting the outlier, Tang et al. (2002) suggested improving the LOF in estimating local density by a new approach called the connectivity-based outlier Factor (COF). This model isolates the outlier by connecting a data point with its nearest neighbors. Tang and Ngan (2016) introduced the density based bounded LOF method (BLOF) after using the principal component analysis (PCA) to detect the outliers.

The clustering-based outlier detection is an unsupervised method that processes data by dividing the whole data into groups based on their distribution. The Clustering-based outlier method aims to cluster data points and then detect the outlier (Wang et al., 2019). Some

algorithms use a small cluster, which represents a small number of points as an outlier. Other methods used the threshold concept to define the outlier who is far from the cluster.

Ensemble-based outlier detection is a new strategy for detecting outlier(s) by combining one set of results with the results of another outlier method in order to present and create a robust outlier detection method. In Cheng et al. (2019), the authors proposed combining the Ensemble-based outlier detection with the density-based outlier detection to solve both IF and LOF limitations. The developed method focused on clipping data points to detect the outlier according to a set of candidate outliers. Several authors have introduced extended versions of the IF to deal with several types of outliers. Staerman et al. (2019) improved the IF by using a new algorithm called Function isolation Forest (FIF) to identify and quantify outliers. Ding and Fei (2013) used the concept of the sliding window for data stream in the IF method.

4.3 Context, Dataset, And Methodology

4.3.1 Concrete Material Components and Dataset

Concrete is a primary component in the construction of various projects. Concrete ingredients have recently changed a lot by introducing various materials and admixtures that were either added before or during mixing; most of these materials are waste by-products, known as Supplementary Cementitious Materials (SCMs). Fly ash, silica fume, and blast furnace slag are the most common types of SCMs used in the concrete industry. These waste by-products enhance short-term properties, such as compressive strength, tensile strength, and workability, and they significantly improve concrete durability over time (Bach et al., 1993; Berra et al., 1991; Islam, 2010; Islam & Ghafoori, 2011; Léger et al., 1996). Moreover, concrete is a multifarious material, and its properties are significantly affected by the individual properties of its constituents.

In this paper, the concrete data collection was obtained from the University of California Irvine (UCI) machine-learning repository that was released in Yeh (1998) and Dua and Graff (2019). The data collection included the results of the compressive strength of 1030 concrete mixtures. Compressive strength is considered one of the most important parameters that are used by the engineering community in structural concrete design, including such critical structures as bridges and the like. Table 4.1 shows the range of ingredients that have been used in the 1030 concrete mixtures.

Table 4.1 Range of Concrete Ingredients Used in This Study

Component	Minimum (kg/m³)	Maximum (kg/m³)	Average
Cement	71	600	232.2
Fly ash	0	175	46.4
Blast furnace slag	0	359	79.2
Water	120	228	186.4
Superplasticizer	0	20.8	3.5
Coarse Aggregate	730	1322	943.5
Fine Aggregate	486	968	819.9
Compressive Strength	2.33	82.6	35.8

Finding the outliers in each component could improve the quality and reliability of the data to be processed. Our task was to calculate the IFS-LOF method's efficiency in identifying the outliers in the UCI concrete data. The proposed algorithm generates better performance than state-of-the-art LOF algorithms.

4.4 Components and Workflow

4.4.1 The Isolation Forest

The Isolation Forest (IF) is an unsupervised method used in the collective-based model to isolate the anomalies by measuring the isolation score for all data points. The IF has the same concept of using the tree model as the random forest algorithm, and then it processes data points into recurrent random splits that are dependent on the selecting features (Liu et al., 2008). The main advantage of the IF algorithm is how it processes the data. Instead of processing all the data points, it uses a decision tree to isolate the outliers, which reduces the execution or processing time and the corresponding memory requirement (Domingues et al., 2018). The IF technique operates by partitioning the model into several segments that are required for the subsampling size, as illustrated in Figure 4.2. An anomaly score is used to create a path length for the tree to isolate the outlier, as shown in Algorithm 1 in Table 4.2.

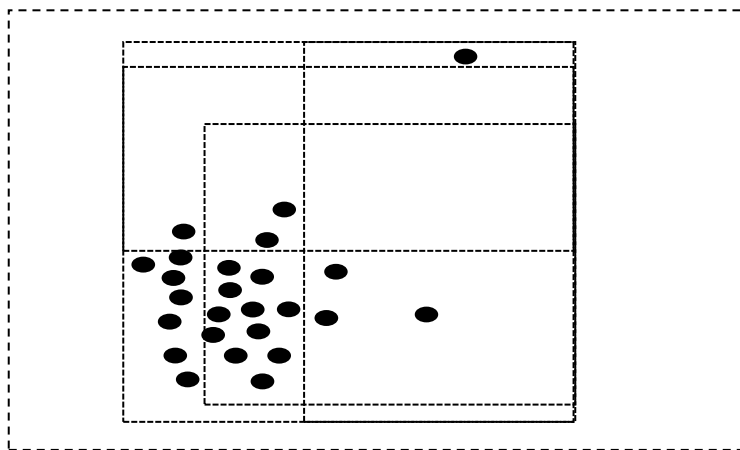


Figure 4.2 Illustration of Subsampling Size in the Isolation Forest for Processing Data Points

The IF calculation begins with a certain data point value. Then, according to the selected value, it sets a range between the maximum and the minimum values to determine the outlier score for

each data point in the tree. The score is calculated to set a path length to isolate the outlier. For more details, the reader should refer to Liu et al. (2008).

Table 4.2 Isolation Forest [IF] Algorithm

Algorithm 1: I Forest (D, t, x)

Input: D – Input data set for the data points t – number of tree x – subsampling size s

Output: a set of t iTree

- 1 **Init** Forest
- 2 set height limit l – ceiling $\log_2 x$
- 3 **For** $i = 1$ to t **do**
- 4 $D' \leftarrow$ sample D, x
- 5 Forest \leftarrow Forest \cup iTree $D', 0, l$
- 6 **End for**
- 7 **Return** Forest

4.4.2 Local Outlier Factor

The Local Outlier Factor (LOF) is another unsupervised approach in density-based outlier detection to search the anomaly based on a score to determine if a data point is considered outlier or normal. LOF evaluates data points according to a degree of measurement, i.e., the outlier factor regarding the density of the local neighbors. The definition of LOF was described in the work of Latifee (2016) and Rangaraju (2016) and illustrated as:

Definition 1: *k-distance of a data point pt*

For given two data points (pt, o) , the distance between them is measured by the Euclidean distance in n -dimensional space

$$Distance (pt, o) = \sqrt{\sum_{i=1}^n (pt_i - o_i)^2} \quad [\text{Eq. 4-1}]$$

Definition 2: *k-nearest neighbor of a data point (pt)*

By having a point pt in a dataset D and k as a positive integer. To measure the k -nearest neighbors of pt , a data point q has a distance from data point pt and does not surpass the k -distance of pt . Equation 2 describes the k -nearest neighbor of a data point pt .

$$N_{k\text{-distance}(pt)}(pt) = \{ q \in D \setminus \{pt\} \mid \text{distance}(pt, q) \leq k\text{-distance}(pt) \} \quad [\text{Eq. 4-2}]$$

Definition 3: Reachability distance (RD) of point pt regarding to the o point

Equation 3 defines the reachability distance of point pt to any point o :

$$\text{Reach-distance}_k(pt, o) = \max \{ k\text{-dist}(o), \text{distance}(pt, o) \} \quad [\text{Eq. 4-3}]$$

According to Definition 3, the distance is calculated based on the k -distance (o) in two ways. If the actual distance is far from the k -distance (o), it measures as a reachable distance, and in the other case, if the distance is shorter than the k -distance of o , it will be calculated as k distance (o). Figure 4.3 represents the computation of the reachable distance when $k = 4$.

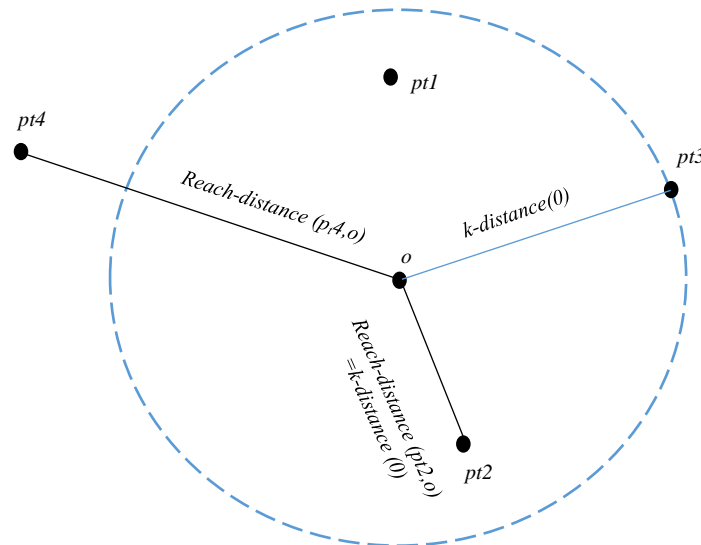


Figure 4.3 : Illustration of the Reachable Distance in Various Data Points as $k = 4$

Definition 4: *Local Reachability Distance (LRD) of point p in regard to o*

The local reachability distance is determined by two parameters: the minimum number of data points and the size of the sample. The size is used by the reachable distance of $\text{Reach-dist}_{\text{Min-point}}(pt, o)$ as shown in equation 4:

$$\text{Lrd}_{\text{Min-points}}(pt) = 1 / \left(\frac{\sum_{o \in N_{\text{Minpoint}}(pt)} \text{Reach-dist}_{\text{Min-point}}(pt, o)}{|N_{\text{Min-point}}(pt)|} \right) \quad [\text{Eq. 4-4}]$$

Definition 5: *The local outlier factor (LOF) of pt*

The LOF of a data point pt can be obtained by equation 5 with all the previous definition described above.

$$\text{LOF}_{\text{Min-point}}(P_t) = \frac{\sum_{p \in P_{\text{Min-point}}(pt)} \frac{\text{Lrd}_{\text{Min-point}}(o)}{\text{Lrd}_{\text{Min-point}}(pt)}}{|P_{\text{Min-point}}(pt)|} \quad [\text{Eq. 4-5}]$$

The LOF generates the score dependent on the local reachable distance (LRD) and the minimum point of pt . a threshold score θ is used to assess whether pt is an outlier or not.

4.4.3 The Isolation Forest Based on Sliding Window for the Local Outlier Factor (IFS-LOF)

This section describes the proposed IFS-LOF objective for finding an outlier. It proposes increasing the accuracy of detecting the outlier by using the sliding window concept to select the outlier candidates from the IF algorithm. The proposed IFS-LOF algorithm has two stages: the processing and detection stages, as shown in Table 4.3 and Figure 4.4.

Table 4.3 The Isolation Forest Based on the Sliding Window for Local Outlier Factor (IFS-LOF Algorithm)

Algorithm 2: IFS-LOF

Input: D – Input dataset for the data points t – number of tree S - sliding windows k -number of nearest neighbor x -outlier candidate data point

Output: outlier score

1 **Init** Forest

2 x outlier candidate set \rightarrow Call Algorithm 1 with D, t, w, S

3 **For** $j=1$ to D **do** \rightarrow Call LOF with k, x

4 **If** the LOF for X -temp is $> \theta$ **then**
 X -Temp is outlier

5 **End**

6 **End for**

7 **End**

Table 4.3 illustrates how the IFS-LOF algorithm process works. In the processing phase (lines 1-2), the isolation forest processes the concrete mixture dataset determines the tree's number to build and determines the sampling size. Then, the sliding window is used as a window size (w_s) to store the data points from the IF algorithm. In the detection phase, the LOF threshold θ is used to calculate the data input from the sliding windows to determine the outlier score. Any data point that exceeds the threshold value is considered an outlier (lines 3-5).

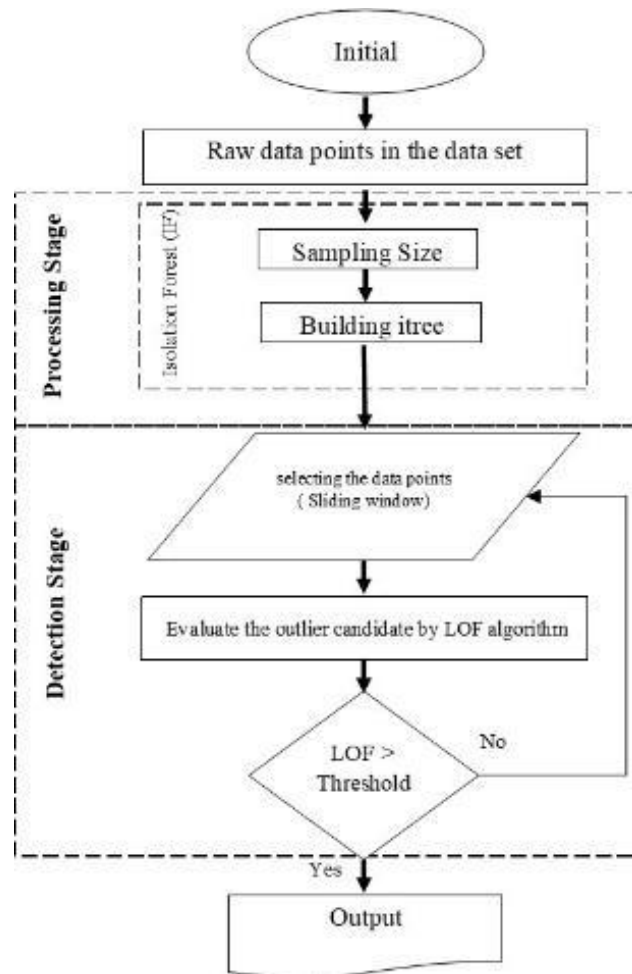


Figure 4.4 Structure of the Proposed IFS-LOF Algorithm

4.5 Experimental Results and Discussion

This section describes the experimental results after comparing the IFS-LOF, LOF-Sliding Window (LOF-SW), and LOF with different window sizes (w_s). The purpose of the proposed IFS-LOF is to answer the following questions:

- Does IFS-LOF perform better than LOF and LOF-SW in the accuracy of outlier detection?
- Does the Sliding Window improve the accuracy of the outlier detection?
- Does IFS-LOF perform faster than LOF and LOF-SW in execution time?

4.6 Experimental Settings

All algorithms (LOF, LOF-SW, and IFS-LOF) were implemented in Java and operated on a machine that runs on operating system of Windows 10 (64-bit) with Intel Core (MT) i7-4940MX CPU, 16 GB RAM, and 1 TB SSD hard disk. The accuracy of the outlier detection for IFS-LOF, LOF-SW, and LOF methods was calculated by using the ROC Curve (AUC) method, as set out in (Bueno et al., 2020; Latifee, 2013). In particular, AUC (area under the ROC curve) was used to answer the first question to obtain the accuracy rate. ROC is a probability and the AUC-ROC curve is a performance measure of categorization of various difficulties under various threshold Settings. The sliding window strategy was adopted in the second question in order to compare the performance between the IFS-LOF and LOF-SW methods for the accuracy of outlier detection. The parameter of the KNN was set at 8 for all algorithms, including LOF, LOF-SW, and IFS-LOF. The IFS-LOF had a selecting feature that was set at 0.25 for the IF algorithm. Different sizes of windows were used to evaluate the performance of each algorithm as presented in Table 4.4. The window size (ws) has different values for the comparison between the algorithms: $ws = \{100, 200, 300, 400\}$.

4.7 Discussion

4.7.1 The Accuracy of Outlier Detection

The accuracy of outlier detection was assessed by applying AUC, as shown in Table 4.4. The IFS-LOF, LOF-SW, and LOF algorithms processed each element in the UCI concrete dataset.

Table 4.4 Accuracy Rate of the LOF, LOF-SW and IFS-LOF for Different Window Sizes

W size / Component	100			200			300			400		
	LOF	LOF-SW	IFS-LOF	LOF	LOF-SW	IFS-LOF	LOF	LOF-SW	IFS-LOF	LOF	LOF-SW	IFS-LOF
cement	90.89	89.01	90.44	96.68	92.10	95.40	94.49	95.38	92.66	94.67	96.55	97.48
Blast Furnace Slag	80.50	80.20	82.49	79.77	89.93	91.67	93.50	92.85	94.52	93.77	91.12	93.65
Fly Ash	67.80	72.05	67.36	93.80	85.54	93.68	94.70	92.45	94.28	93.81	93.77	94.28
Superplasticizer	77.39	78.01	90.91	84.41	80.69	93.13	88.57	86.21	88.97	82.94	89.56	89.20
Coarse Aggregate	98.46	85.58	85.83	92.08	91.14	93.20	97.65	95.23	96.44	97.28	94.59	96.51
Fine Aggregate	85.77	84.89	90.95	89.77	87.21	90.40	93.09	96.99	94.70	95.24	95.95	96.62
Age	82.83	86.46	88.56	90.03	93.10	86.46	94.09	90.47	94.18	90.04	88.15	94.73
Water	85.13	62.63	90.53	96.23	92.78	94.69	91.35	93.82	92.16	94.37	91.63	93.24
Concrete compressive strength	94.39	85.52	94.72	90.74	89.49	92.78	90.03	90.27	94.26	95.07	93.26	95.51

Figure 24.5 illustrates the comparison of the accuracy rate with different window sizes (ws). Based on the results for each element or component, we were able to illustrate the most suitable method to use for a greater accuracy rate. For the cement element, both IFS-LOF and LOF-SW had a higher accuracy rate for most of the window sizes compared to LOF. The reason is because of the size of the windows used to process the data in the memory. LOF performed better with smaller sizes of the windows, while both LOF-SW and IFS-LOF had an advantage using larger sizes of windows. The IFS-LOF method surpassed all other methods with an accuracy rate of 97.48% when it reached $ws = 400$.

Based on IFS-LOF's performance, it had a better accuracy rate for both the superplasticizer element and concrete compressive strength for all ws. The IFS-LOF's performance was

inconsistent in the concrete elements was seen in the blast furnace slag, coarse aggregate, and water.

LOF performed better than IFS-LOF in larger sizes of windows. In addition, in the coarse aggregate element, the gap of the accuracy was noticeable when w_s reached $w = 100$. However, when the size of the windows increased, IFS-LOF performed better than LOF when it reached $w_s = 200$. Despite the low accuracy rate performance, in most of the w_s sizes IFS-LOF had a better accuracy rate than LOF as illustrated in the blast furnace Slag element. Also, LOS-SW showed lower performance than the LOF $w_s = 100$ and 200 in the cement and fine aggregate elements, and the performance was better than the LOF at higher windows sizes.

4.7.2 Sliding Window Strategy for Improving Outlier Detection

The sliding window strategy has improved the accuracy rate for most of the concrete components. Still, one of the drawbacks of the method is related to the size of the window used to process the data. For example, LOF-SW produced a lower accuracy rate, when the size of the window was increased. This is due to the amount of data used in the sliding window, which has an impact on the results of the accuracy performance.

To improve the accuracy rate in the sliding window technique, the IFS-LOF algorithm strengthens the accuracy output in the sliding window by using the IF algorithm. The IF algorithm enhances the sliding window by selecting the isolation data point instead of processing all of the data. IFS-LOF improves its usability in comparison with LOF-SW (Figure 4.5). IFS-LOF presented the most consistently higher accuracy in most of the w_s compared to the other remaining algorithms.

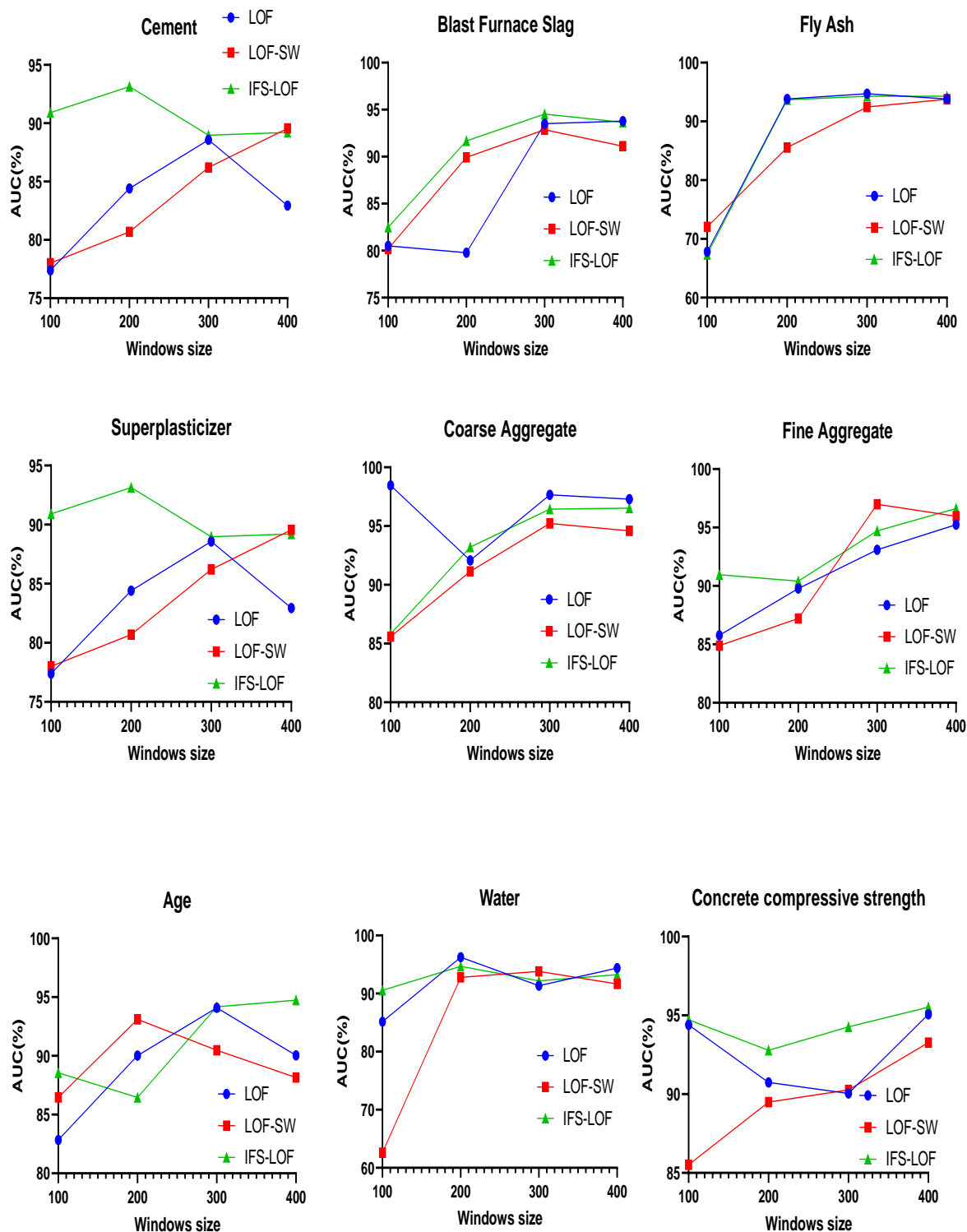


Figure 4.6 Comparing accuracy result between LOF, LOF-SW, and IFS-LOF. IFS-LOF presents most consistently higher accuracy in most of the ws comparing to the other remaining algorithms

4.7.3 Execution Time

Table 4.5 represents the execution time for the concrete data elements by comparing LOF, LOF-SW, and IFS-LOF. All algorithms were measured in seconds. In general, LOF was slightly better in execution time than either LOF-SW or IFS-LOF for most of the elements when it reached $ws = \{100,200\}$. The Superplasticizer and coarse aggregate elements were executed faster than LOF-SW and IFS-LOF in all ws . For the remaining windows at $ws = \{300,400\}$, we noticed both LOF-SW and IFS-LOF execution times were much lower compared to the LOF algorithm. The main reason was related to the sliding window technique for reducing execution time. The LOF-SW algorithm was slightly better than the IFS-LOF in the execution time. However, it had a lower accuracy rate than LOF-SW.

Table 4.5 Execution Times of the LOF, LOF-SW, and IFS-LOF for Different Window Sizes

Execution Time / Component	100			200			300			400		
	LOF	LOF-SW	IFS-LOF	LOF	LOF-SW	IFS-LOF	LOF	LOF-SW	IFS-LOF	LOF	LOF-SW	IFS-LOF
cement	1.55	1.62	1.58	4.34	4.83	5.19	9.25	8.93	10.09	16.24	16.17	18.98
Blast Furnace Slag	8.05	8.02	8.24	7.97	8.99	9.16	9.35	9.28	9.45	9.37	9.11	9.36
Fly Ash	1.58	1.74	1.78	6.76	8.33	7.47	22.21	19.32	15.84	48.81	50.75	53.48
Superplasticizer	1.66	1.57	1.95	4.3	7.05	5.2	9.81	22.39	10.77	19.67	48.67	21.38
Coarse Aggregate	1.71	1.55	1.7	5.57	5.15	6.04	10.81	11.04	12.07	20.24	21.68	23.45
Fine Aggregate	1.7	1.44	2.08	4.4	4.45	5.62	9.72	9.15	10.72	17.39	17.1	20.03
Age	1.65	1.7	2.17	4.4	4.79	5.33	9.46	9.34	11.37	16.35	16.08	19.37
Water	2.38	1.8	2.19	8.88	9.28	8.14	31.77	18.29	23.2	40.36	37.95	50.91
Concrete compressive strength	1.69	1.68	1.75	4.47	4.63	5.45	9.06	9.42	11.12	16.19	16	18.85

4.8 Benefits of Using the Outlier Detection in Concrete Mix Design

Outlier detection, which is part of data mining, aims at finding a point or group of points in the dataset that are significantly deviating in behavior from the rest of the data points. Different factors influence the recognition of an item as an outlier. One of the factors could be seen in the quality of the data. The main causes of the poor quality of data included defective data processing methods. The data is often generated from various heterogeneous sources; human or machine error may occur at data entry or processing. These issues may be found in practical applications. For example, Yu et al. (2015) illustrated the poor quality of the data used because of the lack of reliability from the sensors used.

Another benefit of outlier detection is that it can enhance the strength assessment of the construction process. The strength assessment is usually carried out at 7–28 days after the concrete has been poured. The quality assessment of concrete may include some unusual data. Using the IFS-LOF outlier detection method can improve the reliability of data processing during the concrete mixture design, reducing the expenses and time.

Chapter 5: Conclusions and Recommendations

A detailed analysis of SCMs used in cement mixtures to mitigate ASR was done with the help of the latest reliable testing methods: namely the ASTM AMBT C1260 for determination of deleterious aggregate reactions in concrete, the ASTM C1437 Flow Test for the determination of mortar workability, and the ASTM C 109/C 109M – 02 Hydraulic cement Compression Test for the test of compressive strength in concrete. American testing standards were maintained during these procedures to ensure the reliability of results.

The mortar mix was made by mixing Portland cement with fine aggregate particles in a W/C ratio of 0.47. Afterward, the supplementary materials were mixed with the aggregates by replacing cement. Currently, there are a variety of supplementary materials that claim to mitigate ASR, with varying degrees of success, in concrete structures. Metakaolin, waste glass powder, and Basalt fibers were used as SCMs in our experiments as these are economically viable options and are easily available for use in concrete. Mortar was made with varying percentages (10%, 20%, and 30%) to determine the effect of SCM concentrations in ASR mitigation.

After comparing the results of the different tests, we can see that all the SCMs used in our experiments have varied between either decreasing or increasing the mortar bars ASR expansion based on the SCM replacement level. Metakaolin has been shown to be a great ASR mitigating agent by reducing the amount of ASR gel formed in concrete. Metakaolin, which has pozzolanic properties, was mixed in different ratios as cement replacement. When Metakaolin was used at a 10% replacement, it completely mitigated the harmful effects of ASR in concrete by showing a significant reduction of the concrete expansion below the 0.1% threshold level. However, Metakaolin reduced the flow of concrete and slightly reduced compressive strength at 7 and 14-days.

Microparticles of waste glass powder did not show positive results in the mitigation of ASR reaction in concrete. The mortar bars made with these particles showed no resistance to changes in length and crossed the safety thresholds. Basalt fiber did not show promising results in mitigating the harmful effects of ASR in concrete. All samples went straight into expansion without delay. Moreover, the tiny fibers did not affect the concrete compressive strength.

The combination of waste glass powder and Metakaolin showed good positive results. The concrete showed increased resistance to alkalinity and increases in compressive strength. The ASR mitigation was effective at concentrations of 20% or more. The 10% cement replacement was not that effective at stopping the expansion of concrete. Overall, the method used for testing, the AMBT C1260, was an effective, quick measure of the effectivity of the reactivity of aggregate particles and the highly alkaline concrete mixtures. Specific conclusions were:

- In the samples with 10%, 20%, and 30% where Metakaolin was added, the expansion was 79%, 89%, and 88% less than that of the control specimen.
- The GP decreased the expansion compared to control specimens by 20%, 43%, and 75% at the 10%, 20%, and 30% replacement levels, respectively. It can be concluded that GP of 30% replacement level is recommended.
- Mixtures 9 and 10 of MK+GP showed a significant reduction of ASR by 86% and 90% for the 20% and 30% replacement levels, respectively.
- The binary mixtures of GP+MK at the 20% and 30% levels were more effective than the individual mixtures of MK or GP in reducing the ASR below the threshold limit. The mixtures were effective in decreasing the ASR expansion (60 % reduction) compared to the control mixture at 10% replacement.

- The sample with 10% Lithium and MK showed an excellent reduction in the expansion caused by ASR (92% reduction). The 14th day results showed a total expansion was almost 0.1%, which is at the safe condition of the ASTM 1260 test.
- The cement replacement of 10% with GP+lithium, resulted in 0.209% expansion (51% reduction). However, the 20% and 30% reduction was not enough to pass the ASTM test, and the total expansion went above the 0.1% total expansion safe limit of the test.
- Therefore, the mixture of NCM and Lithium was not an effective solution for ASR reduction in concrete.
- The results showed that basalt fibers were not helping in stopping ASR in concrete. After the third day, all samples had crossed the safety threshold of 0.10% expansion, and the results were very comparable to the control mixtures.

The study suggests using more than one SCM in concrete to make it more resistant to varying parameters. More research is needed to reach reliable and specific results for the concrete mixtures, especially with the continuous demand for concrete mixes. Using manufacturing materials in future research can support the concrete durability and help have better solutions for ASR.

In addition, a cost analysis of the mixtures has been conducted based on the unit price of each material and the quantities used in all mixtures. All mixture's cost was compared to the cost of the control mixture (100% cement). The labor cost was not taken into account. It was found that the MK mixtures were higher in price compared to the control mixtures by 29%, 59%, and 88% for the 10%, 20%, and 30% replacement levels. It can be seen that as the percentage of replacement increases, the cost increases; however, MK has proved to be very effective in reducing the ASR expansion levels. The most expensive mixture was for the 30% replacement level of GP as a SCM, where the cost has reached 148% more compared to the control mixture.

The cheapest mixture was for the NCP at a 10% replacement level, where the cost was almost 50% less than the control mixture (100% cement). In addition, the 3.5% basalt fiber has shown 655% more costly than the control mixture. In conclusion, the manufacturer should compare the high initial cost of using SCMs such as MK and GP compared to the maintenance and rehabilitation of the concrete members. A life cycle assessment should be conducted before making any final decisions.

The IFS-LOF algorithm was developed and compared with LOF and LOF-SW. Dataset of 1030 concrete mixtures datasets was used in the study to investigate the accuracy rate of the IFS-LOF. The concrete mixtures included various material proportions of water, cement, fine aggregate, coarse aggregate, fly ash, slag, and superplasticizers. In addition, the compressive strength and concrete age of all mixtures were included in the analysis. The benefits and drawbacks have been analyzed in the concrete dataset to enhance the strength and workability of concrete mixtures by searching the outlier by measuring the accuracy rate and execution time. The main objective of IFS-LOF is to enhance the accuracy rate in each ingredient of the concrete data and solve the limitation of LOF.

The outcome of the IFS-LOF demonstrated greater improvement in the accuracy rate than other state-of-the-art LOF algorithms. Moreover, the popular LOF algorithm needs broad memory to hold all the data before identifying the local outlier. In addition, it is flawed with respect to the sequences of an outlier.

References

1. Adam, J. T. (2004). Potential concrete aggregate reactivity in northern Nevada [Master's thesis]. UMI Microform.
2. K. Afshinnia, P. Rangaraju, Effectiveness of ground glass powder from recycled glass in mitigating alkali-silica reaction in concrete. *J. Trans. Res. Board*, 2508.
3. Alghushairy, Omar & Alsini, Raed & Ma, Xiaogang & Soule, Terence. (2020). A genetic-based incremental local outlier factor algorithm for efficient data stream processing. 10.1145/3388142.3388160.
4. Aquino, W., Lange, D. & Olek, J., 2001. The Influence of Metakaolin and Silica Fume on the Chemistry of Alkali-Silica Reaction Products. *Cement and Concrete Composites*, Volume 23, pp. 485-493.
5. Aligizaki, K. K. (2006). Pores structure of cement-based material, testing, interpretation and requirements: Modern concrete technology. Taylor & Francis.
6. American Association of State Highway and Transportation Officials (AASHTO). (2014). 110-14: Standard method of test for potential alkali reactivity of aggregates and effectiveness of ASR mitigation measures (Miniature concrete prism test, MCPT). Author.
7. American Association of State Highway and Transportation Officials (AASHTO). (2019). T 380: Standard method of test for potential alkali reactivity of aggregates and effectiveness of ASR mitigation measures (Miniature concrete prism test, MCPT). Author.
8. American Society for Testing and Materials (ASTM). (1995). C. ASTM, 1293-95: Standard test method for concrete aggregates by determination of length change of concrete due to alkali-silica reaction. Author.
9. American Society for Testing and Materials (ASTM). (2003). ASTM B. Stand. Vol. 04.02, ASTM C 295-03: Standard guide for petrographic examination of aggregates for concrete. Author.
10. American Society for Testing and Materials (ASTM). (2007). A. Standard, C1260: Standard test method potential alkali react. Aggregates (Mortar-Bar Method). Author.
11. Aquino, W., Lange, D. & Olek, J. (2001). The Influence of Metakaolin and silica fume on the chemistry of alkali-silica reaction products. *Cement and Concrete Composites*, 23, 485-493.
12. Bach, F., Thorsen, T. S., Nielsen, M. P. (1993). Load-carrying capacity of structural members subjected to alkali-silica reactions. *Constr. Build. Mater.* 7, 109–115.
13. Bažant, Z. P., & Steffens, A. (2000). Mathematical model for kinetics of alkali-silica reaction in concrete. *Cem. Concr. Res.* 30, 419–428.
14. Beaver, J., Jiang, L., & Sherman, M. (2013). Inspection and monitoring of ASR-affected structures at Seabrook Station, NH.

15. Bérubé, M.-A., Duchesne, J., Dorion, J. F., & Rivest, M. (2002). Laboratory assessment of alkali contribution by aggregates to concrete and application to concrete structures affected by alkali-silica reactivity. *Cem. Concr. Res.* 32, 1215–1227.
16. Bérubé, M.-A., & Fournier, B. (1993). Canadian experience with testing for alkali-aggregate reactivity in concrete. *Cem. Concr. Compos.* 15, 27–47.
17. Bérubé, M. A., Fournier, B., Mongeau, P., Dupont, N., Ouellet, C., & Frenette, J. (1992). Effectiveness of the accelerated mortar bar method, ASTM C-9 proposal P 214 or NBRI, for assessing potential AAR in Quebec (Canada), in: *Proceedings of the 9th International Conference Alkali-Aggregate React. Concr. Concr. Soc. London, Publ. CS*, pp. 92–101.
18. Bérubé, M.-A., & Frenette, J. (1994). Testing concrete for AAR in NaOH and NaCl solutions at 38 C and 80 C. *Cem. Concr. Compos.* 16, 189–198.
19. Berra, M., Mangialardi, T., Paolini, A. E., & Turriziani, R. (1991). Critical evaluation of accelerated test methods for detecting the alkali-reactivity of aggregates. *Adv. Cem. Res.* 4, 29–37.
20. Bradley, A. P. (1997). The use of the area under the ROC curve in the evaluation of machine learning algorithms. *Pattern Recognition*, 30(7), 1145–1159.
21. Breunig, M.M. et al. (2000). L of *Proceedings of the 2000 ACM SIGMOD International Conference on Management of Data. SIGMOD 00*, 29, pp. 93–104.
22. Bueno, E. T., Paris, J. M., Clavier, K. A., Spreadbury, C., Ferraro, C.C., & Townsend, T. G. (2020). A review of ground waste glass as a supplementary cementitious material: A focus on alkali-silica reaction. *J. Clean. Prod.* 257(120180).
23. Chandola, V., Banerjee, A. & Kumar, V. (2009). Anomaly detection: A survey. *ACM Computing Surveys (CSUR)*, 41, 15.
24. Cheng, Z., Zou, C. & Dong, J. (2019). Outlier detection using isolation forest and local outlier factor. *Proceedings of the Conference on Research in Adaptive and Convergent Systems*.
25. Chowdhury, M. S. & Mishra, D., 2009. Implementing AASHTO TP 110 for Alkali-Silica Reaction Potential Evaluation of Idaho Aggregates, Boise, Idaho: Boise State University.
26. Cole, W. F., Lancucki, C. J., & Sandy, M. J. (1981). Products formed in an aged concrete. *Cem. Concr. Res.* 11, 443–454.
27. Dang, T. T., Ngan, H. Y. & Liu, W. (2015). Distance-based k-nearest neighbors outlier detection method in large-scale traffic data. *2015 IEEE International Conference on Digital Signal Processing (DSP)*, pp.507–510.
28. De Beauchamp (1995) “The Progress of Remedial Measures at Chambon Dam.” AAR in Hydroelectric Plants and Dams: *Proceedings of the 2nd International Conference*, Chattanooga, USA, United States Committee on Large Dams, 209-220.
29. Diamond, S. (1992). Alkali aggregate reactions in concrete: An annotated bibliography, 1939-1991.

30. Diamond, S. (2000). Chemistry and other characteristics of ASR gels, in: Proceedings of the 11th International Conference Alkali-Aggregate React. Concr: pp. 31–40.
31. Ding, Z. & Fei, M. (2013). An anomaly detection approach based on isolation forest algorithm for streaming data using sliding window. IFAC Proceedings, 46(20), 12–17.
32. Domingues, R. et al. (2018) . A comparative evaluation of outlier detection algorithms: Experiments and analyses. Pattern Recognition, 74, 406–421.
33. Dron, R., & Brivot, F. (1992). Thermodynamic and kinetic approach to the alkali-silica reaction. Part 1. Concepts, Cem. Concr. Res. 22, 941–948.
34. Dron, R., & Brivot, F. (1993). Thermodynamic and kinetic approach to the alkali-silica reaction. Part 2: Experiment. Cem. Concr. Res. 23, 93–103.
35. Dua, D. & Graff, C. (2019). UCI Machine Learning Repository. Irvine, CA: University of California, School of Information and Computer Science. <http://archive.ics.uci.edu/ml>
36. El-Chabib, H., & Ibrahim A. (2013). The performance of ultra-strength flowable concrete made with binary, ternary, and quaternary binder in hot climate. Construction and Building Materials, 47, 245–253.
37. Fanijo, E., Babafemi, A. J., & Arowojolu, O. (2020). Performance of laterized concrete made with palm kernel shell as replacement for coarse aggregate. Constr. Build. Mater. 250(118829).
38. Farny, J., & Kerkhoff, B., 2007. Diagnosis and control of alkali-aggregate reactions in concrete. Portland cement Association, Skokie, Illinois, USA, (413), 26.
39. Farny, J. A., & Kosmatka, S. H. (1997). Diagnosis and control of alkali-aggregate reactions in concrete, Portland cement Association Skokie, IL.
40. Federal Highway Administration, 2007. The use of lithium to prevent or mitigate alkali-silica reaction in concrete pavements and structures [Online]. Accessed March 23, 2020.
41. Fernández-Jiménez, A., García-Lodeiro, I., Palomo, & A. (2007). Durability of alkali-activated fly ash cementitious materials. J. Mater. Sci. 42, 3055–3065.
42. Folliard, K. J., Barborak, R., Drimalas, T., Du, L., Garber, S., Ideker, J., Ley, T., Williams, S., Juenger, M., & Fournier, B. (2006). Preventing ASR/DEF in new concrete.
43. Forster, S. W., Boone, R. L., Hammer, M. S., Lamond, J. F., Lane, D. S., Miller, R. E., Parker, R. E., Pergalsky, A., Pierce, J. S., Robert, M. Q., Schmitt, J. W., & Tobin, R. E. (1998). State-of-the-art report on alkali-aggregate reactivity reported by ACI Committee, 221(98), 1–31.
44. Gholizadeh-Vayghan, A., & Rajabipour, F. (2017). The influence of alkali–silica reaction (ASR) gel composition on its hydrophilic properties and free swelling in contact with water vapor. Cement and Concrete Research, 94, 49–583.
45. Gillerman, V. S., & Weppner, K. N. (2014). Lithologic characterization of active ITD aggregate sources and implications for aggregate quality, Idaho. Transportation Department.

46. Gillott, J. E., & Swenson, E. G. (1969). Mechanism of the alkali-carbonate rock reaction. *Q. J. Eng. Geol. Hydrogeol.* 2, 7–23.
47. Glasser, F. P. (1992). Chemistry of the alkali-aggregate reaction. *Alkali-Silica React. Concrete*, 30–53.
48. Guo, Z., Wan, C., Xu, M. & Chen, J., 2018. Review of Basalt Fiber-Reinforced Concrete in China: Alkali Resistance of Fibers and Static Mechanical Properties of Composites. *Sustainable Building Materials and Technologies*, Volume 2018.
49. Godart, B., de Rooij, M. R., & Wood, J. G. M. (2013). Guide to diagnosis and appraisal of AAR damage to concrete in structures. Springer.
50. Godart, B., I. Sims, P. Nixon, B. Capra, M. de Rooij, J. Wood, O. Expert Consultant, F. Avon, The RILEM guidance on appraisal and management of structures damaged by AAR, in: *Proc. 13th Int. Conf. Alkali-Aggregate React. Concr.*, 2012.
51. Goguel, R. Alkali release by volcanic aggregates in concrete, *Cem. Concr. Res.* 25 (1995) 841–852.
52. Goldstein, M. & Uchida, S. (2016). A Comparative Evaluation of Unsupervised Anomaly Detection Algorithms for Multivariate Data. *Plos One*, 11(4).
53. P.E. Grattan-Bellew, Laboratory evaluation of alkali-silica reaction in concrete from Saunders Generating Station, *Mater. J.* 92 (1995) 126–134.
54. P.E. Grattan-Bellew, L. Mitchell, Preventing concrete deterioration due to alkali-aggregate reaction, Institute for Research in Construction, National Research Council of Canada, 2002.
55. P.E. Grattan-Bellew, L.D. Mitchell, J. Margeson, D. Min, Is alkali-carbonate reaction just a variant of alkali-silica reaction $ACR = ASR?$, *Cem. Concr. Res.* 40 (2010) 556–562.
56. Guo, Z., Wan, C., Xu, M. & Chen, J., 2018. Review of Basalt Fiber-Reinforced Concrete in China: Alkali Resistance of Fibers and Static Mechanical Properties of Composites. *Sustainable Building Materials and Technologies*, Volume 2018.
57. Haddad, R. & Smadi, M. M., 2004. Role of fibers in controlling unrestrained expansion and arresting cracking in Portland cement concrete undergoing alkali-silica reaction. *Cement and Concrete Research*, 34(1).
58. Haddad, R. & Smadi, M. M., 2004. Role of fibers in controlling unrestrained expansion and arresting cracking in Portland cement concrete undergoing alkali-silica reaction. *Cement and Concrete Research*, 34(1).
59. L. Halsey, W. Heyen, Evaluation of Nebraska's aggregate reactivity by the miniature concrete prism test method—AASHTO T380, (2019).
60. S. Han, M. Fang, Alkali-aggregate reaction under high temperature, high pressure and high alkali content, *J. Nanjing Inst. Chem. Technol.* 2 (1984) 1–10.
61. Hanley, J.A. & Mcneil, B.J. (1982). The meaning and use of the area under a receiver operating characteristic (ROC) curve. *Radiology*, 143(1), pp.29–36.

62. R. Helmuth, D. Stark, S. Diamond, M. Moranville-Regourd, Alkali-silica reactivity: an overview of research, *Contract*. 100 (1993) 202.
63. D.W. Hobbs, "Alkali-Silica Reaction in concrete", Thomas Telford, London (1988), (n.d.).
64. D.W. Hobbs, W.A. Gutteridge, Particle size of aggregate and its influence upon the expansion caused by the alkali-silica reaction, *Mag. Concr. Res.* 31 (1979) 235-242.
65. R.D. Hooton, New aggregates alkali-reactivity test methods. Ministry of Transportation, (1991).
66. Ibrahim A., and El-Chabib, H., (2013). Ultra-strength flowable concrete made with high volume of supplementary cementitious materials. *ASCE Journal of Materials in Civil engineering*, 25, No. 12. pp. 1830-1839. DOI: 10.1061/ (ASCE) MT.1943-5533.0000746.
67. Ibrahim A., and Mahmoud E., and Ali, T. (2013). Macroscopic Compressive Strength of High-Strength Self-Consolidating concrete with high volume of cementitious materials based on real digital image. *Construction and Building Materials*, 38, 1161-1169, DOI: 10.1016/j.conbuildmat.2012.09.066.
68. Ibrahim A., Mahmoud E., and Khodair Y., (2013). Fresh, Mechanical, and Durability Characteristics of Self-Consolidating Concrete Incorporating Recycled Asphalt Pavements. *ASCE, Journal of Materials in Civil Engineering*, 26(4), 668-675. DOI: 10.1061/ (ASCE) MT.1943-5533.0000832.
69. T. Ichikawa, M. Miura, Modified model of alkali-silica reaction, *Cem. Concr. Res.* 37 (2007) 1291-1297.
70. J.H. Ideker, B.L. East, K.J. Folliard, M.D.A. Thomas, B. Fournier, The current state of the accelerated concrete prism test, *Cem. Concr. Res.* 40 (2010) 550-555.
71. M.S. Islam, Performance of Nevada's aggregates in alkali-aggregate reactivity of Portland cement concrete, (2010).
72. M.S. Islam, S. Akhtar, A critical assessment to the performance of alkali-silica reaction (ASR) in concrete, *Can. Chem. Trans.* 1 (2013) 253-266.
73. M.S. Islam, N. Ghafoori, Comparison of concrete expansion and stiffness due to alkali-silica reactivity, in: *Proc. Concr. Solut. Ser. (The 4th Int. Conf. Concr. Repair)*, 2011: pp. 243-250.
74. W. Jin, Alkali-silica reaction in concrete with glass aggregate: A chemo-physico-mechanical approach., (1999).
75. Justyna, Z.-S., 2017. Alkali Silica Reaction In The Presence Of Metakaolin - The Significant Role of Calcium Hydroxide. *IOP Conference Series: Materials, Science and Engineering*, Volume 245.
76. S. Kandasamy, M.H. Shehata, The capacity of ternary blends containing slag and high-calcium fly ash to mitigate alkali silica reaction, *Cem. Concr. Compos.* 49 (2014) 92-99.
77. Kara De Maeijer, P., 2014. Challenge of ASR in the Use of Waste Glass Slurry. *Riga: s.n.*

78. Ke, G. et al. 2018. Mitigation Effect of Waste Glass Powders on Alkali–Silica Reaction (ASR) Expansion in cementitious Composite. *Int J Concr Struct Mater*, 12(67).
79. Knorr, E.M. & Ng, R.T. (1998). Algorithms for Mining Distance-Based Outliers in Large Datasets. *Algorithms for Mining Distance-Based Outliers in Large Datasets | Proceedings of the 24th International Conference on Very Large Data Bases*. Available at: <https://dl.acm.org/doi/10.5555/645924.671334>.
80. J.T. Kolawole, R. Combrinck, W.P. Boshoff, Rheo-viscoelastic behaviour of fresh cement-based materials: cement paste, mortar and concrete, *Constr. Build. Mater.* 248 (2020) 118667. <https://doi.org/https://doi.org/10.1016/j.conbuildmat.2020.118667>.
81. T. Kuroda, S. Inoue, A. Yoshino, S. Nishibayashi, Effects of particle size grading and content of reactive aggregate on ASR expansion of mortars subjected to autoclave method, in: *Proc. 12th Int. Conf. Alkali-Aggregate React. Concr.* Beijing, China, 2004.
82. D.S. Lane, Alkali-silica reactivity in Virginia., Virginia Transportation Research Council, 1994.
83. E. Latifee. Miniature concrete prism test-A new test method for evaluating the ASR potential of aggregates, the effectiveness of asr mitigation and the job mixture, (2013).
84. E.R. Latifee, State-of-the-art report on alkali silica reactivity mitigation effectiveness using different types of fly ashes, *J. Mater.* 2016 (2016) 1–7
85. E.R. Latifee, S. Akther, K.A. Hasnat, Critical review of the test methods for evaluating the ASR potential of aggregates, in: *Proc. 10th Glob. Eng. Sci. Technol. Conf.*, 2015: pp. 2–3.
86. E.R. Latifee, P.R. Rangaraju, Miniature concrete prism test: rapid test method for evaluating alkali-silica reactivity of aggregates, *J. Mater. Civ. Eng.* 27 (2015) 4014215
87. P. Léger, P. Côté, R. Tinawi, Finite element analysis of concrete swelling due to alkali-aggregate reactions in dams, *Comput. Struct.* 60 (1996) 601–611.
88. Lenke, L. R. & Malvar, L. J., 2009. Alkali Silica Reaction Criteria for Accelerated Mortar Bar Tests Based on Field Performance Data. Lexington, World of Coal Ash (WOCA).
89. M. Lima, R. Salamy, D. Miller, CFRP Strengthening of ASR affected concrete piers of railway bridges, in: *Maintenance, Safety, Risk, Manag. Life-Cycle Perform. Bridg. Proc. Ninth Int. Conf. Bridg. Maintenance, Saf. Manag. (IABMAS 2018)*, 9-13 July 2018, Melbourne, Aust., CRC Press, 2018: p. 346.
90. J. Lindgård, Ö. Andiç-Çakır, I. Fernandes, T.F. Rønning, M.D.A. Thomas, Alkali–silica reactions (ASR): Literature review on parameters influencing laboratory performance testing, *Cem. Concr. Res.* 42 (2012) 223–243. <https://doi.org/https://doi.org/10.1016/j.cemconres.2011.10.004>
91. Lipatov, Y., Manylov, M. S. & Gutnikov, S. I., 2015. High alkali-resistant basalt fiber for reinforcing concrete. *Materials and Design*, Volume 73.

92. Liu, F.T., Ting, K.M. & Zhou, Z.-H. (2008). Isolation Forest. 2008 Eighth IEEE International Conference on Data Mining.
93. F. Locati, S. Marfil, E. Baldo, Effect of ductile deformation of quartz-bearing rocks on the alkali-silica reaction, *Eng. Geol.* 116 (2010) 117–128.
94. D. Lu, B. Fournier, P.E. Grattan-Bellew, Z. Xu, M. Tang, Development of a universal accelerated test for alkali-silica and alkali-carbonate reactivity of concrete aggregates, *Mater. Struct.* 41 (2008) 235–246.
95. D. Lu, X. Zhou, Z. Xu, X. Lan, M. Tang, B. Fournier, Evaluation of laboratory test method for determining the potential alkali contribution from aggregate and the ASR safety of the Three-Gorges dam concrete, *Cem. Concr. Res.* 36 (2006) 1157–1165.
96. Mahmoud E., Ibrahim A., and El-Chabib H., (2013). Laboratory investigation of self-consolidating concrete containing sustainable technologies: Recycled asphalt pavements, fly ash, & slag. *International Journal of Concrete Structures and Materials*, 7(2), 155-163. DOI 10.1007/s40069-013-0044-1.
97. L.J. Malvar, G.D. Cline, D.F. Burke, R. Rollings, T.W. Sherman, J.L. Greene, Alkali-silica reaction mitigation: state of the art and recommendations, *Mater. J.* 99 (2002) 480–489.
98. L.J. Malvar, L.R. Lenke, Efficiency of fly ash in mitigating alkali-silica reaction based on chemical composition, *ACI Materials Journal*, 2006, 103(5), 319-326.
99. K. Mather, & B. Mather, Method of petrographic examination of aggregates for concrete, in: *PROCEEDINGS-AMERICAN Soc. Test. Mater., AMER SOC TESTING MATERIALS 100 BARR HARBOR DR, W CONSHOCKEN, PA 19428-2959, 1950: pp. 1288–1313.*
100. M. Moisson, M. Cyr, E. Ringot, A. Carles-Gibergues, EFFICIENCY OF REACTIVE AGGREGATE POWDER IN CONTROLLING THE EXPANSION on CONCRETE AFFECTED BY ALKALI-SILICA REACTION (ASR), in: *第十二届国际混凝土碱集料反应会议论文集 (I)*, 2004.
101. P.J.M. Monteiro, K. Shomglin, H.R. Wenk, N.P. Hasparyk, Effect of aggregate deformation on alkali-silica reaction, *Mater. J.* 98 (2001) 179–183.
102. R.D. Moser, A.R. Jayapalan, V.Y. Garas, K.E. Kurtis, Assessment of binary and ternary blends of Metakaolin and Class C fly ash for alkali-silica reaction mitigation in concrete, *Cem. Concr. Res.* 40 (2010) 1664–1672.
103. S. Multon, M. Cyr, A. Sellier, P. Diederich, L. Petit, Effects of aggregate size and alkali content on ASR expansion, *Cem. Concr. Res.* 40 (2010) 508–516.
104. T.R. Naik, Sustainability of concrete construction, *Pract. Period. Struct. Des. Constr.* 13 (2008) 98–103.
105. Niennattrakul, V., Keogh, E. & Ratanamahatana, C.A. (2010). Data Editing Techniques to Allow the Application of Distance-Based Outlier Detection to Streams. 2010 IEEE International Conference on Data Mining.

106. Nixon, P., & Sims, I. Testing aggregates for alkali-reactivity, *Mater. Struct.* 29 (1996) 323–334.
107. Oberholseter & Davies (1986), National Building Research Institute (NBRI)
108. K. Ono, Damaged concrete structures in Japan due to alkali silica reaction, *Int. J. Cem. Compos. Light. Concr.* 10 (1988) 247–257.
109. M. Palacios, F. Puertas, Effect of carbonation on alkali-activated slag paste, *J. Am. Ceram. Soc.* 89 (2006) 3211–3221.
110. A. Pedneault, Development of testing and analytical procedures for the evaluation of the residual potential of reaction, expansion, and deterioration of concrete affected by ASR, *M. Sc. Mem. Laval Univ. Québec City, Canada.* 133 (1996).
111. A.B. Poole, Introduction to alkali-aggregate reaction in concrete, in: *Alkali-Silica React. Concr.*, CRC Press, 1991: pp. 17–45.
112. A.B. Poole, Alkali-silica reactivity mechanisms of gel formation and expansion, in: *Proc. 9th Int. Conf. Alkali-Aggregate React. London*, Concrete Society Publications CS, 1992: pp. 782–789.
113. Ramaswamy, Sridhar & Rastogi, Rajeev & Shim, Kyuseok. (2000). Efficient Algorithms for Mining Outliers from Large Data Sets.. *ACM SIGMOD Record.* 29. 427-438. 10.1145/335191.335437.
114. P. Rangaraju, A. Kaveh, S. Enugula, E. Latifee, Evaluation of alkali-silica reaction potential of marginal aggregates using miniature concrete prism test (MCPT), in: *Proc. 15th Int. Conf. Alkali-Reaction Concret. Sao Paulo, Brazil*, 2016: pp. 4–7.
115. R. Ranc, L. Debray, Reference test methods and a performance criterion for concrete structures, in: *NINTH Int. Conf. ALKALI-AGGREGATE React. Concr. JULY 1992, LONDON*, Vol. 2, 1992.
116. P. Rivard, M.-A. Bérubé, J.-P. Ollivier, G. Ballivy, Alkali mass balance during the accelerated concrete prism test for alkali–aggregate reactivity, *Cem. Concr. Res.* 33 (2003) 1147–1153.
117. P. Rivard, M.A. Bérubé, J.P. Ollivier, G. Ballivy, Decrease of pore solution alkalinity in concrete tested for alkali-silica reaction, *Mater. Struct.* 40 (2007) 909–921.
118. A.K. Saha, M.N.N. Khan, P.K. Sarker, F.A. Shaikh, A. Pramanik, The ASR mechanism of reactive aggregates in concrete and its mitigation by fly ash: A critical review, *Constr. Build. Mater.* 171 (2018) 743–758.
119. S.M.H. Shafaatian, A. Akhavan, H. Maraghechi, F. Rajabipour, How does fly ash mitigate alkali–silica reaction (ASR) in accelerated mortar bar test (ASTM C1567)?, *Cem. Concr. Compos.* 37 (2013) 143–153.
120. C.-S. Shon, D.G. Zollinger, S.L. Sarkar, Evaluation of modified ASTM C 1260 accelerated mortar bar test for alkali–silica reactivity, *Cem. Concr. Res.* 32 (2002) 1981–1987.

121. Y. Shao, T. Lefort, S. Moras, D. Rodriguez, Studies on concrete containing ground waste glass, *Cem. Concr. Res.* 30 (2000) 91–100.
122. A. Shayan, A. Xu, H. Morris, Comparative study of the concrete prism test (CPT 60 degrees Celsius, 100 per cent RH [relative humidity]) and other accelerated tests, in: *Int. Conf. Alkali-Aggregate React. Concr. (ICAAR)*, 13th, 2008, Trondheim, Norw., 2008.
123. M.H. Shehata, M.D.A. Thomas, The effect of fly ash composition on the expansion of concrete due to alkali–silica reaction, *Cement and Concrete Research*, 2000, 30(7), 1063-1072.
124. C. Shi, Z. Shi, X. Hu, R. Zhao, L. Chong, A review on alkali-aggregate reactions in alkali-activated mortars/concretes made with alkali-reactive aggregates, *Mater. Struct.* 48 (2015) 621–628.
125. Staerman, G., Mozharovskyi, P., Cléménçon, S. & d'Alché-Buc, F.. (2019). Functional Isolation Forest. *Proceedings of The Eleventh Asian Conference on Machine Learning*, in PMLR.
126. Stanton, T., 1940. Influence of cement and aggregate on concrete expansion. *Engineering News-Record*.
127. T.E. Stanton, *Expansion of concrete through reaction between cement and aggregate*, 2008.
128. Stark, D. and Depuy, G., Alkali-silica reaction in five dams in southwestern United States. *Proceedings of the Katherine and Bryant Mather International Conference on Concrete Durability*, Atlanta, Georgia (USA), April 1987, ACI SP-100, pp. 1759-1786, 1987.
129. D. Stark, B. Morgan, P. Okamoto, S. Diamond, Eliminating or minimizing alkali–silica reactivity. *Strategic Highway Research Program, SHRP-P-343*, Washington, DC, 1993.
130. R.N. Swamy, *The alkali-silica reaction in concrete*. Blackie and Son Ltd., Glasgow, London, (1992).
131. Tang, J. et al. (2002). Enhancing Effectiveness of Outlier Detections for Low Density Patterns. *Advances in Knowledge Discovery and Data Mining Lecture Notes in Computer Science*, pp.535–548.
132. Tang, Jialing & Ngan, Henry Y.T.. (2016). Traffic Outlier Detection by Density-Based Bounded Local Outlier Factors. *IT in Industry*. 4. 6-18.
133. N. Thaulow, U.H. Jakobsen, B. Clark, Composition of alkali silica gel and ettringite in concrete railroad ties: SEM-EDX and X-ray diffraction analyses, *Cem. Concr. Res.* 26 (1996) 309–318.
134. M.D.A. Thomas, B. Fournier, K.J. Folliard, Y. Resendez, *Alkali-Silica Reactivity Field Identification Handbook*, United States. Federal Highway Administration. Office of Pavement Technology, 2011.
135. M. Thomas, A. Dunster, P. Nixon, B. Blackwell, Effect of fly ash on the expansion of concrete due to alkali-silica reaction–Exposure site studies, *Cem. Concr. Compos.* 33 (2011) 359–367.

136. Thomas, M. & Fournier, B., 2006. Test methods for evaluating preventive measures for controlling expansion due to alkali-silica reaction in concrete. *Cement and Concrete Research* 36(10), 1842-1856.
137. M.D.A. Thomas, B. Fournier, K.J. Folliard, Selecting measures to prevent deleterious alkali-silica reaction in concrete: rationale for the AASHTO PP65 prescriptive approach., United States. Federal Highway Administration, 2012.
138. M.D.A. Thomas, B. Fournier, K.J. Folliard, J.H. Ideker, Y. Resendez, The use of lithium to prevent or mitigate alkali-silica reaction in concrete pavements and structures., Turner-Fairbank Highway Research Center, 2007.
139. M. Thomas, B. Fournier, K. Folliard, J. Ideker, M. Shehata, Test methods for evaluating preventive measures for controlling expansion due to alkali-silica reaction in concrete, *Cem. Concr. Res.* 36 (2006) 1842–1856.
140. W. Touma, D.W. Fowler, R.L. Carrasquillo, Alkali-silica reaction in portland cement concrete: testing methods and mitigation alternatives, 2001.
141. Ulm, F., Coussy, O., Kefei, L. & Larive, C., 2000. Thermo-chemo-mechanics of ASR expansion in concrete structures. *Thermo-chemo-mechanics of ASR expansion in concrete structures*, 126(3), pp. 233-242.
142. Wang, H., Bah, M.J. & Hammad, M. (2019). Progress in Outlier Detection Techniques: A Survey. *IEEE Access*, 7, pp.107964–108000.
143. X. Wang, M. Nguyen, M.G. Stewart, M. Syme, A. Leitch, Analysis of climate change impacts on the deterioration of concrete infrastructure—part 1: mechanisms, practices, modelling and simulations—a review, Publ. by CSIRO, Canberra. ISBN. 9780 (2010) 8.
144. H. Woods, Durability of concrete construction, (1968).
145. H. Xu, On the alkali content of cement in AAR, in: *Concr. Alkali-Aggregate React. Proc. 7th Int. Conf.* Ed. by Grattan-Bellew, Patrick E., Noyes Publ. Park Ridge, New Jersey, 1987: pp. 451–455.
146. Yan, Y. et al. (2017). Distributed Local Outlier Detection in Big Data. *Proceedings of the 23rd ACM SIGKDD International Conference on Knowledge Discovery and Data Mining*.
147. Yan, Y., Cao, L. & Rundensteiner, E.A. (2017). Scalable Top-n Local Outlier Detection. *Proceedings of the 23rd ACM SIGKDD International Conference on Knowledge Discovery and Data Mining*
148. Yan, Hang & Yang, Nan & Peng, Yi & Ren, Yitian. (2020). Data mining in the construction industry: Present status, opportunities, and future trends. *Automation in Construction*. 119. 103331. 10.1016/j.autcon.2020.103331
149. Yeh, I.-C. (1998). Modeling of strength of high-performance concrete using artificial neural networks. *Cement and Concrete Research*, 28(12), pp.1797–1808

150. Yu, A. W. (2017, September 13). Investigating a big dam concrete problem. MIT News. Concrete Sustainability Lab. <https://news.mit.edu/2017/concrete-researchers-investigate-big-dam-problem-0913>
151. Yu, Zhun & Haghghat, Fariborz & Fung, Benjamin. (2015). Advances and challenges in building engineering and data mining applications for energy-efficient communities. *Sustainable Cities and Society*. 10.1016/j.scs.2015.12.001.
152. Zhang, Mengxi & Li, Mingchao & Shen, Yang & Ren, Qiubing & Zhang, Jinrui. (2019). Multiple mechanical properties prediction of hydraulic concrete in the form of combined damming by experimental data mining. *Construction and Building Materials*. 207. 661-671. 10.1016/j.conbuildmat.2019.02.169.
153. C. Zhang, A. Wang, M. Tang, B. Wu, N. Zhang, Influence of aggregate size and aggregate size grading on ASR expansion, *Cem. Concr. Res.* 29 (1999) 1393–1396.
154. P. Nixon, B. Fournier, Assessment, Testing and Specification, Alkali-Aggregate React.
155. *Concr. A World Rev.* (2017).
156. Najafi, Fazil, and Sarah Rajkumari Jayasekaran. "A Graduate Research on the Cost-Effective Analysis and Environmental Impact of Using Industrial Byproducts as Supplementary Cementitious Materials in Building Construction." 2017 ASEE Annual Conference & Exposition Proceedings, doi:10.18260/1-2
157. "Concrete Cracking – A Destructive Kind." Western Technologies, wt-us.com/concrete-cracking-a-destructive-kind/.
158. Toutanji, H., et al. "Effect of Supplementary Cementitious Materials on the Compressive Strength and Durability of Short-Term Cured Concrete." *Cement and Concrete Research*, vol. 34, no. 2, 2004, pp. 311–319., doi:10.1016/j.cemconres.2003.08.017.
159. Islam, G.M. Sadiqul, et al. "Waste Glass Powder as Partial Replacement of Cement for Sustainable Concrete Practice." *International Journal of Sustainable Built Environment*, vol. 6, no. 1, 2017, pp. 37–44., doi:10.1016/j.ijjsbe.2016.10.005.
160. H. Hu, Y. Liu,(2010). 11 - High modulus, high tenacity yarns, Editor(s): R. Alagirusamy, A. Das, In Woodhead Publishing Series in Textiles, Technical Textile Yarns, Woodhead Publishing, 2010.
161. Aquino, W., Lange, D. & Olek, J., 2001. The Influence of Metakaolin and Silica Fume on the Chemistry of Alkali-Silica Reaction Products. *Cement and Concrete Composites*, Volume 23, pp. 485-493.
162. Chowdhury, M. S. & Mishra, D., 2009. Implementing AASHTO TP 110 for Alkali-Silica Reaction Potential Evaluation of Idaho Aggregates, Boise, Idaho: Boise State University.
163. Farny, J. & Kerkhoff, B., 2007. Diagnosis and Control of Alkali-Aggregate Reactions in Concrete. Portland Cement Association, Skokie, Illinois, USA, Issue 413, p. 26.

164. Federal Highway Administration, 2007. The Use of Lithium to Prevent Or Mitigate Alkali-Silica Reaction in Concrete Pavements and Structures. [Online] Available at: <https://www.fhwa.dot.gov/publicationsresearch/infrastructure/pavements/concrete/06133/002.cfm> [Accessed 23 March 2020].
165. Guo, Z., Wan, C., Xu, M. & Chen, J., 2018. Review of Basalt Fiber-Reinforced Concrete in China: Alkali Resistance of Fibers and Static Mechanical Properties of Composites. Sustainable Building Materials and Technologies, Volume 2018.
166. Haddad, R. & Smadi, M. M., 2004. Role of fibers in controlling unrestrained expansion and arresting cracking in Portland cement concrete undergoing alkali-silica reaction. Cement and Concrete Research, 34(1).
167. Justyna, Z.-S., 2017. Alkali Silica Reaction In The Presence Of Metakaolin - The Significant Role of Calcium Hydroxide. IOP Conference Series: Materials, Science and Engineering, Volume 245.
168. Kara De Maeijer, P., 2014. Challenge of ASR in the Use of Waste Glass Slurry. Riga: s.n.
169. Ke, G. et al., 2018. Mitigation Effect of Waste Glass Powders on Alkali-Silica Reaction (ASR) Expansion in Cementitious Composite. Int J Concr Struct Mater, 12(67).
170. Lenke, L. R. & Malvar, L. J., 2009. Alkali Silica Reaction Criteria for Accelerated Mortar Bar Tests Based on Field Performance Data. Lexington, World of Coal Ash (WOCA).
171. Lipatov, Y., Manylov, M. S. & Gutnikov, S. I., 2015. High alkali-resistant basalt fiber for reinforcing Concrete. Materials and Design, Volume 73.
172. Stanton, T., 1940. Influence of Cement and aggregate on concrete expansion. Engineering News- Record.
173. Thomas, M. & Fournier, B., 2006. Test Methods for Evaluating Preventive Measures for Controlling Expansion due to Alkali-Silica Reaction in Concrete. Cement and Concrete Research 36, Volume 10, pp. 1842-1856.
174. Ulm, F., Coussy, O., Kefei, L. & Larive, C., 2000. Thermo-chemo-mechanics of ASR expansion in concrete structures. Thermo-chemo-mechanics of ASR expansion in concrete structures, 126(3), pp. 233-242.
175. Gholizadeh-Vayghan, A. and Rajabipour, F., 'The influence of alkali-silica reaction (ASR) gel composition on its hydrophilic properties and free swelling in contact with water vapor', Cement and Concrete Research 94 (2017) 49-583.
176. K. K. Aligizaki, Pores structure of cement-based material, testing, interpretation and requirements, Modern concrete technology, Taylor & Francis, 2006.
177. M.H. Shehata, M.D.A. Thomas, The effect of fly ash composition on the expansion of Concrete due to alkali-silica reaction, Cement and Concrete Research, 2000, 30(7), 1063-1072.

178. L.J. Malvar, L.R. Lenke, Efficiency of fly ash in mitigating alkali-silica reaction based on chemical composition, *ACI Materials Journal*, 2006, 103(5), 319-326.

Appendix

A.1. Guidelines for Use Dosage

The dosage of MasterLife ASR 30 admixture is based on the alkali content of the cement but may be adjusted depending on the particular ingredients of the concrete mixture (see Note 1).

A. Determine the amount of cement (lb/yd³ or kg/m³) in the mixture.

$$=1466.24 \text{ g}$$

$$=1.46624 \text{ KG/m}^3$$

B. Determine the alkali content of the cement (%).

high-alkali content (Na₂O_{eq} of 0.88%) with Blaine's fineness of 383 m³/kg

C. Determine the preferred dosage multiplier. If you are using gal/yd³, multiplier is 0.55. If you are using L/m³, multiplier is 4.6.

D. Dosage = (A) x (B) x (C) 100

A.2. Chemical composition of the used materials

a. Cement



1601 Rockwell Road LaSalle, IL 61301
(815)224-2112

MILL TEST REPORT

Cement Type: I
Production Period: November 1 - 30, 2020
Report Date: January 13, 2021

Chemical Data		Test Result
Al ₂ O ₃ (C 114)	%	5.3
Fe ₂ O ₃ (C 114)	%	2.45
MgO (C 114)	%	2.7
SO ₃ (C 114)	%	4.15
Na ₂ O (C 114)	%	0.35
Ignition Loss (LOI) (C 114)	%	2.0
Equivalent Alkalies (C 150)	%	1.01
Insoluble Residue (C 114)	%	0.71
Limestone (C 150)	%	3.6
CaCO ₃ in Limestone (C 150)	%	77
CO ₂ (C 114)	%	1.2
Potential Cement Phase Composition (C 150-09)		
C ₃ S	%	55
C ₂ S	%	12
C ₄ AF	%	7
C ₃ A	%	10
Physical Data		Test Result
Air Content (C185)	%	6.5
Blaine Fineness (C204)	cm ² /g	3779
325 Fineness (C430)	% <	95.9
Expansion, Autoclave (C 151)	%	0.12
Expansion, Mortar Bar (C 1038)	%	0.008
Compressive Strength (C109)		
1 day	psi	2762
3 days	psi	3997
7 days	psi	4977
28 days	psi	5872
Time of Setting (Vicat) (C191)		
Initial	min	91
Final	min	210

Notes:

We certify that the above described cement at the time of shipment meets the chemical and physical requirements of the ASTM C 150, and AASHTO M 85 specifications. The above data represents the average for above stated production period.



Kevin Jensen
Chief Chemist

1/13/2021

Date

We are an AASHTO accredited laboratory


b. NewCem Plus

LAFARGE
NORTH AMERICA

Cement

NewCem Plus

Analysis by: Lafarge Concrete Lab
Sample from : Seattle Blending Facility
Average Analysis: May 2020
Mill Certificate ID: 5-20 BSCM


 Certified to
 NSF/ANSI 61

Chemical Analysis

Total Alkalies as Equivalent Na ₂ O	2.05 %
Available Alkali as Equiv. Na ₂ O (previous month's result)	0.5 %
CaO Fly Ash *	15
SO ₃ Fly Ash *	1.2 %
SO ₃ Slag **	2.8 %
S Ion Slag **	0.8 %

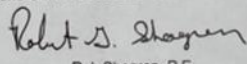
Physical Analysis

Ground Granulated Blast Furnace Slag SAI, 28 Day **	110 %
Class/Type F Fly Ash Pozzolanic Activity Index, 28 Day *	107 %
LOI Fly Ash *	0.59 %
Autoclave Fly Ash *	0.04 %
Autoclave Slag **	0.00 %
45 _μ Fly Ash*	17.5 %
45 _μ Slag**	4.5 %
Density	2.75 Mg/m ³

Cementitious Blend

Class/Type F Fly Ash Blend Percentage	50 %
Ground Granulated Blast Furnace Slag Blend Percentage	50 %

We hereby certify this blended SCM product meets the requirements of
 ASTM C-1697 SCMb-50S/50F and CSA A-3000 BMB-50F/S.

Certified: 
 Rob Shogren, P.E.
 Technical Engineer
 Lafarge North America

* 5-20F Centralia Class/Type F Fly Ash Cert
 ** SEA_NEWCEM May 2020 Ground Granulated Blast Furnace Slag Cert

c. Metakaolin

Chemical Composition, Wt.:

<i>SiO₂</i>	<i>52-55%</i>	<i>CaO</i>	<i><0.20%</i>
<i>Al₂O₃</i>	<i>41-44%</i>	<i>MgO</i>	<i><0.10%</i>
<i>Fe₂O₃</i>	<i><1.90%</i>	<i>Na₂O</i>	<i><0.05%</i>
<i>TiO₂</i>	<i><3.0%</i>	<i>K₂O</i>	<i><0.75%</i>
<i>SO₄</i>	<i><0.05%</i>	<i>L.O.I.</i>	<i><0.50%</i>
<i>P₂O₅</i>	<i><0.2%</i>		

A.3. The Algorithm

```

package lofalgorithm;

import be.cylab.java.roc.Roc;
import java.awt.Point;
import java.io.BufferedReader;
import java.io.BufferedWriter;
import java.io.File;
import java.io.FileNotFoundException;
import java.io.FileReader;
import java.io.FileWriter;
import java.io.IOException;
import java.io.InputStreamReader;
import java.io.PrintWriter;
import java.util.ArrayList;
import java.util.Collections;
import java.util.List;
import java.util.Scanner;

public class LOF {

    static long startTime;
    static long endTime;

    static List<List<Double>> points = new ArrayList<>(); //Points
after converted to Double Coordinates
    static List<String> rawPoints = new ArrayList<>(); //For points
entered from input

    private static int k=8;

    static Double [] threshold = {0.80, 0.90 ,0.95, 1.0 ,1.05,
1.10, 1.15, 1.20,1.30,2.0, 3.0 }; //Threshold values

    public ArrayList<Double> getDisList(List<Double> data) {
        ArrayList<Double> disList = new ArrayList<Double>();
        for (List<Double> point : points) {
            if (!point.equals(data)) {
                disList.add(Math.abs(point.get(0) -
data.get(0))
                                + Math.abs(point.get(1) -
data.get(1)));
            }
        } //End of for loop

        return disList;
    } //End of getDistList

```

```

public double kdistance(List<Double> data) {
    ArrayList<Double> disList = getDisList(data);
    Collections.sort(disList);
    return disList.get(k - 1);
} //End of kdistance

public ArrayList<List<Double>> nk(List<Double> data) {
    ArrayList<List<Double>> nk = new
ArrayList<List<Double>>();
    double kdis = kdistance(data);
    for (List<Double> point : points) {
        if (!point.equals(data)) {
            if (kdis >= Math.abs(point.get(0) -
data.get(0))
                                + Math.abs(point.get(1) -
data.get(1))) {
                nk.add(point);
            }
        }
    }
    return nk;
} //End of nk

public double reactDist(List<Double> data1, List<Double> data2)
{
    return Math.max(
        Math.abs(data1.get(0) - data2.get(0))
        + Math.abs(data1.get(1) -
data2.get(1)),
        kdistance(data2));
} //End of reactDist Function

public double lrd(List<Double> data) {
    double ret = 0, deno = 0;
    for (List<Double> point : nk(data)) {
        deno += reactDist(data, point);
    }
    ret = nk(data).size() / deno;
    return ret;
}

public double lof(List<Double> data) {
    double ret = 0;
    ArrayList<List<Double>> nk = nk(data);
    for (List<Double> point : nk) {
        ret += lrd(point);
    }
    ret /= lrd(data);
    ret /= nk.size();
    return ret;
} //End of LOF Function

```



```

public static void main(String[] args) {

    startTime = System.currentTimeMillis(); //For Seconds

    LOF lof = new LOF();

    //Reading data from the file until the end of file
    BufferedReader br = null;
    try {
        File f = new
File("C:\\Users\\Alienware\\Desktop\\testisolate\\concrete.txt");
//File location
        br = new BufferedReader(new FileReader(f));
// br = new BufferedReader(new InputStreamReader(System.in));
        String s;
        while ( (s = br.readLine()) != null) {
            rawPoints.add(s);
        }
    } catch (FileNotFoundException e) {
        e.printStackTrace();
    } catch (IOException e) {
        e.printStackTrace();
    } finally {
        if (br != null) {
            try {
                br.close();
            } catch (IOException e) {
                e.printStackTrace();
            }
        }
    }
} //End of input try-catch

List<String> randomPoints = new ArrayList<>();

for(int i=0; i <= 500; i++) //Loop to number of wanted points
{
    int range = ( rawPoints.size() - 0) + 1;
    int random = (int) (Math.random() * range) + 0;

    randomPoints.add(rawPoints.get(random));
    rawPoints.remove(random); //To not duplicate selected points

} //End of for loop

for(String dataPoint: randomPoints) {
    String[] stringCoordinates = dataPoint.split(",");

```

```

        List<Double> dataCoordinates = new ArrayList<>();
        for(int i =0; i < stringCoordinates.length; i++){
dataCoordinates.add(Double.parseDouble(stringCoordinates[i]));
        }
        points.add(dataCoordinates); //Add Double coordinates list
to another list
    } //End of for-each loop

List<Double> score = new ArrayList<Double>();
    for (List<Double> data : points) {
        score.add(lof.lof(data));
    } //End of score for loop

//print points' anamolies score
for(int j=0; j < threshold.length ; j++){
// System.out.println("*"+threshold[j]+" : ");
    int min=0,max=0;
    for(int i =0; i < score.size(); i++)
    {
        if(score.get(i) <= threshold[j])
        {

            min ++;

// System.out.println(score.get(i));
        }
        else
        {

            max ++;
        } //End of else if

    } //End of j

        System.out.println(" "+ ((min * 1.0) /
score.size()));
        System.out.println(" "+ ((max * 1.0) /  score.size()));

// Double Accuracy = (1.0 * min)/score.size();
// System.out.println( "Accuracy: " + (Accuracy ) ) ;

} //End of for loop

System.out.println();

    endTime = System.currentTimeMillis();

```

```
float sec = (endTime - startTime) / 1000F;  
System.out.println("Exution Time: "+ sec + " seconds");
```

```
    } //End of Main function
```

```
} //End of Class
```

A.4. Copyright

1. Report No. FHWA-HIF-13-019	2. Government Accession No.	3. Recipient's Catalog No.	
4. Title and Subtitle Alkali-Aggregate Reactivity (AAR) Facts Book		5. Report Date March 2013	
		6. Performing Organization Code	
7. Author(s) Thomas, M.D.A., Fournier, B., Folliard, K.J.		8. Performing Organization Report No.	
9. Performing Organization Name and Address The Transtec Group, Inc. 6111 Balcones Drive Austin, TX 78731		10. Work Unit No.	
		11. Contract or Grant No. DTFH61-06-D-00035	
12. Sponsoring Agency Name and Address Office of Pavement Technology Federal Highway Administration 1200 New Jersey Avenue, DE Washington, DC 20590		13. Type of Report and Period Covered Final Report March 2013	
		14. Sponsoring Agency Code	
15. Supplementary Notes Contracting Officer's Representative (COR): Gina Ahlstrom, HIAP-10			
16. Abstract This document provides detailed information on alkali-aggregate reactivity (AAR). It primarily discusses alkali-silica reaction (ASR), covering the chemistry, symptoms, test methods, prevention, specifications, diagnosis and prognosis, and mitigation. Alkali-carbonate reaction (ACR) is also addressed.			
17. Key Words Alkali-silica reactivity, alkali-aggregate reaction, reactive aggregates, ASR, concrete durability, symptoms, identification, prevention, mitigation, lithium		18. Distribution Statement No restrictions. This document is available to the public through the National Technical Information Service, Springfield, VA 22161.	
9. Security Classif. (of this report)	20. Security Classif. (of this page)	21. No of Pages 211	22. Price